ARCHIVES OF ACOUSTICS
6, 3, 219-228 (1981)

ANALYSIS OF THE ACOUSTIC FIELD ENERGY DISTRIBUTION IN A RECTANGULAR HALL FOR MANY SOUND SOURCES*

MARIA TAJCHERT

Institute of Radioelectronics, Warsaw Technical University
(00-665 Warszawa, ul. Nowowiejska 15/19)

This paper presents conclusions regarding the relations of the energy distribution of the field of reflected waves for a simultaneous action of many sources with such parameters as: the dimensions of the hall, the proportion of the dimensions of the floor, and the position of the most powerful sound sources.

1. Introduction

The difficulty in analyzing the acoustic field in enclosures by the wave method and the insufficient results of analysis by the statistical method have caused scientists to seek simpler and more accurate methods. Recent years have brought development of the numerical approach in the geometrical methods: "the ray tracing method" [1, 2] and "the image source method" [3, 4, 7]. Papers [5, 6, 8] presented a geometrical–numerical method of investigation of the acoustic field energy distribution in a rectangular room. This method uses an array of image sources determined by a computer. The powers of the image sources are relatively lower than the power of a real source, depending on the value of the absorption coefficient of the walls and on the distance from the observation points. In addition to simplifying assumptions related to the present implementation of the geometrical–numerical method [8], in analyzing the field with many sources acting simultaneously it was assumed that the energies of waves from all the sources sum up at the observation point. The programme is so designed that the energy of the direct waves, the reflected waves as well as the total energy are calculated for each sound source and each observation point. The algorithm does not impose any restrictions on the order of reflection. In practice, some restrictions are necessary due to time limit and calculation cost.

The input data are: the dimensions of the hall, the absorption coefficients of the walls, the number of sources, the number of observation points, the power

* These investigations were supported by grant MR.I.24.

of the sources and the energy attenuation constant in the air. The results are obtained in the form of two tables: the sound pressure levels of direct and reflected waves from individual sources at successive observation points and the sound pressure levels of direct, reflected and resultant waves from all the sources at the successive observation points.

The present algorithm can be used in twofold manner. First of all, it can be used for analysis of the energy distribution in a hall, i.e. for seeking some general regularities of the acoustic field for variations in particular parameters. Another possibility is making computations for specific real cases, for example, seeking the most efficient means of noise reduction in a given area or point. The same computations can be made for the design of industrial halls, provided that it is defined what acoustic conditions are the most desired from the point of view of noise control. If one is interested in the acoustic conditions in the entire hall rather than at a specific "work post", for a uniform distribution of sources, the calculations can be limited to include the field of reflected waves only. The field of direct waves is related only to the distance of sources from observation points, i.e. it does not depend on regularities which result from variations of the other parameters of the system. Obviously, the energy of the resultant field as a sum of the direct field energy and of the energy of reflected waves will vary in a slightly different manner than the energy of reflected waves. However, it seems that this difference is not significant in the investigations of the general regularities of the sound field.

2. Discussion of the results

In the investigation of the dependence of the energy distribution on the acoustic system parameters it is possible to seek regularities but it is difficult to compare individual cases, since (apart from the criterion of minimum energy level) no good comparative criteria exist.

The effect of the following parameters on the energy distribution was analyzed: the size of the hall, the proportions of the floor dimensions (for approximately the same floor area) and the position of the most powerful sources for a constant density of sources, i.e. a constant floor area per one sound source (i.e. a machine) and a constant hall height $h = 7.8$ m. The dimensions of halls, the values of absorption coefficients of walls and also other data are close to the real values, e.g. sources and observation points are at a height of 1.5 m above the floor.

2.1. *The effect of the hall size*

Fig. 1 shows the arrangement of sources of equal power ($L_N = 101$ dB) and observation points in one of the examples for which the computations were made. The other two examples involve computations in halls with a floor

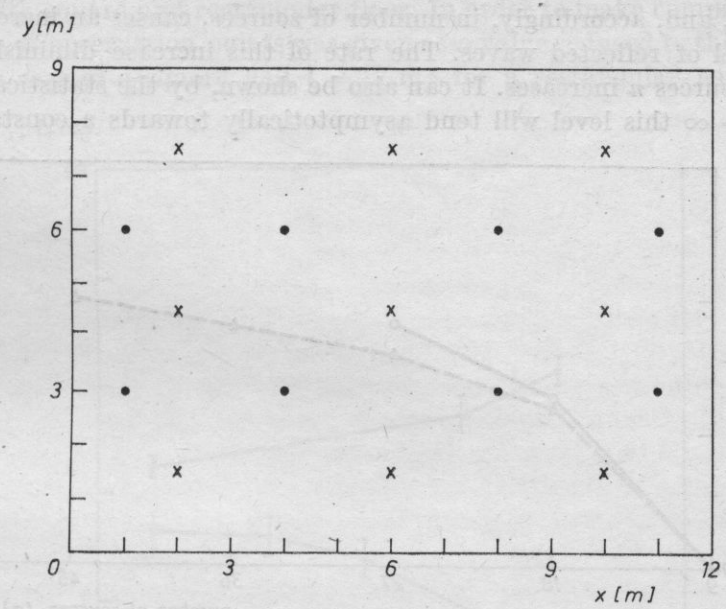

Fig. 1. The projection of the floor of the hall with dimensions 9 × 12 m with plotted positions of sources (x) and observation points (●); the height of the hall $h = 7.8$ m

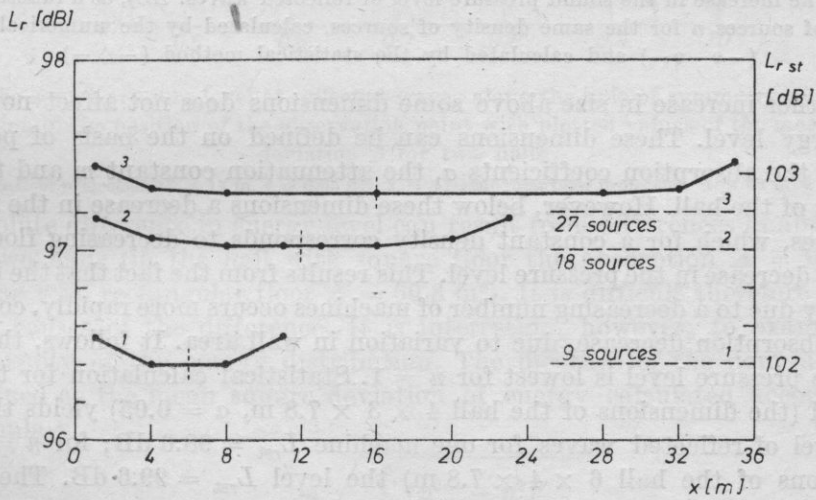

Fig. 2. The sound pressure level of reflected waves along the x axis as a function of the distance of the observation point from the wall, $x = 0$

1 – a hall with dimensions 9 × 12 × 7.8 m, *2* – a hall with dimensions 9 × 36 × 7.8 m; on the left calculation results by the numerical method, on the right those by the statistical method, the density of sources $G = 12$ m²/machine

area twice as large and three times as large, respectively, but with the same density of identical sources ($G = 12$ m²/machine). Fig. 2 shows the results of numerical calculations and those of statistical calculations. For a constant density of sources and a constant hall height an increase in hall size, i.e. also

in floor area, and, accordingly, in number of sources, causes an increase in the pressure level of reflected waves. The rate of this increase diminishes as the number of sources n increases. It can also be shown, by the statistical method, that for $n \to \infty$ this level will tend asymptotically towards a constant value.

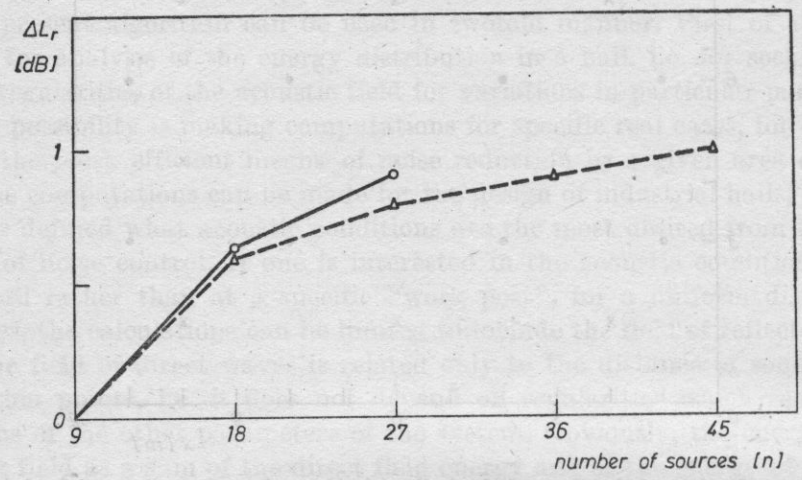

Fig. 3. The increase in the sound pressure level of reflected waves. ΔL_r, as a function of the number of sources n for the same density of sources, calculated by the numerical method (—o—o—) and calculated by the statistical method (—△—)

Any further increase in size above some dimensions does not affect noticeably the energy level. These dimensions can be defined on the basis of power of sources, the absorption coefficients a, the attenuation constant m and the proportions of the hall. However, below these dimensions a decrease in the number of sources, which for a constant density corresponds to decreasing floor area, causes a decrease in the pressure level. This results from the fact that the increase in energy due to a decreasing number of machines occurs more rapidly, compared to the absorption decrease, due to variation in wall area. It follows, therefore, that the pressure level is lowest for $n = 1$. Statistical calculation for the data assumed (the dimensions of the hall $4 \times 3 \times 7.8$ m, $a = 0.05$) yields the pressure level of reflected waves for one machine $L_{rst} = 98.6$ dB; for $n = 2$ (the dimensions of the hall $6 \times 4 \times 7.8$ m) the level $L_{rst} = 99.6$ dB. The results for larger n are given in Fig. 2.

2.2 *The effect of the proportion of dimensions of the floor*

The following quantities are invariable in the computations: the density of sources of equal power ($L_N = 101$ dB), the floor area (the number of sources), the absorption coefficients $a = 0.05$ and the energy attenuation constant in the air $m = 0.004$. The proportions of the dimensions of the floor varied, however, from 1:1 to 1:2 to 1:3.6. In view of slight differences in the energy distribution between the first and second cases, only the first and third cases were considered,

i.e. halls with square and rectangular floor. In order to make comparison easier the position of observation points was given as a value reduced to the hall length x/l; in the case of a square hall $l = 17$ m; for a rectangular hall $l = 32$ m.

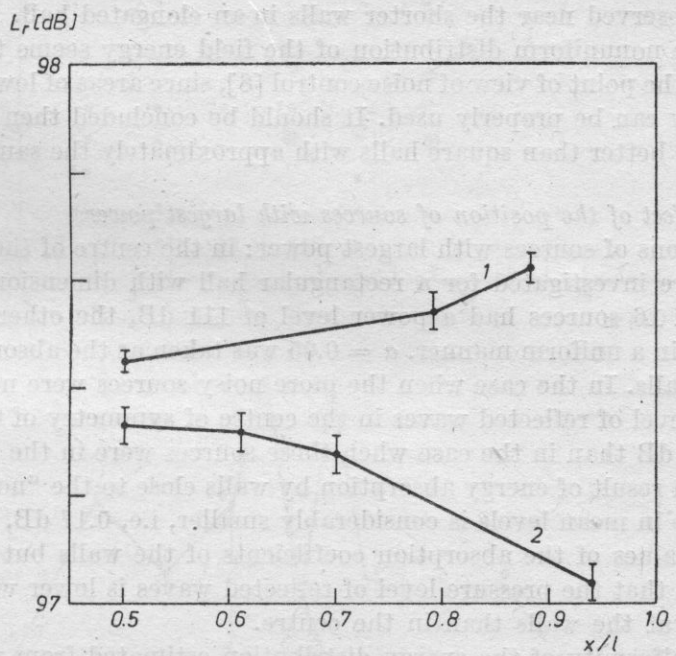

Fig. 4. The sound pressure level of reflected waves along the axis of symmetry of the floor as a function of the position of the observation point with plotted values of the mean square deviation δ for two halls

1 – a square floor projection 17 × 17 m, $\delta = 0.05$ dB; *2* – a rectangular floor projection 9 × 32 m, $\delta = 0.07$ dB

The absolute difference in energy level can result from differences in absorption in the two halls (in the hall with square floor the absorption $A = 55.4$ m²), in the one with rectangular floor $A = 60.8$ m²). It is difficult therefore to analyze the causes of the difference. It is interesting, however, to examine the nonuniformity of the energy distribution. The measure of the nonuniformity was defined as the mean square deviation of energy calculated according to the formula

$$\delta = \sqrt{\frac{\sum_{i=1}^{n} (p_{\mathrm{av}}^2 - p_i^2)^2}{n}},$$

where p_{av}^2 – the value of mean square sound pressure for all points, p_i^2 – the value of mean square sound pressure at the ith observation point, n – the number of observation points.

The deviation is 0.5 % for a hall with square floor, 0.8 % for a rectangular hall with the constant coefficient $\alpha = 0.05$ for all walls and 0.86 % and 1.12 %, respectively, for the absorption coefficient of the ceiling $\alpha = 0.8$ and $\alpha = 0.05$

for the walls. Therefore, the nonuniformity of energy distribution is smaller in a square hall than in a rectangular one and obviously increases for different absorption coefficients of the surface area. A noticeable decrease in the energy level can be observed near the shorter walls in an elongated hall. For constant energy a more nonuniform distribution of the field energy seems to be advantageous from the point of view of noise control [8], since areas of lower or greater energy density can be properly used. It should be concluded then that rectangular halls are better than square halls with approximately the same floor area.

2.3 *The effect of the position of sources with largest power*

Two positions of sources with largest power: in the centre of the hall and at the walls, were investigated for a rectangular hall with dimensions $9 \times 18 \times \times 7.8$ m. 4 of 16 sources had a power level of 111 dB, the other had 96 dB, all positioned in a uniform manner. $\alpha = 0.05$ was taken as the absorption coefficient of the walls. In the case when the more noisy sources were near the walls the pressure level of reflected waves in the centre of symmetry of the floor was lower by 1.52 dB than in the case when these sources were in the centre of the floor. This is a result of energy absorption by walls close to the "noisy" sources. The difference in mean levels is considerably smaller, i.e. 0.17 dB, which is due to very low values of the absorption coefficients of the walls but still permits the statement that the pressure level of reflected waves is lower when the loud machines are at the walls than in the centre.

The nonuniformity of the energy distribution estimated from values of the mean square deviation of energy is greater when more powerful machines are in the centre of the hall. The mean square deviations are respectively 7.1 and 6.6%. However, in the case when the ceiling is covered with a highly absorbent material ($\alpha = 0.8$) a greater nonuniformity occurs when the "noisy" sources are near the walls (the mean square deviations being 4.6 and 4.4%, respectively). For different absorption coefficients of the walls the energy distribution due to the arrangement of sources of different power varies essentially due to the arrangement of sound absorbing materials (Fig. 5b, c).

Increased value of the absorption coefficient of the walls at which the "louder" sources are placed considerably decreases the pressure level of reflected waves [8]. This may lead to another conclusion that in the case when materials of different values of the absorption coefficient of the walls are used it is better to set the "loud" machines at the walls rather than in the centre of the hall because of a lower noise level and greater nonuniformity of the energy distribution. However, for low values of the absorption coefficient of the walls the criterion of the nonuniformity of the energy distribution seems more essential, and it follows, therefore, that it is better to set the more powerful machines in the centre of the hall. Some discrepancy in estimations suggests that computations should be made for specific cases and that machines should be set according to the results of these computations.

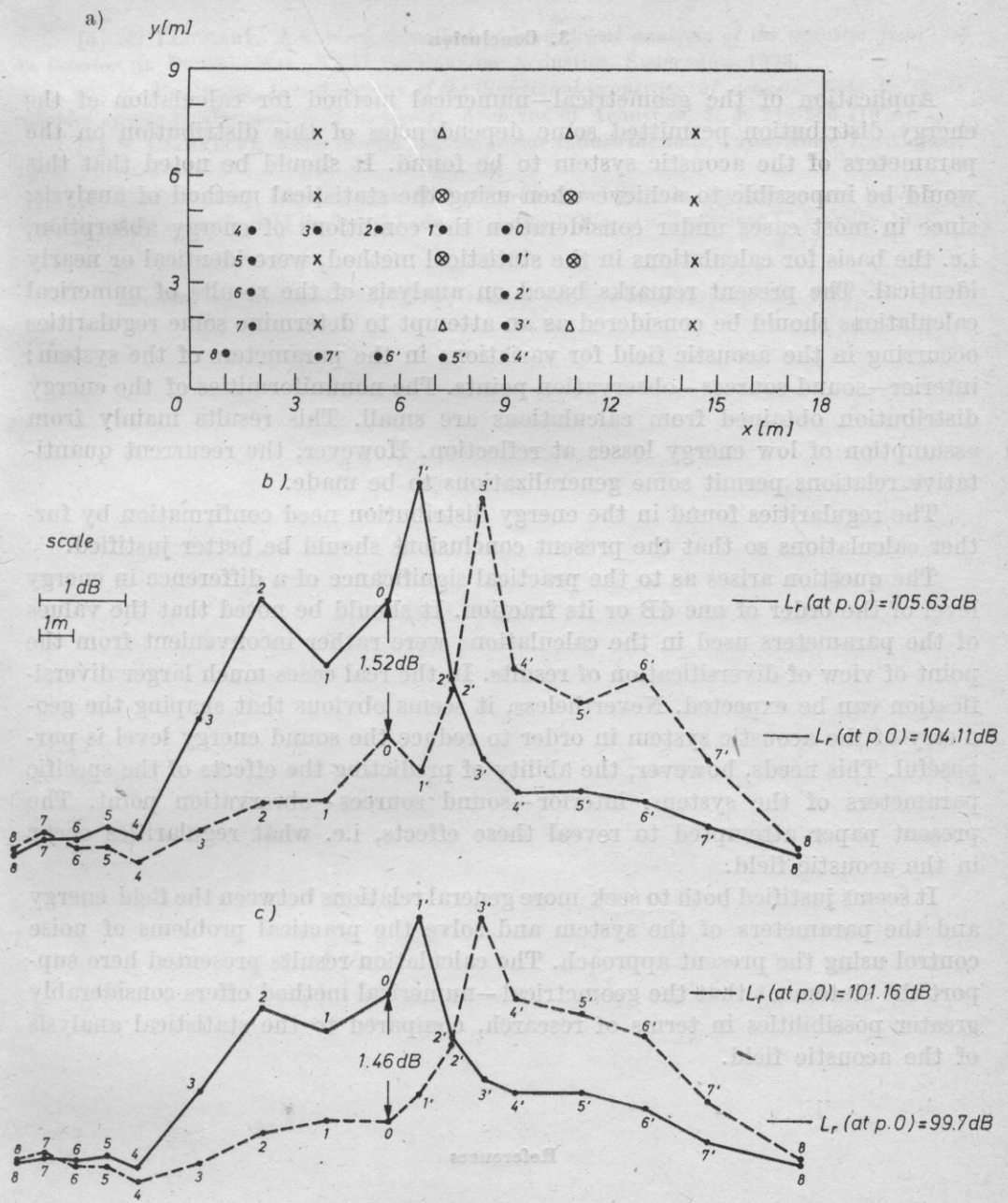

Fig. 5. a) A floor projection with plotted positions of sources of different power levels of 111 dB (△), 108 dB(⊗) and 96 dB (x) and positions of observation points (●); b) The sound pressure level of reflected waves in successive observation points (numbered as in Fig. 5a) as a function of the distance along the x axis or y axis for the same value of the absorption coefficient $\alpha = 0.05$; —— "noisy" sources in the middle, — — — "noisy" sources near the walls; c) as in b) but for different values of the absorption coefficient; $\alpha = 0.08$ for the ceiling and $\alpha = 0.05$ for the walls

3. Conclusion

Application of the geometrical–numerical method for calculation of the energy distribution permitted some dependencies of this distribution on the parameters of the acoustic system to be found. It should be noted that this would be impossible to achieve when using the statistical method of analysis, since in most cases under consideration the conditions of energy absorption, i.e. the basis for calculations in the statistical method, were identical or nearly identical. The present remarks based on analysis of the results of numerical calculations should be considered as an attempt to determine some regularities occurring in the acoustic field for variations in the parameters of the system: interior–sound sources–observation points. The nonuniformities of the energy distribution obtained from calculations are small. This results mainly from assumption of low energy losses at reflection. However, the recurrent quantitative relations permit some generalizations to be made.

The regularities found in the energy distribution need confirmation by further calculations so that the present conclusions should be better justified.

The question arises as to the practical significance of a difference in energy level of the order of one dB or its fraction. It should be noted that the values of the parameters used in the calculations were rather inconvenient from the point of view of diversification of results. In the real cases much larger diversification can be expected. Nevertheless, it seems obvious that shaping the geometry of the acoustic system in order to reduce the sound energy level is purposeful. This needs, however, the ability of predicting the effects of the specific parameters of the system: interior–sound sources–observation point. The present paper attempted to reveal these effects, i.e. what regularities occur in the acoustic field.

It seems justified both to seek more general relations between the field energy and the parameters of the system and solve the practical problems of noise control using the present approach. The calculation results presented here support the statement that the geometrical–numerical method offers considerably greater possibilities in terms of research, compared to the statistical analysis of the acoustic field.

References

[1] A. Krokstad, S. Strom, *Calculation of the acoustical room response by the use of a ray tracing technique*, Journal of Sound and Vibration, **8** (1968).

[2] A. Kulowski, *A numerical method of modelling the acoustic field in interiors* (in Polish) (doctoral diss.), Politechnika Gdańska 1979.

[3] M. Gibbs, D. Jones, *A simple image method for calculation of the distribution of sound pressure levels within an enclosure*, Acustica, **26** (1972).

[4] Y. Hirata, *Geometrical acoustics for rectangular rooms*, Acustica, **43** (1979).

[5] M. TAJCHERT, *A numerical method of geometrical analysis of the acoustic field in an interior* (in Polish), Mat. XXII Seminar on Acoustics, Świeradów 1975.

[6] M. TAJCHERT, *Investigations of the directional properties of acoustic field in finite cuboidal spaces (geometrical field analysis)*, Archives of Acoustics, **3**, 4, 249-265 (1978).

[7] S. CZARNECKI, *Noise control aspects inside industrial halls*, Inter-Noise 75, August, 1975.

[8] M. TAJCHERT, *Interpretation of the reverberation effect in the geometrical method of analysis of the acoustic field* (in Polish) (doctoral diss.), Warsaw Technical University 1978.

Received on November 26, 1979; revised version on February 19, 1981.

ARCHIVES OF ACOUSTICS
6, 3, 229-238 (1981)

GENERALIZED DISCRIMINATION THRESHOLDS AND EVALUATION OF SIMULTANEOUS VARIATIONS IN THE INTENSITY AND FREQUENCY OF A TONE

ALICJA CZAJKOWSKA

Department of Acoustics, Mickiewicz University
(60-769 Poznań, ul. Matejki 48/49)

The investigations presented in this paper were based on the concept of an interrelation between simultaneously evaluated variations in loudness and pitch of the same tonal signal with varying intensity and frequency. As an example, some elements of this interrelation – related to the perceptibility and to the evaluation of the magnitude of variations in loudness and pitch – were examined for a chosen tone. The results obtained were represented in the form of new, so-called generalized, discrimination thresholds and of the curve of the variations in loudness and pitch sensed to be equal. The results permit the statement that it is possible to sum up the subthreshold effects caused by the simultaneous variations in the signal intensity and frequency and thus to obtain the superthreshold effect in the form of a sensation of loudness variations. For greater variations in the physical parameters, a sort of mutual "masking" of the simultaneous variations in loudness and pitch of the same tone was found, and in the case when both variations were audible simultaneously it was found that it was possible to compare these in terms of magnitude.

1. Introduction

An analysis of the curves of equal loudness and the curves of equal pitch shows some interrelations between the variations in loudness and pitch of a tone. Both subjective characteristics of the tone, loudness and pitch, depend simultaneously on the two physical parameters of the tone, i.e. intensity and frequency. Therefore, in changing the loudness of the tone only by varying the intensity, it is difficult to avoid the simultaneous variation in the pitch of this tone over some ranges. And conversely, when changing the pitch of the tone by modulation of the frequency only, it is possible to achieve simultaneously a change in its pitch.

The investigations presented in this paper were based on the concept of the existence of some interrelation between the variations in loudness and pitch. This interrelation occurs in simultaneous evaluation of these two variations with respect to tonal signals in which simultaneous variations in intensity and frequency occur. It was acknowledged that this interrelation may be significant for deeper knowledge of the mechanism of forming the sensations of loudness and pitch of a tone and an attempt was made to analyze preliminarily some of its elements related to the sensation itself and to the evaluation of the magnitude of simultaneous variations in loudness and pitch.

The investigations consisted in experimental determination of discrimination thresholds different from the previously used, which were called generalized discrimination thresholds, and of curves resulting from an evaluation of variations in intensity and frequency, which were called the curves of variations in loudness and pitch sensed to be equal. It was decided that the investigations were to be performed, for example, for a given tone of 1100 Hz and 70 dB over the range of variation from 0 to 900 Hz and 0 to 20 dB, respectively.

It was decided that "the generalized discrimination thresholds" would refer to a threshold determined for signals in which variations of the two physical parameters, i.e. intensity and frequency, occur simultaneously. Those discrimination thresholds which were known previously and determined for signals involving variations in only one parameter: alternatively, frequency or intensity (the so called frequency discrimination thresholds or intensity discrimination thresholds), were called, in opposition to the new ones, the classical thresholds. Irrespective of considering this division of thresholds from the point of view of the number and quality of variable physical parameters of a signal under examination, it was decided, both in the case of the generalized and classical discrimination thresholds, to specify besides the threshold type the name of the psychoacoustic parameter whose variation undergoes estimation by listeners in terms of perceptibility. For example, "the intensity discrimination threshold for pitch variations" refers to the case when the listener evaluates the perceptibility of variations in pitch in a signal which shows intensity variations. In turn, e.g. "the generalized discrimination threshold for pitch variations" applies to the case when the listener estimates the perceptibility of pitch variations in a signal with simultaneous intensity and frequency variations.

An attempt was made to obtain the curves of variations in loudness and pitch sensed to be equal under the assumption that listeners can perform a kind of evaluation consisting in simultaneous comparison of totally different variations in loudness and pitch in terms of their magnitude.

2. Experimental investigation

In order to achieve in one experiment the data both for the generalized discrimination thresholds and for the curves of variations in loudness and pitch

sensed to be equal, a special method of investigation permitting multiple simultaneous evaluation was developed.

An acoustic generator of the signal of the type *ABAB*... shown schematically in Fig. 1 was designed and constructed. This signal is a sequence of two-

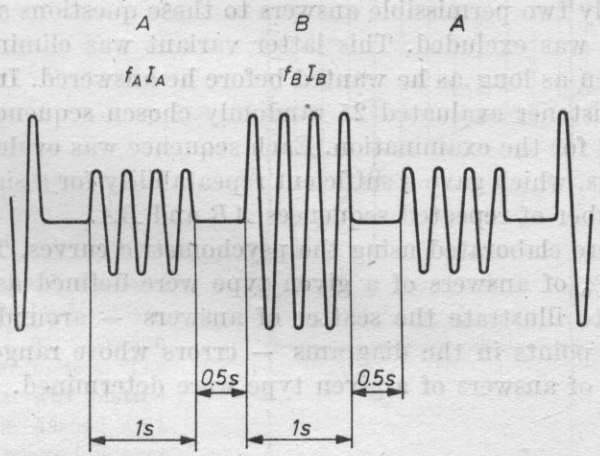

Fig. 1. The signal form used in the investigations

second tonal impulses *A* and *B* of almost rectangular envelope, generated alternatively and after half-second intervals, with the rise and decay times of the order of several milliseconds. In view of the duration of the impulses (and the intervals) these impulses can be simply regarded as tones. One also can neglect the effect on the evaluation of loudness and pitch of these tones, of the randomly changing phase of their start and interruption and the slight, hardly perceptible cracks occurring then. Two constants predetermined for it. and the differences occuring simultaneously between the tones *A* and *B*: in frequency (30 possibilities over the range 0 to 900 Hz) and in intensity (30 possibilities over the range 0 to 20 dB), correspond to a given sequence of tones. These differences were so chosen that in the case when both took values different from zero the tones of higher frequency also had higher intensity.

The signal was supplied to one of listener's ear by earphones in the audiometric booth.

The investigation involved three listerns with normal hearing and different musical ability, chosen from a larger number of listeners in the course of a preliminary examination which at the same time was a training session. In terms of their results these listeners were representative of the whole group examined. At the same time their answers were mostly dilligent, which was confirmed by the infrequent faults in the case of the sequences of the type *AAAA*...

In the case of each sequence *ABAB*... the task of each listener was to answer simultaneously the following three questions:

1. whether the tones *A* and *B* in a given sequence differ in loudness;

2. whether the tones A and B in a given sequence differ in pitch; and when both of these differences were perceived:

3. which of the variations — in loudness or in pitch — was perceived as dominating.

There were only two permissible answers to these questions and the variant "I do not know" was excluded. This latter variant was eliminated since the listener could listen as long as he wanted before he answered. In a single listening session the listener evaluated 25 randomly chosen sequences of over 300 sequences selected for the examination. Each sequence was evaluated ten times in all the listenings, which gave a sufficient repeatability for a signal containing an unlimited number of repeated sequences AB and BA.

The results were elaborated using the psychometric curves. The values corresponding to 50% of answers of a given type were defined as the threshold values. In order to illustrate the scatter of answers — around the threshold values plotted as points in the diagrams — errors whose range corresponded to 25% and 75% of answers of a given type were determined.

3. Investigation results

The results obtained for three chosen listeners showed that despite individual quantitative differences the general trends of the answers were the same and that the same psychoacoustic effects occurred for all the three listeners. Therefore, the results were elaborated for each listener individually, and it was decided that the results of only one of them will be presented here, as an example typical of all the other listeners participating in the investigations. The results were represented as the curves of the generalized discrimination threshold for variations in loudness, the generalized discrimination threshold for variations in pitch, and the curve of variations in loudness and pitch sensed to be equal. In view of the singularity of psychoacoustic effects occurrring for variations in the physical parameters of the order of the classical discrimination thresholds and for greater ones, a division into two ranges, called respectively range I and range II, was introduced.

Fig. 2 shows the generalized discrimination threshold for variations in loudness in range I of variability of the physical parameters. The value of the corresponding classical discrimination thresholds are marked on the co—ordinate axes by the dashed lines. It can be seen that the generalized discrimination threshold for variations in loudness occurs above the classical intensity discrimination threshold for variation in loudness and shows a monotonical increase with increasing the tone frequency simultaneous with the variations in intensity. The same trend also occurs in range II of variations in the physical parameters, i.e. for greater variations than the classical discrimination thresholds. This signifies that the occurrence of frequency variations in a signal may decrease

the perceptibility of the variations in loudness resulting only from variations in the intensity of a tone and that in direct proportion to the increase in frequency variations.

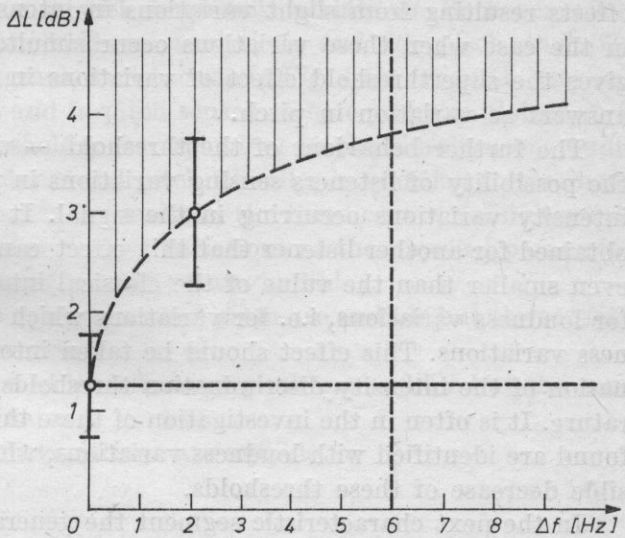

Fig. 2. The generalized discrimination threshold for loudness variations in range I of variation of the physical parameters. The scatter of answers was plotted every ± 25%. The dashed area denotes the region where loudness variations are audible

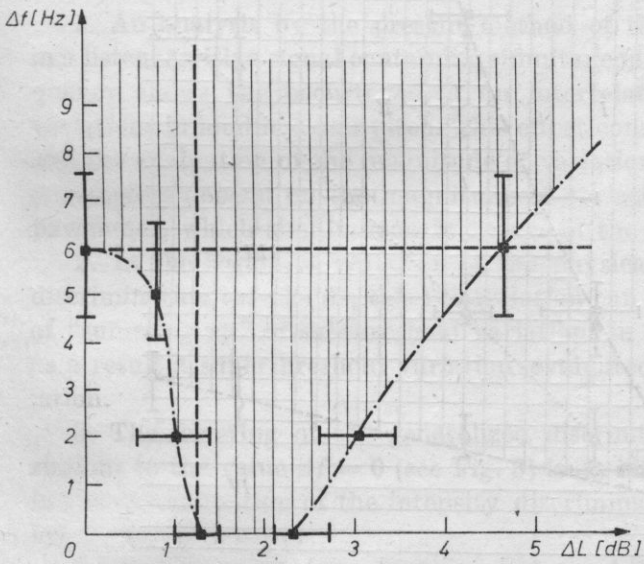

Fig. 3. The generalized discrimination threshold for pitch variations in range I of variations of the physical parameters. The scatter of answers was plotted every ± 25%. The dashed area denotes the region where loudness variations are audible

Fig. 3 shows the characteristic of the simultaneously determined generalized discrimination threshold for variations in pitch in range I. Several segments can be distinguished in this characteristic.

The first one shows a monotonical decrease in this threshold from the value of the classical frequency discrimination threshold for variations in pitch to the

value $\Delta f = 0$ reached for a variation in intensity equal approximately to the value of the classical intensity discrimination threshold for variations in loudness. This decrease suggests the possibility of "summing up" the subthreshold effects resulting from slight variations in intensity and frequency of a signal in the case when these variations occur simultaneously. This "summing up" gives the superthreshold effect of variations in the signal, estimated in most answers as variation in pitch.

The further behaviour of the threshold — under the abscissa — suggests the possibility of listeners sensing variations in pitch as a result of only slight intensity variations occurring in the signal. It can be seen from the results obtained for another listener that this effect can occur for intensity variations even smaller than the value of the classical intensity discrimination threshold for loudness variations, i.e. for variations which do not cause perceptible loudness variations. This effect should be taken into consideration in the determination of the intensity discrimination thresholds as they are called in the literature. It is often in the investigation of these thresholds that all the variations found are identified with loudness variations, which evidently involves the possible decrease of these thresholds.

In the next characteristic segment the generalized discrimination threshold

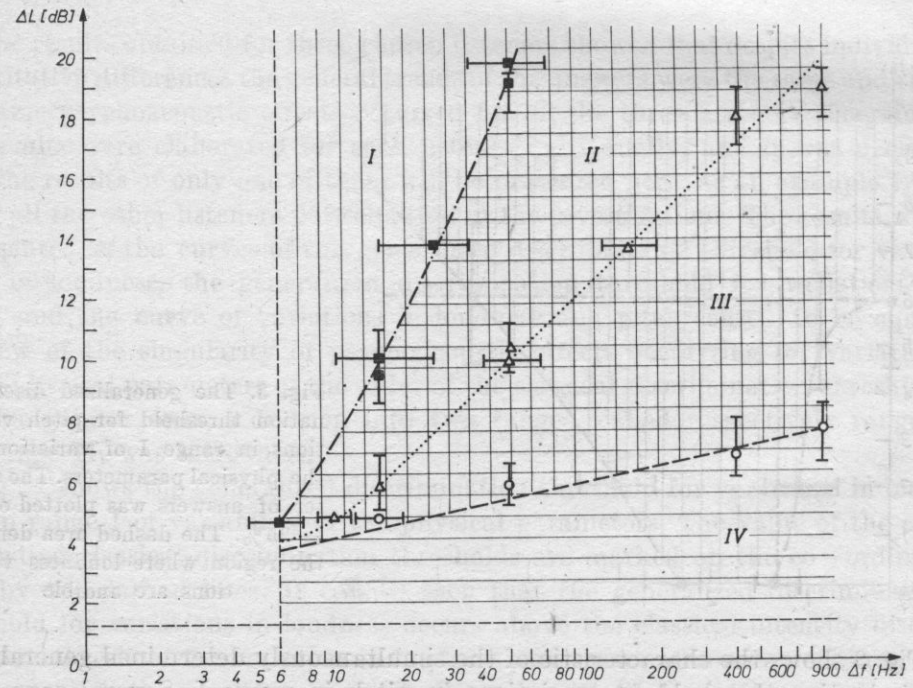

Fig. 4. A comparison of the generalized discrimination threshold for loudness variations —o—, the generalized discrimination threshold for pitch variations, —■—, and the curve of the variations in loudness and pitch sensed to be equal ...△... for range II of variation of the physical parameters. The scatter of answers was plotted every ± 25%

for pitch variations shows a monotonical increase also in range II of variation of the physical parameters. This signifies that the perception of pitch variations can worsen as a result of introduction into a signal of adequately great intensity variations simultaneous with frequency variations. Both generalized discrimination thresholds: for loudness variations and for pitch variations, can be represented in one diagram, as it is done in Fig. 4 for range II. The curve of the variations in loudness and in pitch sensed to be equal was plotted in the area between the above thresholds, corresponding to the simultaneous audibility of both variations in loudness and pitch. Finally, in addition to the inaudibility region, where no variations are audible, the three curves define the following regions in the investigated area of variations of the physical parameters:

range I where only loudness variations are audible;

range II where variations in loudness and pitch are audible but the sensation of loudness variations dominates;

range III where variations in loudness and pitch are audible but the sensation of pitch variations dominates;

range IV where only pitch variations are audible.

4. Conclusions

1. An analysis by the present method of the complex sensation produced in a listener with a signal containing simultaneous variations in intensity and frequency shows the occurrence of an interrelation between the simultaneous variations in loudness and pitch. This effect consists in that both the perception and the evaluation of the magnitude of variation of one of these psychoacoustic parameters depend on the magnitude of variation in the other psychoacoustic parameter, which simultaneously occurs in the same signal.

2. In the region of variation of the physical parameters near the classical discrimination thresholds, this interrelation can be seen in the form (see Fig. 3) of "summing up" of subthreshold variations in intensity and frequency, giving as a result a superthreshold variation evaluated by the listeners as pitch variation.

3. The lowering of the generalized discrimination threshold for pitch variations to the value $\Delta f = 0$ (see Fig. 3) is an effect which should be considered in the determination of the intensity discrimination thresholds as they are called in the literature.

It follows from the investigations performed that slight variations in the tone intensity can produce in a listener a sensation of pitch variation, and therefore, identification of the sensation resulting from intensity variation with only pitch variation can lead to a decrease of the thresholds mentioned above.

In this connection, the necessity mentioned in the introduction of ordering and newly specifying the terms in the field of discrimination thresholds is con-

firmed. It is essential that there should be no doubt as to which variable physical parameters of the signal the given thresholds relate, and with the evaluation of which psychoacoustic parameters they are connected.

4. The increase in the generalized discrimination thresholds both for pitch and loudness variations with respect to the classical discrimination thresholds (Fig. 4) signifies that as if mutual "masking" effect of simultaneous variations in loudness and pitch of the same signal occurs for variations of physical parameters greater than the classical discrimination thresholds.

5. The simultaneous variations in loudness and pitch of the same signal, despite their different nature, can be compared in terms of magnitude. The regularity and monotonical increase of the curve of variations in pitch and loudness sensed to be equal signifies that listeners are quite consistent in the evaluation, based on some standard pattern for the equality of both variations.

6. The effects found cannot be explained by using the curves of equal loudness and the curves of equal pitch, which suggests the particularity of the mechanisms of evaluating simultaneously the variations in loudness and pitch by the hearing organ. There are also no data in the literature which could be comparable enough with those obtained in the present investigations, since investigations of approximately similar problems are mostly fragmentary and diversified (cf. References), and the present approach is different from concepts proposed therein.

Interpretation of the results obtained in terms of the theory of hearing needs further accurate investigations to give a full quantitative image of the psychoacoustic effects and a deeper knowledge of the physiology of hearing.

7. The simultaneous variations in intensity and frequency are characteristic of the natural sounds of speech and music. It seems therefore possible to use, in the future, the results of investigations in this field, first of all in the acoustics of music and audiology, and also in the room acoustics.

References

[1] J. T. ALLANSON, A. F. NEWELL, *Subjective responses to tones modulated simultaneously in both amplitude and frequency*, J. Sound Vib., **3**, 2, 135 (1966).

[2] A. CZAJKOWSKA, *A psychoacoustic analysis of perception and evaluation of simultaneous variations in intensity and frequency of a tone*, doct. diss. (in Polish), Poznań 1980.

[3] F. CONINX, *The detection of combined differences in frequency and intensity*, Acustica, **39**, 3, 137 (1978).

[4] R. FELDTKELLER, E. ZWICKER, *Über die Lautstärke von gleichförmigen Geräuschen*, Acustica, **5**, 303 (1955).

[5] G. B. HENNING, *Frequency discrimination of random amplitude tones*, JASA, 39, 336 (1966).

[6] E. KÖNIG, *Effect of time on pitch discrimination threshold under several psychophysical procedures, comparison with intensity discrimination thresholds*, JASA, 29, 606 (1957).

[7] D. MAIWALD, *Ein Funktionsschema des Gehörs zur Beschreibung der Erkenbarkeit kleiner Frequenz- und Amplitudenänderungen*, Acustica, 18, 81 (1967).

[8] A. RAKOWSKI, *Categorical perception of sound pitch in music* (in Polish), Chopin Academy of Music, Warsaw 1978.

[9] R. J. RITSMA, *Pitch discrimination and frequency discrimination*, Congres International d'Acoustique, Liége 1965, B 22.

[10] G. SHOWER, R. BIDULPH, *Differential pitch sensitivity of the ear*, JASA, 3, 275 (1931).

[11] S. S. STEVENS, *The relation of pitch to intensity*, JASA, 6, 150 (1935).

[12] W. SUCHOWERSKYI, *Beurteilung von Unterschieden zwischen aufeinanderfolgenden Schallen*, Acustica, **38**, 2, 131 (1977).

[13] W. SUCHOWERSKYI, *Beurteilung kontinuierlicher Schalländerungen*, Acustica, **38**, 2, 140 (1977).

[14] I. VERSCHUURE, A. A. van MEETEREN, *The effect of intensity on pitch*, Acustica, **32**, 1, 33 (1975).

[15] E. ZWICKER, *Direct comparison between the sensations produced by frequency modulation and amplitude modulation*, JASA, **34**, 9, 2, 1425 (1962).

Received on November 26, 1979; revised version on January 7, 1981.

ARCHIVES OF ACOUSTICS
6, 3, 239-252 (1981)

MODIFIED CORRECTION CURVES FOR NOISE HAZARD ESTIMATION

GABRIELA KERBER, JACEK KONIECZNY, ANNA PREIS

Department of Acoustics, Adam Mickiewicz University
(60-769 Poznań, ul. Matejki 48/49)

The harmful effect of noise at work stands is established by the ISO Standard of noise which gives the maximum permissible and the mean permissible values of the sound level expressed in dB (A).

Application of the correction curve A does not account for the effects of the temporary threshold shift (TTS) and the permanent threshold shift (PTS) in hearing which results from physiological aging of the hearing organ. Both effects influence the noise induced permanent hearing loss (NIPTS), depending only on the exposure to noise. In addition there is no correspondence between the noise spectrum corrected by the curve A and the distribution of hearing loss established on the basis of the audiogram of a person exposed to this noise.

The present proposal of modified correction curves for noise hazard estimation accounts for the effects mentioned above. Contrary to the previously used methods of noise spectrum correction (by the curves A and D), the distribution of the values of the sound level for individual frequencies, obtained by using the modified correction curves, accounts for the hearing loss induced by the noise. In particular, what is essential here is a good agreement between the position of the spectral maxima and the maximum hearing loss on the frequency scale.

The correction curves proposed were used in the estimation of the noise hazard at the work stand of a cutter-loader.

1. Introduction

The advisability of the correction curve A in noise hazard estimation has been recently more and more questioned [2].

If the curve A corrects well the noise spectrum in noise hazard estimation, the maximum values of the noise level in the corrected spectrum ought to correspond to the maximum hearing loss in the audiogram of a person exposed to this noise.

In practice this relation is not observed [2]. This results from the fact that the main purpose of the correction curve A in its original concept was to serve in the estimation of the noise level in the range of sound pressure levels (SPL) up to 55 dB. Therefore, its application to the correction of harmful noise spectra, i.e. the noise of SPL above 90 dB, does not permit correct evaluation of both the loudness of noise in question and its harmfulness.

2. Selected elements of the physiological principles of perception, used as the basis for the construction of the modified correction curves

The results of investigations of both the temporary (TTS) and the permanent threshold shift (PTS) can be useful in the estimation of noise hazard. Considering the effect of noise on creation of hearing loss apart from "the pathological" hearing loss" resulting from diseases, inflammations etc., the following assumptions should be taken into account.

(a) the sounds of such a low SPL that they do not cause the temporary threshold shift (TTS), do not lead to the permanent threshold shift in the form of occupational hearing loss — the effect of noise induced permanent threshold shift (NIPTS) [1, 6, 7];

(b) the values of hearing loss occurring in the audiogram of a person working under the conditions of noise hazard, are primarily affected by the following two factors: the character of the noise at a given work stand and the so called physiological hearing loss, i.e. the permanent threshold shift, depending on age [9, 12].

In [3] COHEN, ANTICAGLIA and CARPENTER gave three curves representing the temporary shift (TTS) resulting from the exposure to noise of the same SPL of 100 dB (A) but with different shape of the spectral envelope. The SPL of

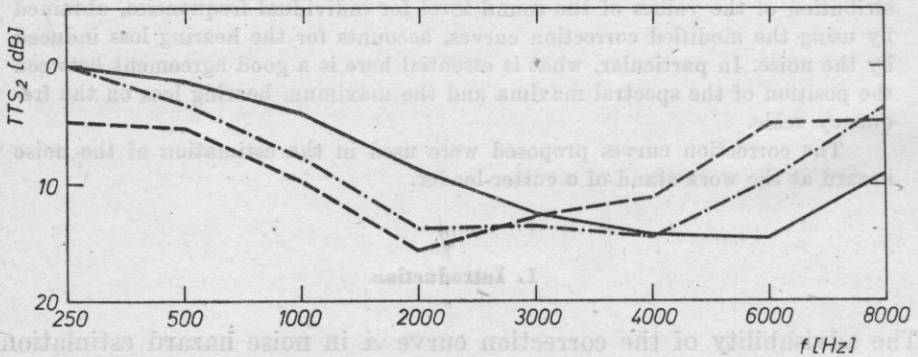

Fig. 1. The mean temporary threshold shift TTS_2 for noise of the same sound level, expressed in dB (A), but of different spectral envelope shapes [3]

"blue noise" — the inclination of the spectral envelope +6 dB/oct.; –·–·–·– "white noise" — the inclination of the spectral envelope O dB/oct.; – – – – – "pink noise" — the inclination of the spectral envelope — 6 dB/oct

100 dB (A) exposed for 30 minutes (based on the standard PN –70/B –02151) corresponds to the exposure to noise of less than 5 hours from the interval of the recommended mean permissible and the maximum permissible values. The above curves of the temporary threshold shift (TTS_2) were obtained 2 minutes after eliminating the source. It follows from analysis of Fig. 1 that the noise of the same SPL, expressed in dB (A), but of different spectral envelope shape, can cause temporay threshold shifts of different kinds, leading as a result to the permanent threshold shift. It is particulary interesting to note the shape of the curve (TTS_2) obtained for the case of white noise. It seems justified to define this curve as the basis of the estimation of the sensitivity of the hearing organ to the temporary threshold shift.

The permanent threshold shift (PTS) occurs not only as a result of harmful exposure of the organism to noise. Fig. 2 shows the curves of the audibility

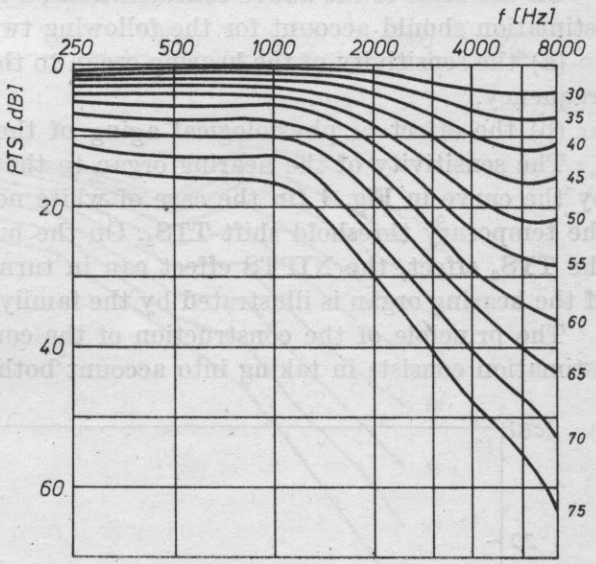

Fig. 2. The dependence of the permanent threshold shift on the frequency and the age of persons examined [3, 12]

threshold changing with age for persons who do not work in the conditions of noise hazard [9, 12]. In this case, therefore, the change in the threshold value of the SPL for components of different frequency is caused only by the physiological aging of the hearing organ. This fact seriously undermines the validity of the application of the curve *A* to the estimation of loudness, and to the estimation of its harmfulness. The concept of the curve of equal loudness is only valid in reference to the evaluation of the SPL of the individual spectral components by a person with normal hearing. In the case of noise loudness estimation by older persons or those with hearing loss (i.e. occupational hearing loss), the statement that the application of the correction curve *A* approximates the estimation of loudness, involves error. This results from the fact that there

is a relation between the loudness of estimated sounds and the value of the hearing loss [4].

Another fact should be mentioned here, namely that the estimation of the loudness of sounds perceived including noise depends on the previous exposure of the organism to noise. This effect is well-known in the literature and is defined as "the temporary loudness shift" (TLS). The dependence of the TLS effect on the physical parameters of stimulation and the conditions of the exposure of the organism to noise is the same as that of TTS. This is additional argument for the necessity of including the TTS effect in constructing the correction curves.

3. The method for the construction of the correction curves for noise hazard estimation

On the basis of the above considerations, a correction curve for noise hazard estimation should account for the following two basic elements:

(a) the sensitivity of the hearing organ to the hearing loss, depending on the frequency,

(b) the effect of physiological aging of the hearing organ.

The sensitivity of the hearing organ to the hearing loss is best represented by the curve in Fig. 1 (in the case of white noise), since this curve represents the temporary threshold shift TTS_2. On the basis of knowledge of the value of the TTS_2 effect, the NIPTS effect can in turn be predicted [7, 8]. The aging of the hearing organ is illustrated by the family of curves in Fig. 2.

The principle of the construction of the correction curves for noise hazard estimation consists in taking into account both these curves. The shape of the

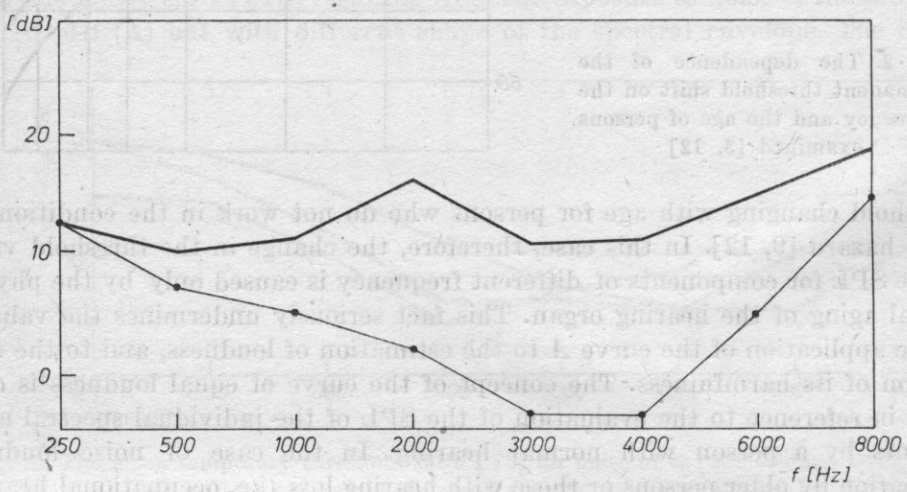

Fig. 3. The mean temporary threshold shift TTS_2: for white noise — the upper curve; the audiobility threshold — the lower curve

correction curve is related to the shape of the TTS_2 curve for the white noise (100 dB (A)). Since this curve is calculated with reference to "the audiometric zero" (cf. Fig. 1), in order to use it for the correction of noise spectrum the threshold values of the SPL (Fig. 3) should be added to the values of the temporary threshold shift. Since the threshold values of the SPL for given frequencies vary depending on the age of persons examined (cf. Fig. 2), it seems correct to introduce a family of correction curves whose parameter is the age of a person exposed to noise. For healthy persons with normal hearing (under 30 years of age) the shape of the correction curve reflects exactly the shape of the curve for the temporary threshold shift shown in Fig. 3. For older persons the shape of the correction curve changes, since it is necessary to include the corrections resulting from physiological aging of the hearing organ (cf. Fig. 2). The correction curves thus obtained for different age groups are reversed with respect to the value of 0 dB and are shown in Fig. 4.

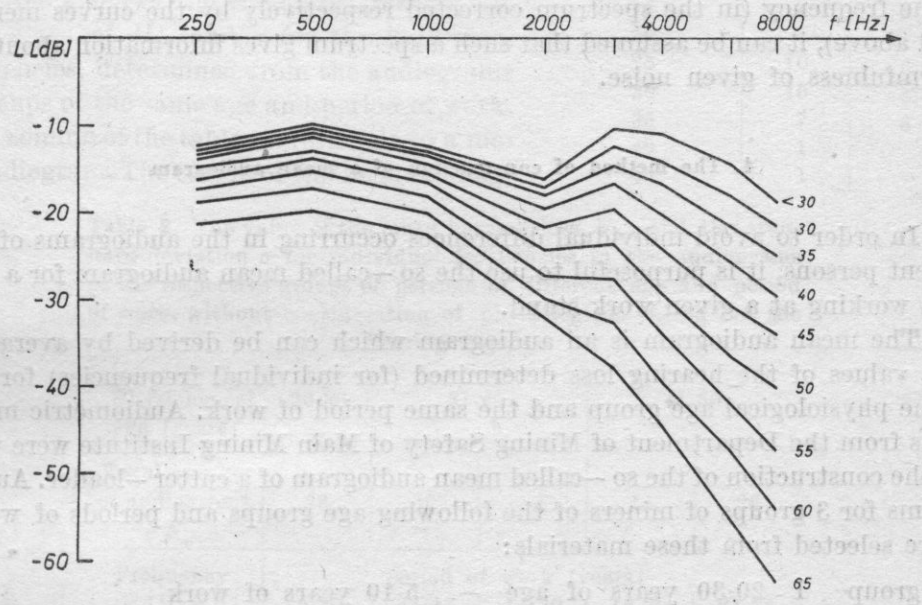

Fig. 4. The family of the correction curves proposed for noise hazard estimation. The parameter of these curves is the age of persons exposed to noise

For comparison, Fig. 5 shows the correction curve A and one of the correction curves proposed by the present authors (for persons under 30 years of age).

In order to estimate to what degree the correction curve proposed is better in the estimation of noise hazard than, for example, the correction curve A, it is necessary to compare the noise spectra corrected by these two curves with the noise induced permanent threshold shifts (NIPTS) occurring in the audiogram of a person exposed to this noise. If this comparison shows that, for exam-

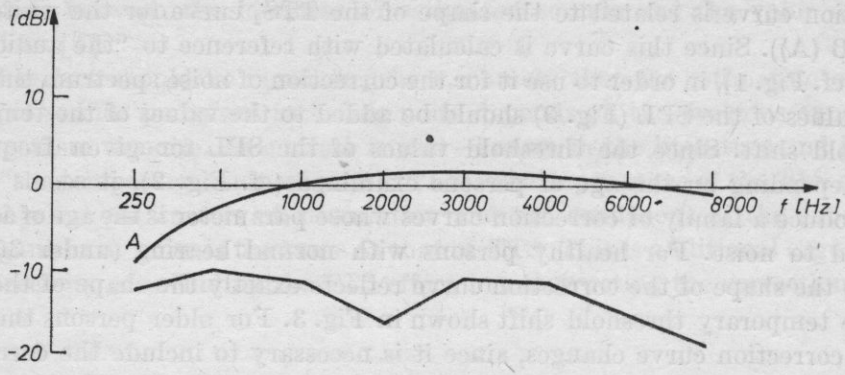

Fig. 5. The comparison of the curve A with the proposed correction curve

ple, the maximum hearing loss corresponds to the maximum noise levels at the same frequency (in the spectrum corrected respectively by the curves mentioned above), it can be assumed that such a spectrum gives information about the harmfulness of given noise.

4. The method of construction of a mean audiogram

In order to avoid individual differences occurring in the audiograms of different persons, it is purposeful to use the so—called mean audiogram for a person working at a given work stand.

The mean audiogram is an audiogram which can be derived by averaging the values of the hearing loss determined (for individual frequencies) for the same physiological age group and the same period of work. Audiometric materials from the Department of Mining Safety of Main Mining Institute were used in the construction of the so—called mean audiogram of a cutter—loader. Audiograms for 3 groups of miners of the following age groups and periods of works were selected from these materials:

group I 20-30 years of age — 5-10 years of work
group II 31-40 years of age — 11-15 years of work; 16-20 years of work
group III 41-50 years of age — 16-20 years of work; 21-25 years of work

The values of the threshold shift at the following 5 selected frequencies: 500, 1000, 2000, 4000 and 6000 Hz were taken into consideration. The values of the threshold shift for the above frequencies are assigned for a given group of miners of the same age, also with consideration of the period of work. As an example, Table 1 shows the data for a frequency of 500 Hz and group III for a cutter—loader's stand. On the basis of the distribution of the value of the

hearing loss for the individual groups of different periods of work the following data were calculated:

(a) the mean statistical threshold shift, i.e. the mean value of the hearing loss U_{av} for each group of persons with the same period of work, at a given frequency, obtained from audiograms,

$$U_{av} = \frac{\sum_{k=1}^{k=n} m_k x_k}{N},$$

where x is the mean value of the kth interval of the individual hearing loss, m is the number of persons with the hearing losses in the given interval k, and N is the total number of persons in a given group.

(b) the value of the standard deviation σ.

Table 2 shows the calculated results, i.e. the values of U_{av} and σ for the individual frequencies, determined from the audiograms of groups of the same age and period of work. Each column of the table corresponds to a mean audiogram. The curves of the mean audiog-

Table 1. The number of the hearing loss in the individual intervals k at a frequency of 500 Hz for a group of miners from 41 to 50 years of age working at a cutter-loader's stand

The value of hearing loss [dB]	Period of work [years]	
	16-20	21-25
5	1	
10	2	2
15	2	2
20	5	1
25	10	6
30	15	6
35	7	9
40	1	
45	1	

Table 2. The value of the mean hearing loss U_{av} and the standard deviation σ for individual frequencies in the audiograms of the respective groups of persons of different age and period of work, without consideration of physiological "aging" of the hearing organ

Physiological age [years]	20-30	31-40		41-50	
Total number of audiograms N	26	40	94	44	26
Frequency [Hz]	period of work [years] 5-10	11-15	16-20	16-20	21-25
500 U_{av}	27.31	25.75	26.54	26.93	27.50
σ	9.01	7.23	8.72	7.84	7.74
1000 U_{av}	17.11	16.62	17.34	18.52	18.65
σ	6.67	5.74	14.07	6.05	5.64
2000 U_{av}	16.54	17.00	17.97	21.36	17.11
σ	7.03	6.20	12.76	11.69	10.81
4000 U_{av}	18.84	20.00	26.65	30.79	36.90
σ	9.76	12.44	13.27	13.77	13.66
6000 U_{av}	20.00	25.87	28.67	30.34	35.00
σ	9.60	9.07	13.70	12.10	14.27

rams for the cutter–loader's stand are shown in Fig. 6. The average values of the hearing loss shown in Table 2 and Fig. 6 include both the noise induced hearing loss and the physiological permanent threshold shift related to the aging of the hearing organ.

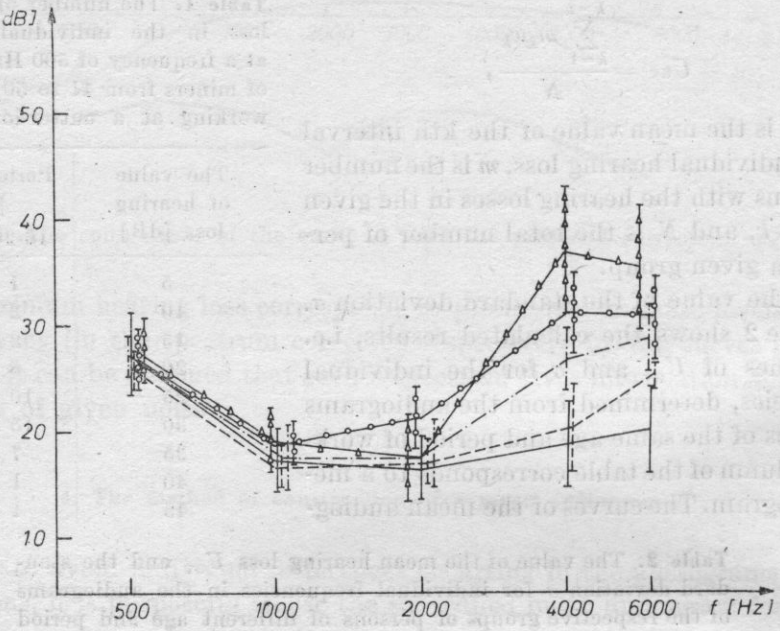

Fig. 6. The mean audiograms of cutter-loaders without consideration of the corrections concerning physiological "aging" of the hearing organ

—— 20-30 years of age, 5-10 years of work; – – – 31-40 years of age, 11-15 years of work; –.–.–. 31-40 years of age, 16-20 years of work; –o–o– 41-50 years of age, 16-20 years of work; –△–△–△– 41-50 years of age, 21-25 years of work

The confidence intervals were determined for the mean values of the hearing loss in the population for each frequency at a confidence level of 0.95. It was assumed in the determination of the confidence intervals in the case when the number of samples was $n > 30$ that the distribution of the mean of the sample was normal. For the group of 20-30 years of age and 41-50 years of age (the group of 21-25 years of work) the number of sample was $n = 26$. In these cases the confidence intervals were determined under the assumption that the sample distribution was a t-distribution [3]. The value of the confidence intervals are plotted in the diagram in Fig. 6. The values of these intervals are on average ± 3 dB. The minimum confidence interval is ± 1 dB, while the maximum one is ± 6 dB.

In order to avoid different values of the physiological permanent threshold shift for different ages the values shown in Table 2 should be corrected in terms of the curves for physiological aging of the hearing organ [9, 12]. Table 3 gives

Table 3. The value of the mean hearing loss U_{av} for individual frequencies in the audiograms for the respective groups of persons of different age and period of work, with consideration of the corrections for physiological aging of the hearing organ

Physiological aging [years]	20-30	31-40		40-50	
Total number of audiograms N	26	40	94	44	26
Frequency [Hz]	period of work [years]				
	5-10	11-15	16-20	16-20	21-25
500 U_{av}	27.31	24.75	25.54	23.33	24.50
1000 U_{av}	17.11	15.62	16.34	15.52	15.65
2000 U_{av}	16.54	15.00	15.97	15.86	11.61
4000 U_{av}	18.84	14.50	21.15	17.79	23.90
6000 U_{av}	20.00	18.87	21.67	14.34	19.00

the hearing loss corrected in terms of physiological age. The corresponding audiograms are shown in Fig. 7. The audiograms corrected in such a way permit comparison of the value of the hearing loss for persons of different physiological age.

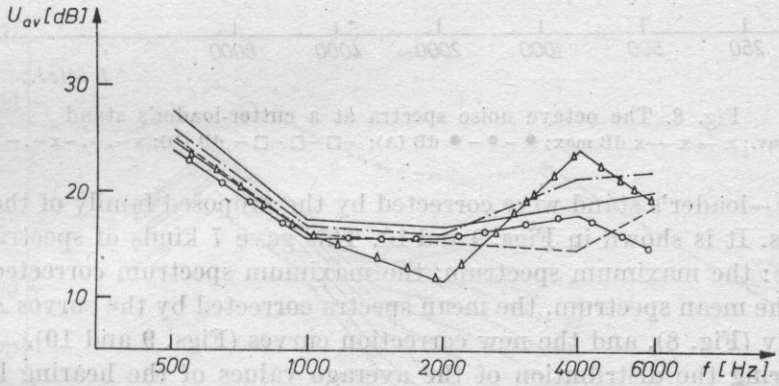

Fig. 7. The mean audiograms of cutter-loaders with consideration of physiological "aging" of the hearing organ

—— 20-30 years of age, 5-10 years of work; — — — 31-40 years of age, 11-15 years of work; —.—.— 31-40 years of age, 16-20 years of work; —o—o— 41-50 years of age, 16-20 years of work; — △ — △ — △ — 41-50 years of age, 21-25 years of work

5. The characteristic of noise at a given work stand

Using a 3347 Brüel and Kjaer Real—Time analyser, the noise at a cutter—loader's stand was analysed four times in order to give:

– the mean spectrum for the time period of 15 s,
– the maximum spectrum,
– the mean spectrum corrected by the curve A,
– the mean spectrum corrected by the curve D.

The above spectra refer to the form of octave spectra (Fig. 8). In addition the maximum spectrum obtained in this way was corrected by the curve A. It is shown in Fig. 8. The mean spectrum and the maximum spectrum of noise

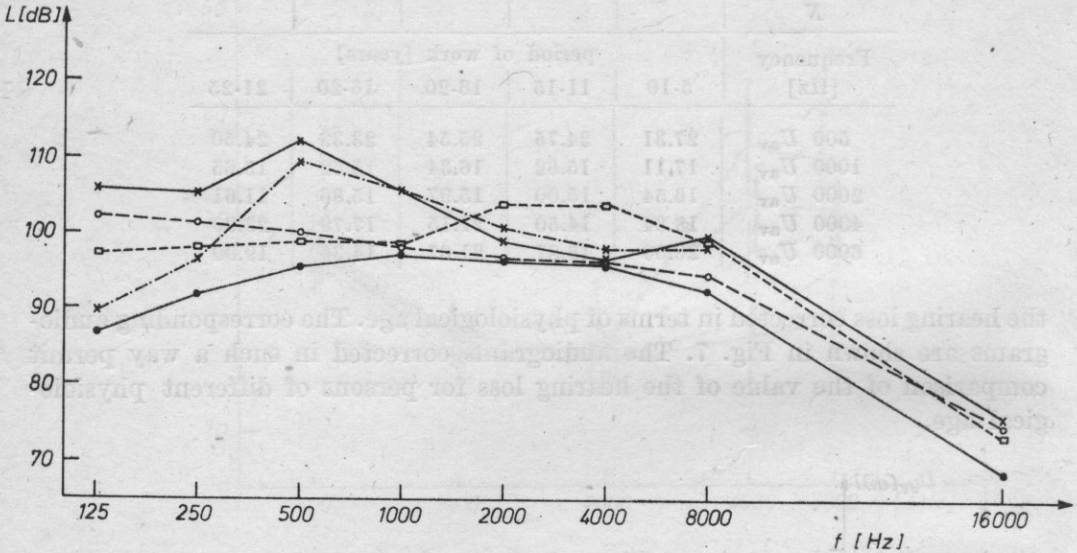

Fig. 8. The octave noise spectra at a cutter-loader's stand
–○–○– dB av.; x——x——x dB max; ●–●–● dB (A); –□–□–□– dB (D); x–.–.–x–.– dB (A)max

at a cutter –loader's stand were corrected by the proposed family of the correction curves. It is shown in Figs. 9 and 10. This gave 7 kinds of spectra for the same noise: the maximum spectrum, the maximum spectrum corrected by the curve A, the mean spectrum, the mean spectra corrected by the curves A and D, respectively (Fig. 8), and the new correction curves (Figs. 9 and 10).

Comparing the distribution of the average values of the hearing loss with the distribution of the values of the noise levels in the spectra corrected (7 forms of spectrum) we can notice some relations between the corresponding maximum and minimum values (i.e. the hearing loss and the noise levels) in these two diagrams.

6. Results

The following conclusions can be drawn from the comparison of the distribution of the average values of the hearing loss with the distribution of the values of the noise level in the noise spectra corrected:

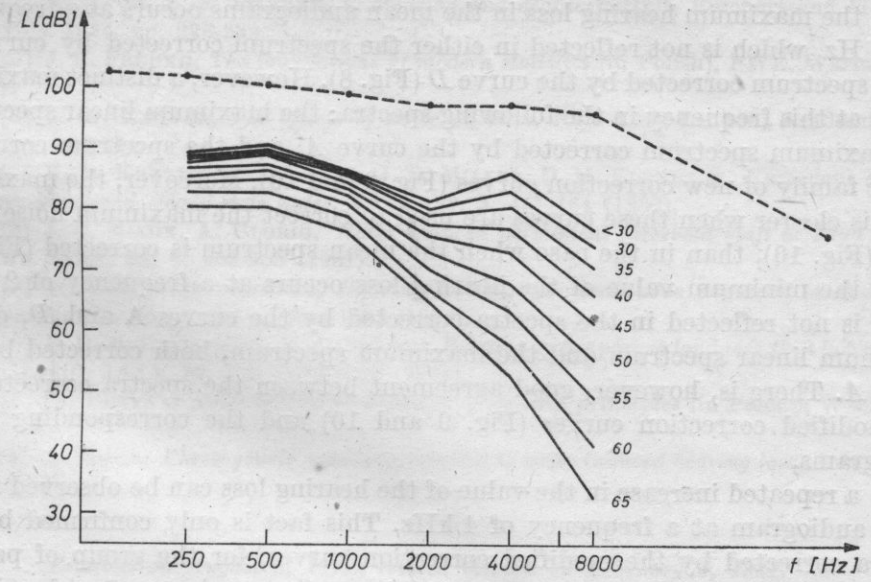

Fig. 9. The dashed curve — the mean octave of noise spectrum at a cutter-loader's stand, the continuous curves — the same spectrum corrected by the modified correction curves for different age

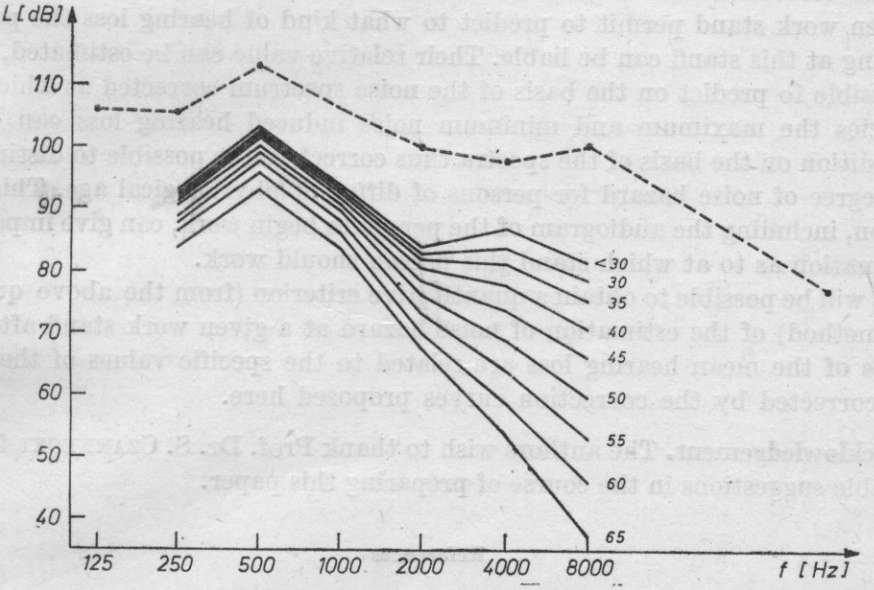

Fig. 10. The dashed curve — the maximum octave noise spectrum at a cutter-loader's stand, the continuous curves — the same spectrum corrected by the modified correction curves for different age

— the maximum hearing loss in the mean audiograms occurs at a frequency of 500 Hz, which is not reflected in either the spectrum corrected by curve *A*, or the spectrum corrected by the curve *D* (Fig. 8). However, a distinct maximum occurs at this frequency in the following spectra: the maximum linear spectrum, the maximum spectrum corrected by the curve *A*, and the spectrum corrected by the family of new correction curves (Fig. 9 and 10). Moreover, the maximum value is clearer when these curves are used to correct the maximum noise spectrum (Fig. 10), than in the case when the mean spectrum is corrected (Fig. 9).

— the minimum value of the hearing loss occurs at a frequency of 2 kHz, which is not reflected in the spectra corrected by the curves A and *D*, or the maximum linear spectrum and the maximum spectrum, both corrected by the curve *A*. There is, however, good agreement between the spectra corrected by the modified correction curves (Fig. 9 and 10) and the corresponding mean audiograms,

— a repeated increase in the value of the hearing loss can be observed in the mean audiogram at a frequency of 4 kHz. This fact is only confirmed by the spectra corrected by the modified correction curves, for the group of persons under 40 years of age. For persons above this age the maximum vanishes in the noise spectra corrected.

7. General conclusions

The correction curves used in the estimation of the spectrum of noise at a given work stand permit to predict to what kind of hearing loss the persons working at this stand can be liable. Their relative value can be estimated, i.e. it is possible to predict on the basis of the noise spectrum corrected at which frequencies the maximum and minimum noise induced hearing loss can occur. In addition on the basis of the spectra thus corrected it is possible to distinguish the degree of noise hazard for persons of different physiological age. This estimation, including the audiogram of the person to begin work, can give important information as to at which stand this person should work.

It will be possible to obtain a quantitative criterion (from the above qualitative method) of the estimation of noise hazard at a given work stand after the values of the mean hearing loss are related to the specific values of the noise evel corrected by the correction curves proposed here.

Acklowledgement. The authors wish to thank Prof. Dr. S. CZARNECKI for his valuable suggestions in the course of preparing this paper.

References

[1] J. H. BOTSFORD, *Theory of temporary threshold shift*, JASA, 49/2, 2, 440-446 (1971).

[2] P. V. BRÜEL, *Noise – Do we measure it correctly*, Naerum-Denmark 1975.

[3] A. COHEN, J. R. ANTICAGLIA, P. L. CARPENTER, *Temporary shift in hearing from exposure to different noise spectra at equal dB (A) level*, JASA, 51, 2, 503-507 (1972).

[4] H. DAVIS, S. R. SILVERMAN, *Hearing and deafness*, Holt, Rinehart and Winstron, New York 1974, pp. 226-232.

[5] J. E. FREUND, *The foundations of modern statistics* (in Polish), PWE, Warsaw 1971, p. 217.

[6] K. D. KRYTER, *The effects of noise on man*, New York-London, Academic Press 1970, pp. 140-144.

[7] K. D. KRYTER, W. D. WARD, J. D. MILLER, D. M. ELDREDGE, *Hazardous exposure to intermittent and steady-state noise*, JASA, **39**, 3, 451-464 (1966).

[8] J. C. NIXON, A. GLORIG, *Noise induced permanent threshold shift at 2000 Hz and 4000 Hz*, JASA, **33**, 7, 904-908 (1961).

[9] W. PASSCHIER-VERMEER, *Hearing loss due to continuous exposure to steady-state broad-band noise*, JASA, **56**, 5, 1585-1593 (1974).

[10] F. D. MCPHERSON, C. V. ANDERSON, *Relation of temporary loudness shift to temporary threshold shift*, JASA, **49**, 4/2, 1195-1202 (1971).

[11] Cz. PUZYNA, *Noise control in industry — general principles* (in Polish), WNT, Warsaw 1974.

[12] A. SPOOR, *Phresbycusis values in relation to noise induced hearing loss*, Int. Audiol., **6**, 52 (1967).

Received on August 1, 1979; revised version on February 4, 1981.

ARCHIVES OF ACOUSTICS
6, 3, 253-272 (1981)

INVESTIGATION OF DIRECTIONAL HEARING

CZESŁAW PUZYNA

Department of Acoustics, Central Institute of Occupational Safety
(00-348 Warszawa, ul. Tamka 1)

This paper presents the results of experimental investigations of the localization of the direction of sound signals. These investigations were performed in a purpose-built laboratory system equipped with 24 loudspeakers disposed in a horizontal plane around the person examined.

The results show that the external auditory canal has dominating influence on the efficiency of localizing signals at low frequencies, while the pinna has a prevailing effect at high frequencies. Application of ear plugs or ear muffs worsens the accuracy of the localization of sound sources in the frequency ranges mentioned above.

The optimum localization was obtained when the source of signals was in front of the person examined, the values of the sound pressure level were from 55 to 80 dB, and their frequency between 250-750 and 1500-3000 Hz. Since least errors in direction localization were committed for signals with large information content, i.e. natural signals, particularly an utterance, on this basis a general statement can be made, that the arrangement and structure of the human hearing organ is from the present point of view best adopted to human oral intercommunication.

1. Introduction

Localization of the sources of acoustic signals results from human ability of determining the distance and direction of the sources of these signals. Particularly, when there is a limited visibility in the place where the information is received, or the listeners are blind, the correct localization of the position of the acoustic sources is particularly important.

For those who can see the correct localization of acoustic signals is equally important, particularly under the industrial conditions, e.g. when the warning signal is emitted by a crane under load moving across the hall, the correct estimation of the direction of the signal may affect the safety of a worker, or in ge-

neral case when —because of the desired quick reaction of the receiver — the distinguishing and identification of the signal against the background of other acoustic signals is not sufficient, but it is very often necessary to localize its position in the environment.

2. Theoretical relations

Man is able to localize the direction of a source of acoustic signals because of his binaural hearing. It should be added here that the zygomatic width of the face which roughly corresponds to the distance D between both ears, is for the Polish adult population [3] on average 14.2 cm for men and 13.4 cm for women (the width of the head is 15.7 cm and 15.1 cm, respectively).

As regards relatively long sound waves, i.e. at a frequency f for which the half wavelength emitted by a sound source is much greater than the width (diameter) of the head, $\lambda/2 = c/2f = 17000/f \gg D$, the determination of the direction is based on the difference between the arrival times of the sound wave for two ears. It can be assumed as an approximation for given values of D that these waves have a frequency $f \ll 1100$ Hz. This case is shown schematically in Fig. 1a.

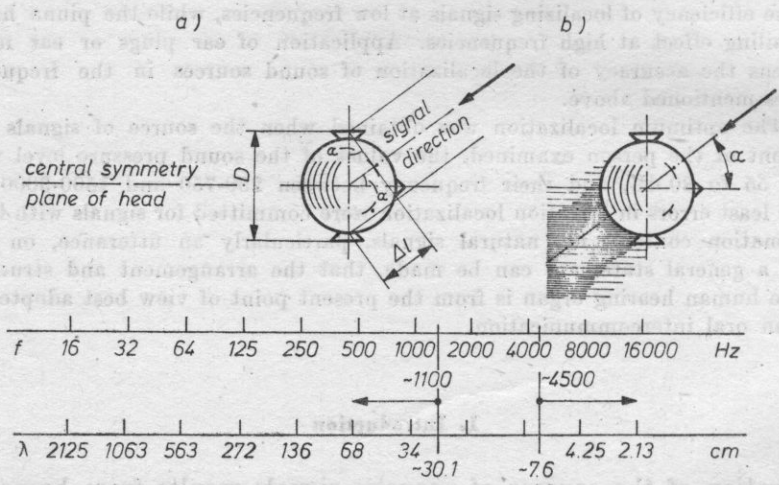

Fig. 1. A schematic diagram of the principle of human perception of acoustic signals at low and high frequencies

Since the human ear is sensitive to differences of the order $1\text{-}3 \cdot 10^{-5}$ s [7], and it can be seen from Fig. 1 that the arrival paths of the sound waves for two ears are proportional to $\sin\alpha$, the location of a sound signal in front or at the back of the head can accordingly be determined theoretically with an accuracy of 2-3°, and for sources on both sides with an accuracy of 10-15° [7].

For relatively short sound waves for which the ratio $D/\lambda \gg 2$, i.e. whose refraction around the barier is low (for the present head sizes these are the waves at a frequency $f \gg 4500$ Hz, approximately), the head constitutes a barrier behind which (cf. Fig. 1b) the "acoustic shade" occurs, and each ear receives the waves falling at some angle as an information signal of a different level [11]. The difference between these levels depends on the angle at which the wave falls, reaching its maximum value for $\alpha = 90°$.

For the sound waves of medium frequency ($1100 < f < 4500$ Hz), i.e. of a length that is approximately double the distance and half the distance between the ears, the determination of the direction of a source should therefore be more difficult from the theoretical point of view.

On the basis of the foregoing argument it can be predicted that the directional hearing characteristics of persons with normal hearing (particularly as far as equal hearing sensitivity of ears is concerned) will be symmetrical with respect

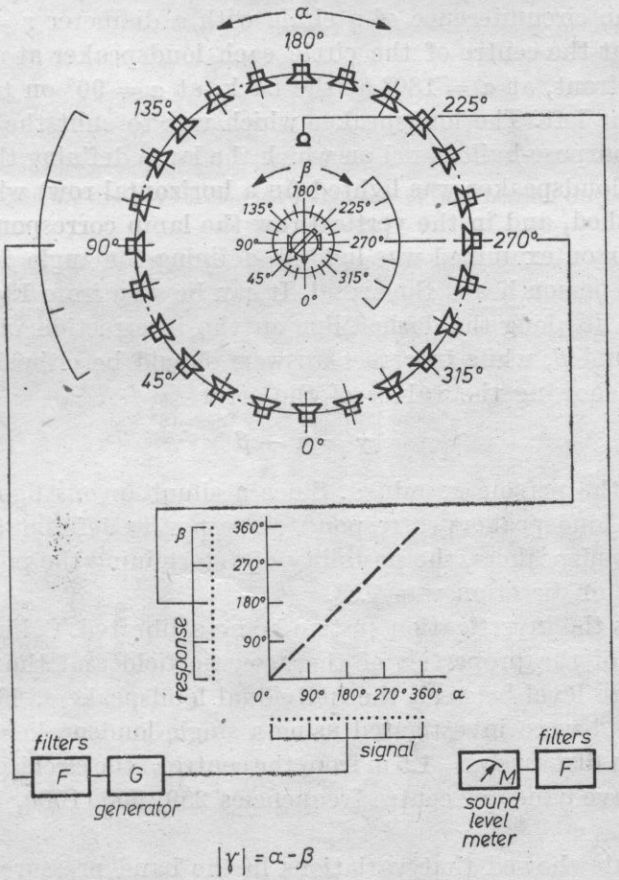

Fig. 2. A schematic diagram of the performance principle of the laboratory system used in the localization of acoustic signals

to the central plane of symmetry of the head, while the determination of the direction of sources of acoustic signals in this plane should be most difficult. Distinguishing between the positions of these sources, i.e. distinguishing between the positions at an angle in front and at the back upwards, will be facilitated by the pinna whose shape favours signals from the front.

3. Procedure

3.1. *Investigation system*

In order to check the validity of the relations discussed above, a series of experimental investigations were performed on a group of 6 persons with normal sight, in whom on the basis of audiometrical tests deviations in hearing from norm were found. These investigations were performed in a special laboratory room [9], well insulated with curtains (for 1000 Hz $\alpha_{QV} = 0.7$), in which (see the diagram in Fig. 2) 24 identical loudspeakers with a power of 0.8 W were placed along the circumference of a circle with a diameter $r = 1.5$ m, so that for the person at the centre of the circle each loudspeaker at an angle $\alpha = 0° = 360°$ was in front, at $\alpha = 180°$ at the back, at $\alpha = 90°$ on the right, and at $\alpha = 270°$ on the left. The loudspeaker which was to emit the signal was controlled from a purpose-built panel on which the lamp defining the angle α of the position of the loudspeaker was lighted (in a horizontal row) when the relevant button was pushed, and in the vertical row the lamp corresponding to the response of the person examined was lighted, defining the angle β of the direction from which the person heard the signal. It can be seen from Fig. 2 that correct answers should lie along the dashed line on the intersection of the corresponding angles α and β, while incorrect answers should be either above or below this line, thus showing the values of the error

$$\gamma = \alpha - \beta$$

committed by the person examined. Since a simultaneous lighting of the two lamps from the loudspeakers corresponds to responses defining the position between the two loudspeakers, the posibility of determining the position of a given signal in terms of direction was 7.5°.

Fig. 3 shows the investigation system being calibrated. Calibration consisted in verification of the properties of the acoustic field and the equality of the acoustic pressure level between the individual loudspeakers. The properties of the acoustic field were investigated using a single loudspeaker which was turned around at a distance $r = 1.5$ m from the centre of the circle, generating a noise signal in octave bands of centre frequencies 250, 500, 1000, 2000, 4000 and 8000 Hz.

Measurements showed that variations in the band pressure level measured at the centre of the circle were $\pm$ 3 dB for 250 Hz and $\pm$ 1.5 dB for 500 Hz, and were negligible for the other bands. This is related to the magnitude of the

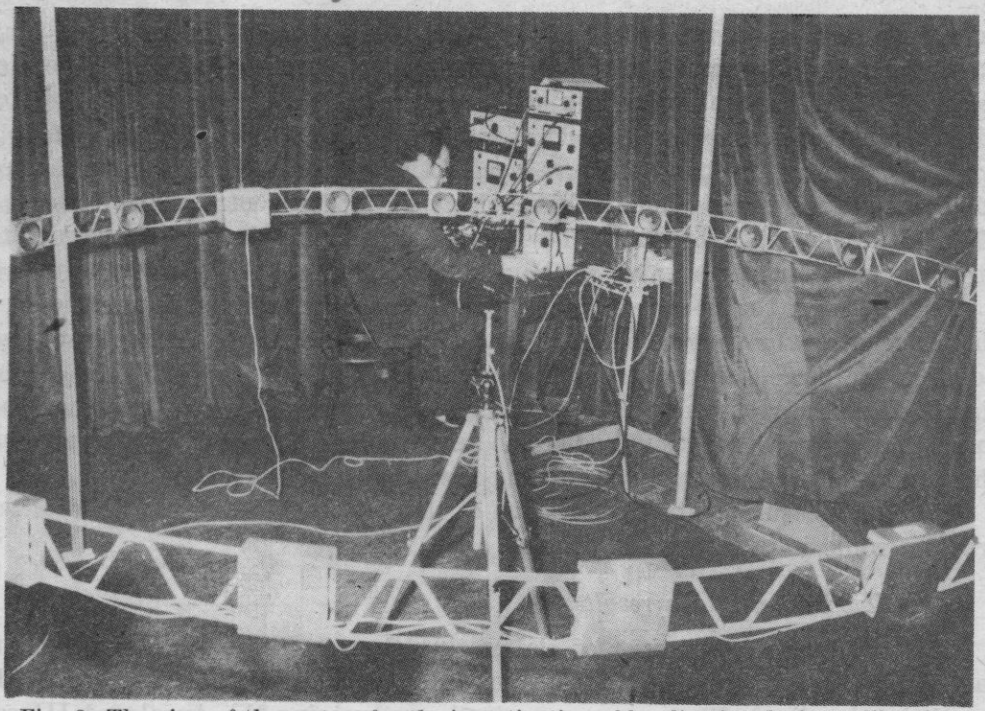

Fig. 3. The view of the system for the investigation of localization during calibration of this system

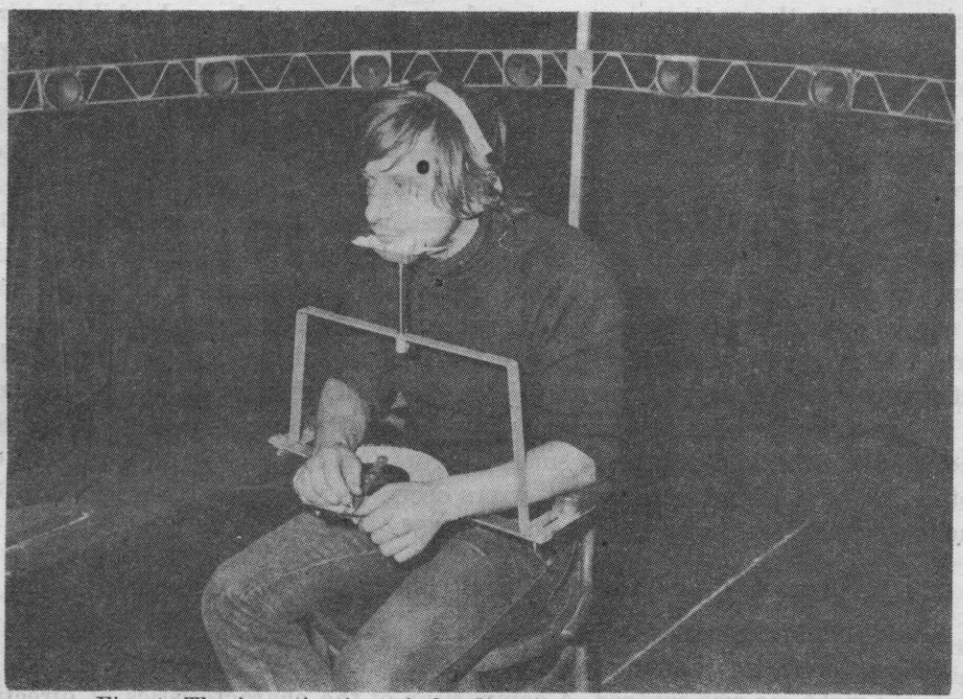

Fig. 4. The investigation of the directional hearing with ear muffs

boundary distance r_g which is 0.87 at a frequency of 2500 Hz and more than 1.5 at the other frequencies, which suggests that for signals at higher frequencies than 500 Hz the examined person at the centre of the circle is in free field of direct sound waves.

Verification of the band pressure level of the individual loudspeakers showed some differences in the value of the level to exist at the centre of the circle. These differences were reduced, however, by replacing the loudspeakers with greatest deviations, to a value of about $\pm$ 2 dB.

Fig. 4 shows the person examined wearing ear protectors. It can be seen that in front of the person there is a shield with an arrow which the person can point in the direction (corresponding to the angle β) from which he hears the signal. The chin rest whose elevation can be adjusted serves to keep the head in position over the rotation axis of the arrow and at the same time to prevent the head — often reflexively — turning towards the source of the signal.

In most measurements the duration of the signal which was to be localized was 3 s while its level was 60 dB (A).

3.2. *Elaboration of the results*

Fig. 5a shows the manner of elaborating the results of the measurements taken in the case when noise in an octave band with a centre frequency od 1000 Hz was being localized. The person examined was wearing the Auralgard III ear protectors on both ears. The curve in the upper part of Fig. 5a shows the results registered directly on the measurement sheet on the control panel, while the circles represent the responses of the person examined obtained for different directions. It can be seen from Fig. 5a that in the present case the sign changed for two angles, i.e. $\alpha' \cong 60°$ and $\alpha'' \cong 33°$, which signifies that with respect to the real location of the sound sources being localized the direction of errors committed moved from right to left and from left to right in terms of this location.

The curve at the centre of Fig. 5a shows the absolute values of errors committed, depending on the direction from which the signal was emitted, while the lower curve shows the directional characteristic of the localization of this signal. It can be seen from this figure that in agreement with expectations this characteristic is symmetrical with respect to the central axis (and, as is known, also with respect to the central plane [4]) of the head, showing for the conditions of the measurements large values of errors committed (up to $\gamma = 135°$) at the back of the head and relatively smaller errors (up to $\gamma = 45°$) in front and on both sides of the head. The lowest errors occurred for a location angle $\alpha = 60°$ and a symmetrically opposite angle $\alpha = 330°$.

3.3 *An example of application of the assumed procedure*

Similarly, Fig. 5b shows the results of measurements in which the shell of the ear protector was removed from the left ear of the person examined, while the right ear was covered. A comparison of the characteristics of directio-

nal localization for both ears covered (Fig. 5a) and for one ear covered (Fig. 5b) shows that baring one ear does not improve the efficiency of the localization at this side of the head, but also makes it worse at the back and at the opposite side. It can be seen from the curve in the upper part of Fig. 5b that in most cases the signal was estimated to be to the right of the real location, and it can be seen from the central curve that for the whole right side of the head (from $= 0°$ to $\alpha = 240°$) the values of error varied from 60° to 140°. The lowest error was also committed only at the left side of the head at an angle

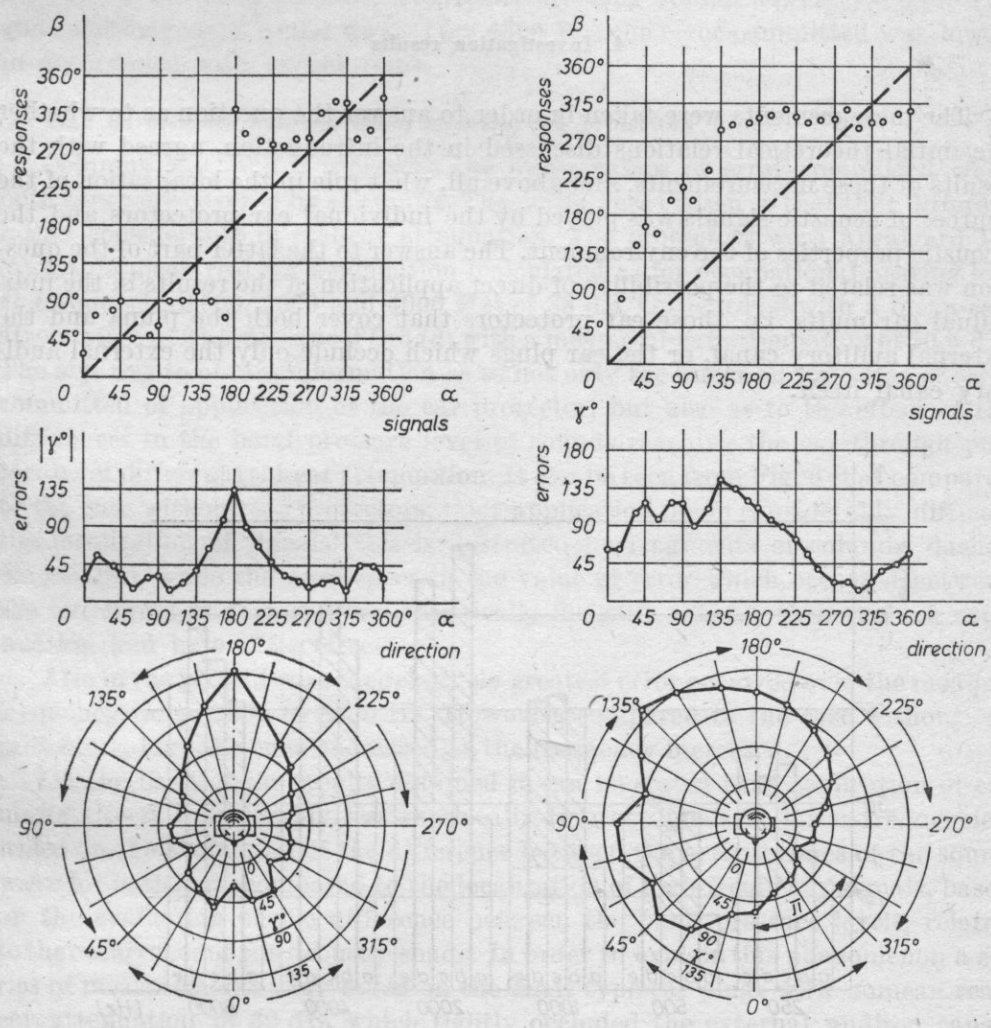

Fig. 5. The successive stages of elaboration of the measurement results; a) a symmetrical directional characteristic of error (both ears covered); b) nonsymmetrical (only the right ear covered)

$\alpha = 300°$; this angle also involved a change in the relative value of the committed errors, i.e. for a small section of the circle in front to the left side the sound source was estimated to be to the left of the real location.

Since the real-ear attenuation of most ear protectors used is similar in its nature to the audiograms of persons with occupational hearing impairment, the characteristics of directional localization in Fig. 5a, b show the difficulty of these persons in correct localization of the sources of acoustic signals, particularly in the case of one-ear defects.

4. Investigation results

The measurements were taken in order to answer the question as to whether the initial theoretical relations discussed in the introduction, agreed with the results of these measurements, and above all, what role in the localization of the sources of acoustic signals was played by the individual ear protectors and the acoustic properties of the environment. The answer to the latter part of the question was related to the possibility of direct application of the results in the individual ear muffs, i.e. those ear protectors that cover both the pinna and the external auditory canal, or the ear plugs which occlude only the external auditory canal itself.

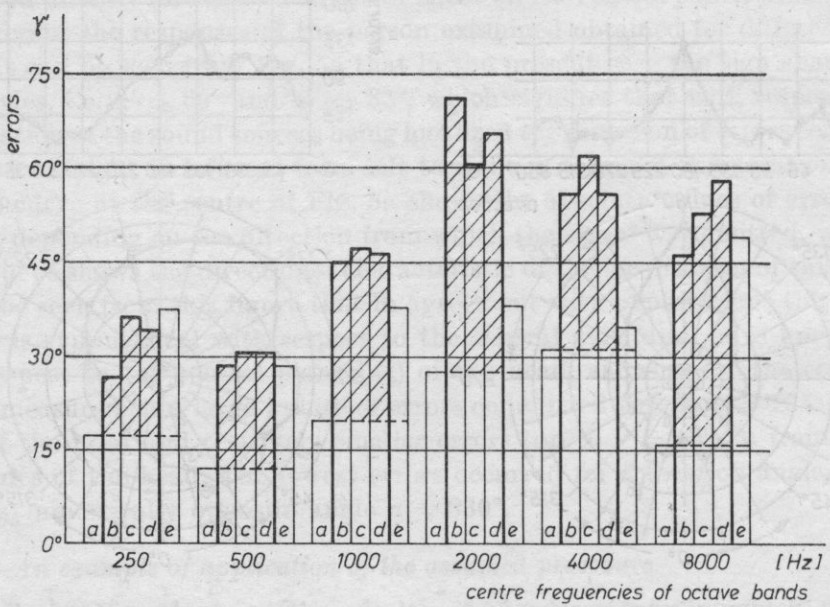

Fig. 6. The averaged values of error in the localization of sound signals at different frequency
a – without ear protectors, *b*, *c*, *d*, – with ear muffs of different real-ear attenuation, *e* – with ear plugs

Fig. 6 shows the results obtained in the form of columns whose height corresponds to the mean values of errors committed in the six groups corresponding to the individual frequencies of the signals used, calculated for 24 directions, i.e. in the course of 144 measurements.

Columns *a* correspond to the case when no protectors were used. It can be seen from Fig. 6 that in this case the relatively greatest error was committed for signals with centre frequencies of 2000 and 4000 Hz, i.e. over the medium frequency range ($1100 < f < 4500$ Hz) for which, in accordance with the theoretical relations discussed above, the localization of direction of the sound sources should be most difficult. For relatively long sound waves ($f < 1100$ Hz) and relatively short sound waves ($f > 4500$ Hz) the error committed was lower, in accordance with expectations.

4.1. *Directional hearing when wearing ear protectors*

Columns *b*, *c*, and *d* represent the mean values of error committed when both ears were covered by ear muffs. The muffs were chosen so that they different rather considerably in real-ear attenuation. The protectors were Auralgard III (*b*) with a mean real-ear attenuation (calculated as for occupational hearing loss at frequencies 1000, 2000 and 4000 Hz) of 38 dB, Optigard (*c*) with a mean-real attenuation of 24.5 dB, and TD-5 (*d*) with a mean real-ear attenuation of 30.5 dB. The aim was to obtain information as to not only the effect on the value of error committed of application of the ear protector, but also as to the effect of the differences in the band pressure level of sounds reaching the ear through protectors of different real-ear attenuation. It can be seen from Fig. 6 that compared to the case without ear protectors, their application made considerably difficult the localization of signals (this is ilustrated by fragments of columns dashed diagonally), while the differences in the value of error which occurred between the individual protectors were statistically insignificant, i.e. their real-ear attenuation had here little effect.

Also in the present case the relatively greatest error occurred over the medium frequency range 2000 to 4000 Hz. However, compared to the case without ear protectors, here the error increased as the frequency increased.

On the basis of the results obtained it can be stated that application of ear muffs affects considerably less the localization of signals at lower frequencies, based on the evaluation of the difference between the arrival times of the sound wave for both ears, compared to the localization of high-frequency signals, based on the evaluation of the difference between the band pressure levels, related to the occurrence of the acoustic shade. In order to explain this phenomenon a series of measurements were taken on the EAR type ear plugs with a mean real-ear attenuation of 32 dB, which tightly occluded the external auditor canal. Columns *e* in Fig. 6 represent the mean values of error committed when the above ear protectors were used. It can be seen from Fig. 6 that at low frequencies (250 and 500 Hz) the error committed is in terms of value close to the error

occurring when the ear muffs are used, while at medium frequencies (1000, 2000 and 4000 Hz) the value of error is lower and closer to that of the error for the uncovered ears. The result obtained permits the statement that occluding the external auditory canal makes difficult the localization based above all on the difference between the arrival times of sound waves for both ears, while it affects to a considerably lesser extent the estimation based on the difference between the band pressure levels.

The effect of high frequencies remains now to be explained. Is the difficulty in accurate localization of signals at high frequencies affected by covering the ear by the bowls of the ear muffs? In order to answer this question measurements were taken, during which the natural irregularities and cavities of the pinna in persons examined were filled with a special Stopper mass of properties close to those of smooth skin surface. In addition, in order to prevent the pinna sticking away from the head, it was pressed to the head by a special thin ring, thus leaving the external auditory canal open.

The results of the measurements taken in this manner and the results of the previous measurements are shown in Fig. 7 where the values of error committed are shown as a function of the frequency of a signal for eight selected characteristic directions of localization. In Fig. 7 the continuous lines represent the case

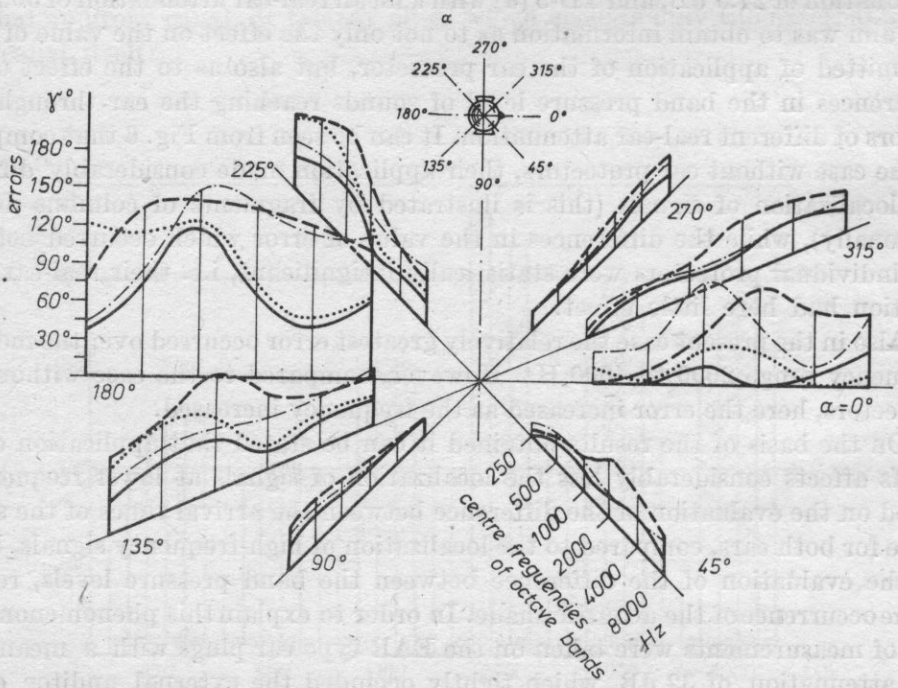

Fig. 7. The values of the error γ determined in a horizontal plane, depending on the frequency of sound signals and on the direction of their localization in the case without ear protectors ————————, with ear muffs — — —, with ear plugs —.—.—, with the pinna covered .....

without ear protectors, the dashed lines, the case with ear muffs, the point and dash lines the case when both external auditory canals were covered by ear plugs and the point lines the case when the pinna was covered. It can be seen from this figure that localization of signals at the back of the head ($\alpha = 180°$) is relatively most difficult, and easiest in front ($\alpha = 45\text{-}315°$); that application of ear muffs increases the error in all the presented directions to a relatively greatest extent in front of the head, and to the least extent on both sides ($\alpha = 90$ and $270°$); and that in most cases the localization of the sources of signals (both with and without ear protectors) is most difficult over the frequency range $1100 < f < 4500$ Hz. The difficulty in the localization of signals at lower and medium frequencies ($f < 1100$ Hz), which causes a considerable increase in error committed, results from limited reception of signals of that frequency in the external auditory canal, while the difficulty in the localization of signals at higher frequencies ($f > 4500$ Hz) — which is particularly conspicuous at the back of the head ($\alpha = 225\text{-}135°$) — results from the covering of the pinna. Since it is confirmed by the results of the measurements that the determination of the direction of signals in the central plane of the head (back-front) is most difficult, the pinna facilitates this localization by concentrating the sound waves reaching it from the environment and directing them in the form of reflections modelled by itself to the external auditory canal. It can be seen from Fig. 7 that this is the case at medium and high frequencies and above all in the space corresponding to the values of the angle α in the limits 90-270°, in front of the person examined.

The present results confirm the results of the investigations of the GARDNERS [4] who in order to explain the localizing effect of the pinna used a similar device made of identical loudspeakers placed in the central plane at a constant distance from the head of the person examined, but, contrary to the measurements described here (Figs. 2, 3 and 4), in a semicircle from the front upwards to the back of the head. By successively covering the individual cavities and irregularities of the pinna they showed that the pinna facilitates the localization of sound signals in front of the head, particularly over the high frequency range. According to these scientists the dashed columns in Fig. 8 represent the values of the index of error committed in reference to the group of small loudspeakers situated from the front upwards, while the columns not dashed refer to the loudspeakers placed downwards and backwards for the pinna with a different degree of covering. The index of 100 % applies to the case when the greatest error is committed in the determination of direction. It can be seen from Fig. 8 that largest differences in the value of this index occurred when the whole pinna was covered, and not covered in the case when high-frequency signals were used, i.e. in bands of 8 and 10 kHz. This result suggests that the pinna facilitates the localization of signals in the central plane of symmetry of the head, i.e. when it is most difficult from the theoretical point of view to determine the location of these signals, particularly over the high frequency range.

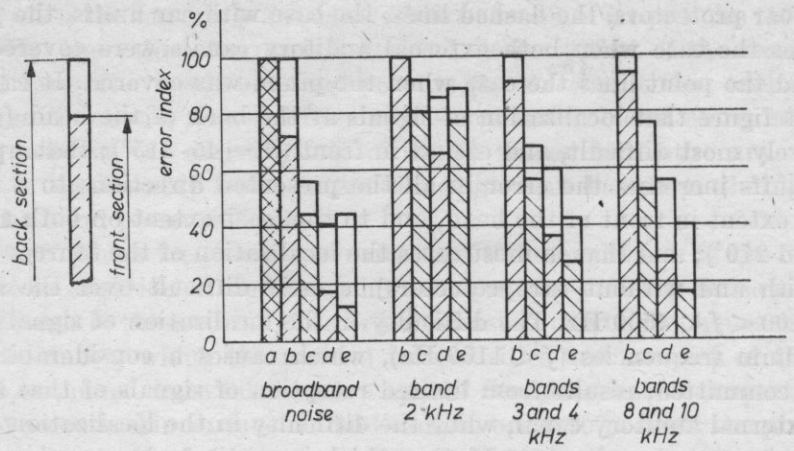

Fig. 8. The values of the index of the error committed in the central plane of the head, after the Gardners, depending on the degree of covering the pinna
with: *a* – the whole pinna covered, *b* – the navicular fossa, cavity and earlap covered, *c* – the navicular fossa and cavity covered, *d* – the cavity covered, *e* – uncovered

In conclusion, it can be stated that application of ear plugs can worsen the localization of sound signals at relatively low frequencies, while application of ear muffs (and also kerchiefs, caps and hairdoes which cover the ears) can worsen this localization in the case of sound signals at relatively high frequencies. For both cases this worsening also occurs over the medium frequency range ($1100 < f < 4500$ Hz) for ear muffs, irrespective of their real-ear attenuation. Therefore in the planning of warning signals these circumstances must be considered.

4.2. *The effect of the acoustic properties of the environment*

4.2.1. *The acoustic conditions* of the room. The measurements whose results were discussed above were taken in a damped laboratory room ($r_g > 1.5$ m), i.e. (for $f > 250$ Hz) under the conditions of the acoustic field close to free space. Under these conditions the values of error committed, calculated for 24 directions of observation, varied in the limits of $\gamma = 10\text{-}20°$. It can be seen from Fig. 9 (columns *a*) that the value of the error was $\gamma = 12.5°$ for the localization of tones at a frequency of 1000 Hz.

In order to examine the masking effect of the reflected sounds, a series of measurements were taken (in the manner discussed above) under the conditions of the acoustic field with greater diffusion, i.e. in a room of average acoustic properties ($r_g < 1$ m) – columns *b* and in a reverberation chamber ($r_g < 0.4$ m) – column *c*. It can be seen from Fig. 9 (columns not dashed *a*, *b* and *c*), that as a result of masking the information about the presence of a signal by reflected sounds the value of the error γ committed increases considerably with increasing diffusivity of the acoustic field, i.e. with decreasing boundary distance r_g.

Since, particularly in these cases, a prevailing role in the determination of the direction of a signal should be played by the beam of direct sound waves, i.e. the beam reaching the ears directly after a given signal has been switched in, a series of measurements were taken in order to confirm this relation. Columns *a* and *b* dashed diagonally in Fig. 9 define the value of the error γ committed when the moment of switching in a signal being localized was masked by another much louder signal. It can be seen from Fig. 9 that in a semi-anechoic laboratory room

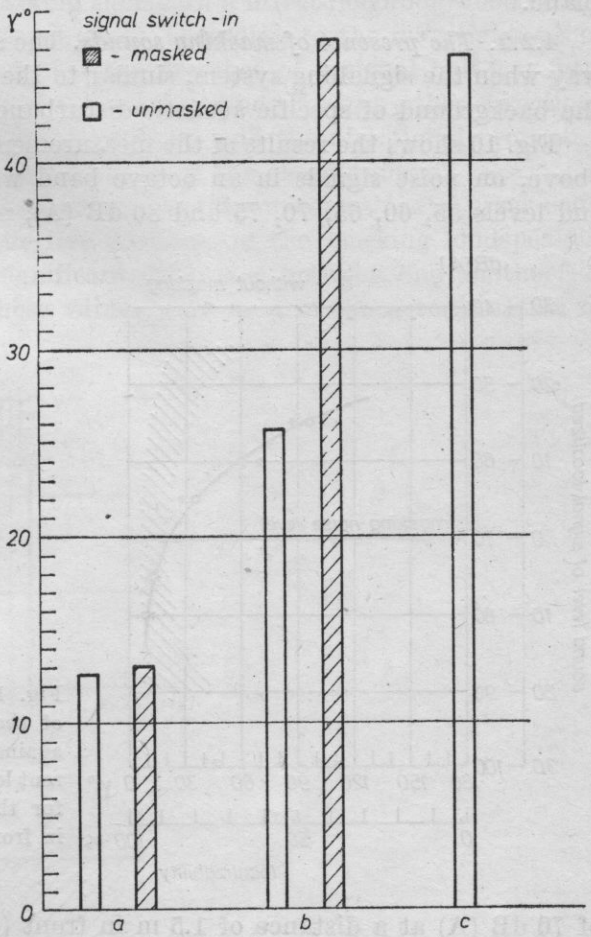

Fig. 9. The effect of the acoustic properties of the room and the contribution of direct waves from the sound wave localized on the value of the error γ
a – semi-anechoic laboratory room, *b* – room of average acoustic properties, *c* – reverberation chamber

(columns *a*), i.e. when the person examined is continuously in the field of direct sound waves, no significant increase in the error γ can be noticed. In a room of average acoustic properties (columns *b*), however, when the sound waves which are not disturbed with reach a given person only at the moment of switching in a signal, a considerable increase in the error occurs. This increase is close in its value to that of the error committed (without masking) in a reverberation chamber.

The acoustic properties of a room also affect the directional characteristic of signal localization. When the position of the person examined in a damped laboratory room with respect to the walls of the room had little effect on the above characteristic (irrespective of its position it was symmetrical to the central plane of the head), the diagonal position, with respect to the walls, of the person examined in a room of smaller absorption caused a fairly distinct rotation of the axis of symmetry of this characteristic with respect to the above plane.

4.2.2. *The presence of masking sounds.* The situation changes in a significant way when the signalling system, similar to the real conditions, operates against the background of specific acoustic disturbances.

Fig. 10 shows the results of the measurements taken in the manner described above, on noise signals in an octave band with a mid-frequency of 2000 Hz and levels 55, 60, 65, 70, 75 and 80 dB (A), masked by white noise at a level

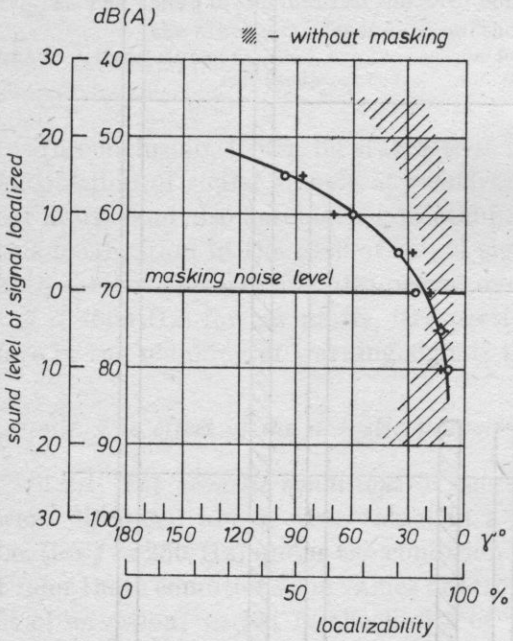

Fig. 10. The effect of masking on the value of the error committed in the localization against the noise of acoustic signals of different level. Circles denote the results obtained for the source of the masking signals placed in front, crosses for the case at the side of the person examined

of 70 dB (A) at a distance of 1.5 m in front (circles) and at the side (crosses) of the person examined. The curve in this figure was plotted against the area (dashed diagonally) corresponding to the case without masking. When it is assumed that an error of less than about 30° (corresponding to the localizability of more than about 85 %) can be admitted, in the present case an error of greater value was committed for signals of a level that was equal to or lower than the masking one. However, in the case without masking less error was committed at a level in the range 55-80 dB, i.e. for the range of human oral intercommunication.

In order to determine the effect of the direction of the source of a masking signal, the position of the loudspeaker generating these signals was changed from successively $\alpha = 0°$ (in front) to 45, 90° (on the right), 135 and 180° (at the back) of the examined person. The characteristic of the error in the localization of the masked signal was determined for each of the above positions in the case with masking and that without masking. It follows from the measurements taken that a distinct decrease in the error committed occurs for the direction corresponding to the position of the masking signal. In a direct neighbourhood of the masking direction the error increases, since, according to the investigations of HAAS [8], the persons examined indicate the presence of a signal half-way between the masking loudspeaker and the masked one. For the other directions the effect of the masking signal is less distinct, and the directional properties of hearing determine the resultant behaviour of the characteristic.

Since for both the described and other cases the mean values of error committed, calculated for each of the five positions of the masking loudspeaker, did not show any statistically significant difference between one another (at a significance level $\alpha = 0.01$), these values were used in the determination of

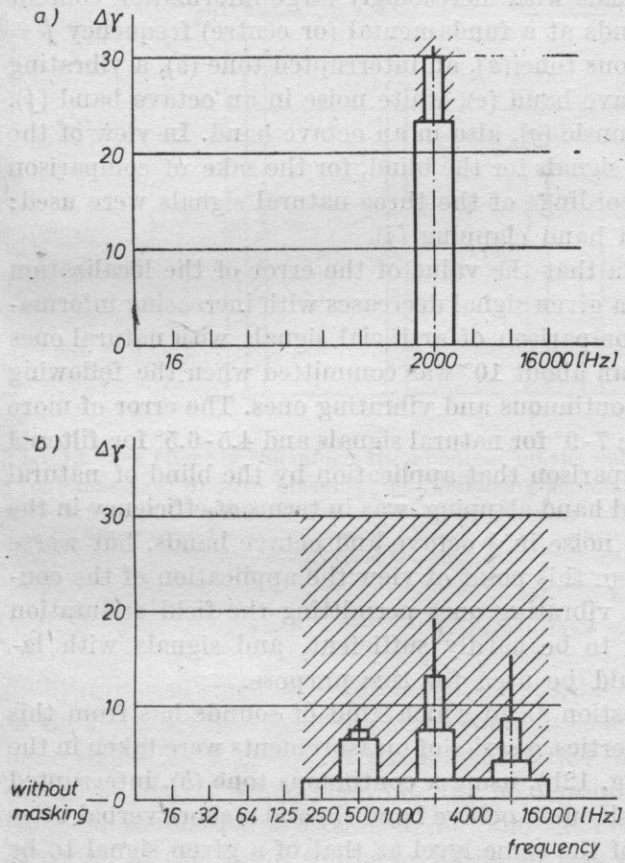

Fig. 11. The dependence of the increase in the mean error with masking and without masking on the bandwidth (the information content) of the masked signal
a) with masking by octave noise, b) with masking by broadband noise

the error committed in the localization of signals with bandwidth equal or narrower than the bandwidth of the masking signal. Fig. 11a shows the results of measurements in the case when the noise of octave width with a midfrequency of 2000 Hz (the area dashed diagonally) masked noise signals at the same frequency and the widths of octave, $\frac{1}{3}$ octave, and tone; Fig. 11b refers to a similar case when broadband noise masked (the area dashed diagonally) the broadband noise and for the noise of the widths of octave, $\frac{1}{3}$ octave and tone at frequencies 500, 2000 and 8000 Hz. It can be seen from Fig. 11 that the increase in the mean value of the error committed $\Delta\gamma$ (defined as the difference in the error between the case with masking and that without) are the greater the lower the information content of the masked signal.

4.2.3 *The effect of the information content of a signal.* The previous experiments used sound signals in the form of continuous tones or noise in $\frac{1}{3}$ octave bands or octave bands, i.e. signals with relatively low information content, which occur rather rarely in practice. In order to define the effect of the content in terms of a warning signal in the successive experiments (whose results are shown in Fig. 12), artificial signals with increasingly large information content were used. These were the sounds at a fundamental (or centre) frequency $f =$ $= 1000$ Hz; namely: a continuous tone (*a*), an interrupted tone (*b*), a vibrating tone (*c*), white noise in a $\frac{1}{3}$ octave band (*e*), white noise in an octave band (*f*), and a fragment of symphonic music (*g*), also in an octave band. In view of the possibility of using information signals for the blind, for the sake of comparison with the above sounds, the recordings of the three natural signals were used: stick tapping (*h*), steps (*i*) and hand clapping (*j*).

It can be seen from Fig. 12a that the value of the error of the localization of the position of the source of a given signal decreases with increasing information content of this signal. A comparison of artificial signals with natural ones shows that the error greater than about 10° was committed when the following tones were used: interrupted, continuous and vibrating ones. The error of more than 7° was committed for noise 7-9° for natural signals and 4.5-6.5° for filtered music. It follows from this comparison that application by the blind of natural signals; stick tapping, steps, and hand clapping, was in terms of efficiency in the orientation in space, similar to noise in $\frac{1}{3}$ octave and octave bands, but worse than that of filtered music. From this point of view the application of the continuous, interrupted tones and vibrating ones permitting the field orientation in space should be considered to be hardly sufficient, and signals with larger information content should be used for this purpose.

In order to answer the question as to which kind of sounds has from this point of view the optimum properties, a series of measurements were taken in the manner described above (cf. Fig. 12b), using a continuous tone (*b*), interrupted noise in an octave band (*i*), music in an octave band (*k*) and a short verbal utterance (*l*), masked by a signal of the same level as that of a given signal to be

localized. It can be seen from Fig. 12b that the least error was committed in the localization of the verbal utterance.

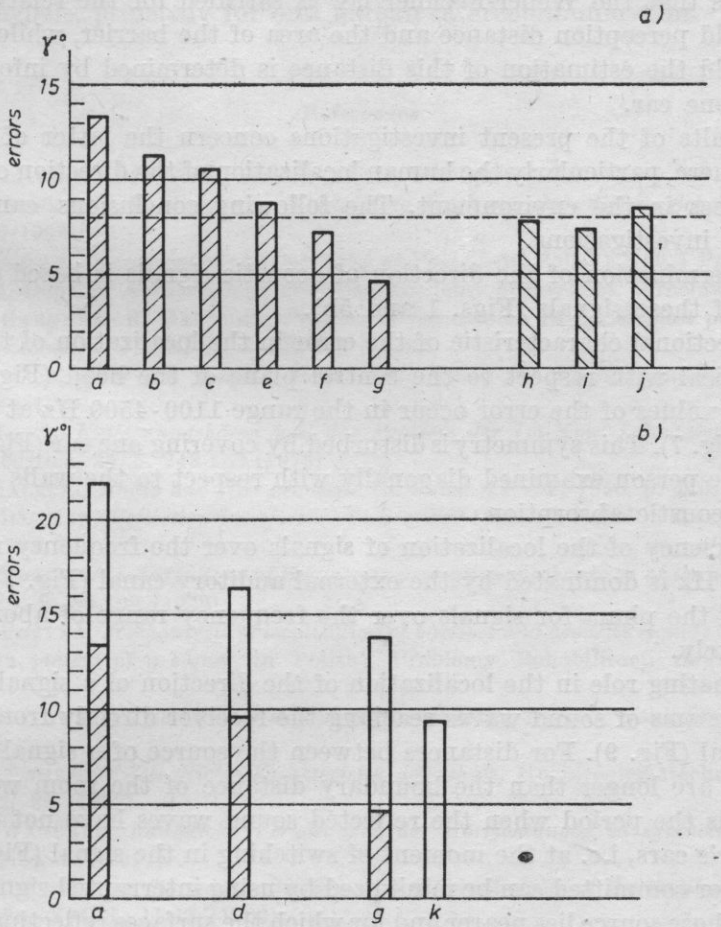

Fig. 12. The effect of the information content on the value of the error γ committed: a) without masking, b) with masking. The following signals were used in the investigations artificial signals: *a* – continuous tone, *b* – interrupted tone, *c* – vibrating tone, *d* – interrupted octave noise, *e* – 1/3 octave noise, *f* – octave noise, *g* – octave music; natural signals: *h* – stick tapping, *i* – steps, *j* – hand clapping, *k* – verbal utterance

5. Conclusions

In the case when it is difficult or impossible to use sight, a dominating role in the human orientation in the surrouding space is played by the audible acoustic signal. Two groups of phenomena based on slightly different mechanisms should be distinguished here, i.e., the perception and estimation of the distance from the sound source or the barrier, and the perception and localization of the direction of the sound source or barier in this space.

The results of the investigation of the former group of phenomena were discussed in reference [9]. On the basis of these investigations it was found among other things that the Weber-Fechner law is satisfied for the relation between the threshold perception distance and the area of the barrier, while in the free acoustic field the estimation of this distance is determined by information received by one ear.

The results of the present investigations concern the latter of the groups mentioned here, particularly the human localization of the direction of the sound signal sources in the environment. The following conclusions can be drawn from these investigations.

The determination of the direction of acoustic signals is based on binaural reception of these signals (Figs. 1 and 5b).

The directional characteristic of the error in the localization of these signals is symmetrical with respect to the central plane of the head (Fig. 5a), while the highest values of the error occur in the range 1100-4500 Hz at the back of the head (Fig. 7). This symmetry is disturbed by covering one ear (Fig. 5b) or positioning the person examined diagonally with respect to the walls of the room with low acoustic absorption.

The efficiency of the localization of signals over the frequency range below about 1500 Hz is dominated by the external auditory canal (Fig. 7), while it is affected by the pinna for signals over the frequency range of above 2000 Hz, approximately.

A dominating role in the localization of the direction of a signal localized is played by beams of sound waves reaching the receiver directly from the source of this signal (Fig. 9). For distances between the source of a signal and the receiver that are longer than the boundary distance of the room what is most important is the period when the reflected sound waves have not yet reached the receiver's ears, i.e. at the moment of switching in the signal (Fig. 9). In the case the error committed can be minimized by using interrupted signals and those signals whose source lies nearer and for which the surfaces reflecting the sounds are further away from where they are received.

In the acoustic field conditions close to free space the localization of the source of the masking signal had little significant effect on the mean value of the error in the localization of the source of the signal masked. This effect is found, however, when the ratio between the information content of the signal masked and that of the masking signal was changed. The higher the ratio was in a given case the higher the error committed (Fig. 10).

Since the optimum conditions of localization of acoustic signals were achieved when the source of these signals was in front of the person examined (Fig. 7), the value of the level of these signals varied over the range 55-80 dB (Fig. 10), their frequency (for $\alpha = 45\text{-}315°$) over the ranges 250-750 and 1500-3000 Hz (Figs. 6 and 7), and the lowest error was commited in the localization of a verbal utterance (Fig. 12), therefore on this basis it can be generally stated that the

arrangement and structure of the human hearing organ are well formed and fitted for the reception of information reaching the listener from the front in the form of natural signals, primarily for oral human intercommunication.

References

[1] J. BLAUERT, *Räumliches Hören*, Hirzel, Stuttgart 1974.

[2] W. BURGTORF, B. WAGENER, *Verdeckung durch subjektiv diffuse Schallfelder*, Acustica, **19** (1967/1968).

[3] S. GÓRNY, *Antropometric photography of Poland* (in Polish) Mat. i Prace Antropometryczne, 84, Dept. of Anthropology of Polish Academy of Sciences, Wrocław 1972.

[4] M. GARDNER, R. GARDNER, *Problem of localization in the median plane: effect of pinnae cavity occlusion*, JASA, **53**, 2 400-408 (1973).

[5] H. HAAS, *Über den Einfluss eines Einfachechos für die Hörsamkeit von Sprache*, Acustica, **1**, 49 (1951).

[6] P. LAWS, *Entfernungshören und das Problem der Im-Kopf-Lokalisiertheit von Hereignissen*, Acustica, **29**, 5, 243-259 (1973).

[7] I. MALECKI, *Radio and film acoustics* (in Polish), PWT, 1950, p. 440.

[8] S. MISZCZAK, *Reflection interference in bounded space* (in Polish), Zeszyty Naukowe COBR-TRV, 293, 1977.

[9] Cz. PUZYNA, *Investigations of the barrier perception mechanisms of the blind*, Archives of Acoustics, **4**, 2, 89-108 (1979).

[10] Cz. PUZYNA, *Mechanisms of localization of barriers and acoustic signals by the blind — the information content of a signal* (in Polish), Problemy Rehabilitacji Zawodowej, 1981 (in press).

[11] M. RAJEWSKI, *Two-channel sterophony* (in Polish), Zeszyty Naukowe CNPT RTV, Warsaw 1980.

[12] W. SCHIRMER, *Die Richtecharakteristik des Ohres*, Hochfrequenztechnik und Electroakustik, **72**, 39 (1963).

[13] B. WAGENER, *Räumliche Verteilungen der Horrichtungen in synthetischen*, Schallfeldern, Acustica, **25** (1971).

[14] A. ZAKRZEWSKI, *Sound localization with different states of the vestibule* (in Polish), Otolaryngologia, **XVI**, 1, 11-15 (1962).

Received on March 18, 1980; revised version on February 12, 1981.

ARCHIVES OF ACOUSTICS
6, 3, 237-285 (1981)

APPROXIMATE METHODS FOR THE SOLUTION OF THE EQUATION OF ACOUSTIC WAVE PROPAGATION IN HORNS

TOMASZ ZAMORSKI, ROMAN WYRZYKOWSKI

Institute of Physics, Higher Pedagogical School
(33-310 Rzeszów, ul. Rejtana 16 A)

In practice, there are acoustic horns designed for which the equation of wave propagation has no exact solution of compact form. The need, therefore, arises for approximate solutions to be used. Accordingly, this investigation sought optimum methods for an approximate solution of the wave equation of a horn. It was assumed that the optimum method should combine the requirement of relatively little time-consuming calculation and the possibility of physical interpretation of the approximate formulae obtained. It was found that the WKB approximation which is recommended in the literature and has been taken directly from quantum mechanics, in general does not satisfy these requirements, and in addition it cannot be used at all in some cases. Therefore, another two approximate methods were developed and their properties analyzed.

1. Introduction

Acoustic wave propagation in horns is described by the well-known Webster equation derived under the assumption of the existence of a plane, harmonic wave that propagates without energy losess [5-9, 11, 15]. This equation, written in the so-called reduced form [1] using the dimensionless variables, is

$$\frac{d^2F}{da^2} + [\mu^2 - V_{(a)}]F = 0, \tag{1}$$

where F is a function defined by the sound pressure p and the cross-section area of the horn S by the formula [12];

$$F = p\sqrt{S}, \tag{2}$$

and a is the so-called dimensionless abscissa. When the axis of abscissae is the geometrical axis of the horn, a can be expressed by the formula [12]

$$a = \frac{x}{x_0}, \tag{3}$$

where x_0 is the coefficient of the divergence of the walls of the horn. The quantity μ is dimensionless frequency defined as the quotient of the absolute frequency and of a constant f_0 [4]

$$\mu = \frac{f}{f_0}, \tag{4}$$

and $f_0 = c/2\pi x_0$, where c is the adiabatic wave propagation velocity. The function $V_{(a)}$ depends on the geometry of the horn and can be given by the so-called dimensionless cross-section radius of the horn ϱ by the formula

$$V_{(a)} = \frac{1}{\varrho}\frac{d^2\varrho}{da^2}, \tag{5}$$

and ϱ can be defined as [12]

$$\varrho = \sqrt{\frac{S}{S_0}}, \tag{6}$$

where S_0 is the cross-section area at the in tlet of the horn.

The solution of equation (1) can be presented in the form [12]

$$F = A\exp^{\pm i\Theta}, \tag{7}$$

where i is an imaginary unit and A and Θ are functions of the variable a satisfying the equations [11, 12]

$$\mu^2 - V_{(a)} + \frac{A''}{A} - \Theta'^2 = 0, \tag{8}$$

$$\frac{2A'}{A} + \frac{\Theta''}{\Theta'} = 0. \tag{9}$$

The dashes in formulae (8) and (9) denote differentiation with respect to the dimensionless abscissa a.

As a final result of considerations based on the reduced form of the Webster equation (1) a general formula for the relative unit admittance of the horn β can be derived [12]

$$\beta = -\frac{i}{\mu}\left(\frac{F'}{F} - \frac{\varrho'}{\varrho}\right). \tag{10}$$

The horns most often considered in the literature were those for which the exact solution of equations (8) and (9) could be achieved. When these equations were to be solved in an approximate manner, however, the approximation known in quantum mechanics was recommended, particulary the WKB (Wentzel, Kramers, Brillouin) method [1, 3, 9, 10]. This resulted from the formal similarity of equation (1) to the onedimensional Schrödinger equation independent of time.

However, the approximate methods used so far in the theory of horns for the solution of equation (1) most often lead to rather tedious calculations possible only when a computer was used and gave so complex approximate formulae that they were hardly useful in physical interpretation. The aim of the present investigation was to find more optimum approximate methods which combine little time-consuming calculations with the requirements of physical interpretation of expressions derived.

2. Discussion of the range of applicability of the WKB method in the theory of horns

The conditions and the range of applicability of the WKB approximation in the theory of horns have to be analysed for two reasons. Firstly, as was mentioned in section 1, the WKB method is recommended for approximate solution of the Webster equation in almost every paper on those horns for which the wave equation has no exact solution [1, 3, 9, 10]. Secondly, in the present paper this method will be a starting point for development of more optimum approximation methods.

In the WKB approximation the approximate solution of equation (1) has the form of (7), and A must be a slowly variable function of a. The requirement of slow variation of $A_{(a)}$ permits the assumption that $A'' \cong 0$, and accordingly equation (8) can be simplified to the form

$$\Theta'^2 = K^2, \tag{11}$$

where the quantity K^2 depends on the frequency and the geometry of the horn

$$K^2 = \mu - V_{(a)}. \tag{12}$$

It follows from (11) that

$$\Theta = \int_{a_0}^{a} K d\bar{a}, \tag{13}$$

where the variation range of the integration limits is restricted by the length of the horn.

Moreover, equation (9) can be integrated directly, thus giving

$$A^2\Theta' = C^2, \tag{14}$$

where the constant C is independent of a and can be only a function of the dimensionless frequency μ.

Consideration of relation (11) in (14) gives

$$A = \frac{C}{\sqrt{K}}. \tag{15}$$

Expression (15) shows that the requirement of slow variation of $A_{(\alpha)}$ is closely related to the requirement of slow variation of $K_{(\alpha)}$. Thus, according to the definition of K (cf. formula (12)) it can be stated that the WKB method can be used at those frequencies and for horns of such geometry for which $K_{(\alpha)}$ is a slowly variable function.

In the case when $K^2 > 0$, from (7), (13) and (15) the solution of the wave equation (1) can be written for the slowly variable function $K_{(\alpha)}$, in the form

$$F = \frac{C_1}{\sqrt{K}} \exp i \left(\int_{a_0}^{a} K d\bar{a} \right) + \frac{C_2}{\sqrt{K}} \exp \left(-i \int_{a_0}^{a} K d\bar{a} \right). \tag{16}$$

In the case, however, when $K^2 < 0$, K is imaginary and formula (16) takes the form

$$F = \frac{C_3}{\sqrt{\chi}} \exp \left(\int_{a_0}^{a} \chi d\bar{a} \right) + \frac{C_4}{\sqrt{\chi}} \exp \left(- \int_{a_0}^{a} \chi d\bar{a} \right), \tag{17}$$

where

$$K = -i\chi. \tag{18}$$

After conversion it can be stated that a differential equation of the second order satisfied exactly by the solutions of (16) and (17) has the form

$$F'' + \left[K^2 - \frac{3}{4} \left(\frac{K'}{K} \right)^2 + \frac{1}{2} \frac{K''}{K} \right] F = 0. \tag{19}$$

Comparison of (19) with (1) (with consideration of formula (12)) shows that the equation satisfied exactly by the approximate solution is different from the reduced wave equation of a horn by the term

$$\Delta = \frac{3}{4} \left(\frac{K'}{K} \right)^2 - \frac{1}{2} \frac{K''}{K}, \tag{20}$$

and this term is subtracted from K^2. This discovery suggests the subsequent approximation in which Δ should be included as a correction, and that equation (11) should have the following form

$$\Theta' = \left[K^2 + \frac{3}{4} \left(\frac{K'}{K} \right)^2 - \frac{1}{2} \frac{K''}{K} \right]^{1/2}. \tag{21}$$

This leads, however, to considerable complexity of the subsequent formulae.

Expressions (16) and (17) can permit good approximation, however, when the quantity Δ is small compared to K^2. This remark permits quantitative formulation of the application condition of the WKB approximation

$$|\gamma| = \left| \frac{\frac{3}{4} \left(\frac{K'}{K} \right)^2 - \frac{1}{2} \frac{K''}{K}}{K^2} \right| \ll 1. \tag{22}$$

On the basis of the foregoing argument in can be stated that in the case of a horn (or a family of horns) of specific shape the usefulness of the WKB method should be determined by the analysis of the function $K_{(\alpha)}$, complemented by examination of condition (22). When this analysis shows that the function $K_{(\alpha)}$ does not satisfy the requirement of slow variation, the WKB method is inefficient, even when using very time-consuming approximations (cf. formula (21)). Accordingly, the next section will give another method for approximate solution of the wave equation (1), which can be used successfully in this case, and which to the authors' knowledge has not been used to date.

3. A method of linear approximation of the function $V_{(\alpha)}$

It follows from formula (12) that the function $K_{(\alpha)}$ for a given frequency μ, is determined by the function $V_{(\alpha)}$ containing information about the geometry of the horn (cf. formulae (5) and (6)). The approach proposed in this section, consists in approximation of the function $V_{(\alpha)}$ by a broken line. In this case the horn is considered to be a multi-element one, where each element corresponds to one section of the broken line. The number of sections depends on the desired accuracy of approximation. It is interesting to note here that for horns used in practice the function $V_{(\alpha)}$ behaves so regularly that the desired accuracy of approximation can be achieved for a small number of sections of the broken line.

Let us assume, as an example, that the function $V_{(\alpha)}$ has the form as in Fig. 1 and was approximated by a broken line of n sections, where $n = 1, 2, 3, \ldots, N$.

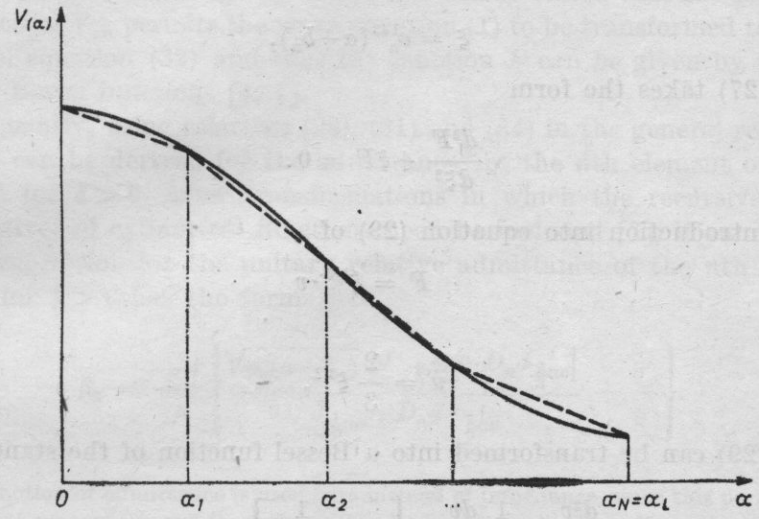

Fig. 1. The approximation of the function $V_{(\alpha)}$ by a broken line consisting of N sections

One can consider the section corresponding to an arbitrary nth section of the horn contained between the points a_{n-1} and a_n. The function $V_{(a)}$ can be approximated over this section by a linear function of the form

$$V_{(a)} = V_{(a_{n-1})} - c_n a, \tag{23}$$

where c_n is the coefficient of directivity of the line. It can be given by the formula

$$c_n = \frac{V_{(a_{n-1})} - V_{(a_n)}}{a_n - a_{n-1}}. \tag{24}$$

After consideration of (23) the reduced wave equation (1) for $a \in [a_{n-1}, a_n]$ takes the form

$$F'' + [\mu^2 - V_{(a_{n-1})} + c_n a] F = 0. \tag{25}$$

Introduction of the abbreviation

$$b_n = \frac{\mu^2 - V_{(a_{n-1})}}{c_n} \tag{26}$$

permits equation (25) to be written in the following form

$$F'' + c_n (a + b_n) F = 0. \tag{27}$$

One can first consider the case $\mu^2 > V_{(a_{n-1})}$, i.e. when the quantity b_n is positive. In this case equation (27) can by way of successive transformations be reduced to the form of a Bessel equation.

After the insertion

$$\xi = c_n^{1/3} (a + b_n), \tag{28}$$

equation (27) takes the form

$$\frac{d^2 F}{d\xi^2} + \xi F = 0. \tag{29}$$

After introduction into equation (29) of

$$F = \xi^{1/2} \cdot v \tag{30}$$

and

$$u = \frac{2}{3} \xi^{3/2}, \tag{31}$$

equation (29) can be transformed into a Bessel function of the standard form

$$\frac{d^2 v}{du^2} + \frac{1}{u} \frac{dv}{du} + \left[1 - \frac{1}{(3u)^2}\right] v = 0. \tag{32}$$

The solution of this equation is Bessel functions of order $\frac{1}{3}$ [4, 7]

$$v = A_n J_{\frac{1}{3}(u)} + B_n J_{-\frac{1}{3}(u)}, \tag{33}$$

where A_n and B_n are constants.

Consideration of formulae (30), (31) and (33) gives

$$F = \xi^{1/2}\left[A_n J_{\frac{1}{3}\left(\frac{2}{3}\xi^{3/2}\right)} + B_n J_{-\frac{1}{3}\left(\frac{2}{3}\xi^{3/2}\right)}\right]. \tag{34}$$

It can now be demonstrated that the solution of (34) for $b_n > 0$ can also be obtained for $b_n < 0$.

It follows from formula (28) that when $|b_n| < a$ we have $\xi > 0$ despite a negative b_n and the foregoing argument (formulae (28)-(34) are still valid).

When, however, $|b_n| > a$, ξ is negative and equation (29) takes the form

$$\frac{d^2F}{d\xi^2} - \xi F = 0. \tag{35}$$

In this case, without changing (30) a substitution different from that in (30) must be used

$$u = -i\frac{2}{3}|\xi|^{3/2}. \tag{36}$$

This substitution permits (35) to be rewritten in the form of (32), and the expression of F takes a form analogous to formula (34)

$$F = \xi^{1/2}\left[A_n J_{\frac{1}{3}\left(-i\frac{2}{3}|\xi|^{3/2}\right)} + B_n J_{-\frac{1}{3}\left(-i\frac{2}{3}|\xi|^{3/2}\right)}\right]. \tag{37}$$

On the basis of the foregoing analysis it can be stated that the linearization of the function $V_{(a)}$ permits the wave equation (1) to be transformed to the form of a Bessel equation (32) and thus the function F can be given by the known tabulated Bessel functions [4, 7].

Subsequently, using relations (28), (31) and (34) in the general relation (10) a formula can be derived for the admittance* of the nth element of the horn considered for $\xi > 0$. After transformations in which the recursive formulae for derivatives of cylindrical functions need be included [7], it can be stated that the expression for the unitary relative admittance of the nth element of the horn for $\xi > 0$ has the form

$$\beta_n = \frac{-i}{\mu}\left\{\frac{\sqrt{c_n(a+b_n)}\left[J_{-\frac{2}{3}(u)} - D_n J_{\frac{2}{3}(u)}\right]}{J_{\frac{1}{3}(u)} + D_n J_{-\frac{1}{3}(u)}} - \frac{\varrho'}{\varrho}\right\}. \tag{38}$$

* The notion of admittance is used here instead of impedance, since this permits simpler mathematical expressions and from the point of view of the final results both notions can be used equally well.

The constant $D_n = B_n/A_n$ which occurs in formula (38) can be determined from the boundary condition at the outlet of the nth element

$$\frac{-i}{\mu}\left\{\frac{\sqrt{c_n(a_n+b_n)}\,[J_{-\frac{2}{3}(u_n)} - D_n J_{\frac{2}{3}(u_n)}]}{J_{\frac{1}{3}(u_n)} + D_n J_{-\frac{1}{3}(u_n)}} - \frac{\varrho'_{(a_n)}}{\varrho_{(a_n)}}\right\} = Re(\beta_{0n+1}) + Jm(\beta_{0n+1}), \quad (39)$$

where, from (28) and (31),

$$u_n = \frac{2}{3}\sqrt{c_n(a_n+b_n)^3}, \quad (40)$$

and $\beta_{0_{n+1}}$ is the inlet admittance of the $(n+1)$th element of the horn.

The admittance of the other elements of the horn can be represented similarly as for the nth elements, e.g. the inlet acoustic admittance of the whole horn can be given by the formula for the inlet acoustic admittance of the first element

$$\beta_{0_1} = \frac{-i}{\mu}\left\{\frac{\sqrt{c_1 b_1}\,[J_{-\frac{2}{3}(u_0)} - D_1 J_{\frac{2}{3}(u_0)}]}{J_{\frac{1}{3}(u_0)} + D_1 J_{-\frac{1}{3}(u_0)}} - \left(\frac{\varrho'}{\varrho}\right)_{(a=0)}\right\}, \quad (41)$$

where, from (28) and (31)

$$u_0 = \frac{2}{3}\sqrt{c_1 b_1^3}. \quad (42)$$

In practice β_{0_1} is calculated in several stages, from the outlet to the inlet. First the inlet admittance of the end element must be determined, considering it as the load of the outlet of the previous element. Subsequently the inlet admittance of this element etc. must be calculated.

Now the case when $\xi = 0$ $(u = 0)$ will be considered. It follows from formula (28) that this case occurs when b_n is negative and satisfies the equation

$$a = |b_n|. \quad (43)$$

After expansion of the functions $J_{-\frac{1}{3}(u)}$ and $J_{-\frac{2}{3}(u)}$ into series [7] and transformations, formula (38) within the limits for $u = 0$ takes the form

$$\beta_n = \frac{-i}{\mu}\left[\frac{(3c_n)^{1/3}\Gamma\left(\frac{2}{3}\right)}{D_n\Gamma\left(\frac{1}{3}\right)} - \frac{\varrho'}{\varrho}\right], \quad (44)$$

where Γ is an Euler function [2, 4].

When $(a+b_n)$ in formula (28) is negative the case $\xi < 0$ occurs. In this case expression (36) must be inserted into formula (38) instead of u and it must be considered that $\sqrt{c_n(a+b_n)}$ is an imaginary number. This gives

$$\beta_n = \frac{-i}{u}\left\{\frac{-i\sqrt{c_n|a+b_n|}\left[J_{-\frac{2}{3}}\left(-i\frac{2}{3}|\xi|^{3/2}\right) - D_n J_{\frac{2}{3}}\left(-i\frac{2}{3}|\xi|^{3/2}\right)\right]}{J_{\frac{1}{3}}\left(-i\frac{2}{3}|\xi|^{3/2}\right) + D_n J_{-\frac{1}{3}}\left(-i\frac{2}{3}|\xi|^{3/2}\right)} - \frac{\varrho'}{\varrho}\right\}. \tag{45}$$

The approximation in the present section leads as a rule to considerable simplification of calculations, compared to the WKB approximation, since it permits the admittance of a horn (i.e. also its impedance) to be determined from the known tabulated Bessel functions [4]. In addition, when compared with the WKB method it has the essential advantage that it can be used in the case when $K_{(a)}$ is not slowly variable.

4. Approximation of the zeroth order

Approximation of the zeroth order can be used practically in estimation of the properties of horns when high accuracy is not necessary. It is assumed in this approximation that $A = \text{const}$. It follows then from equation (9) that Θ' must be constant, and thus Θ is a linear function of a.

At the same time, in view of that from equation (8) A is constant, the application of definition (12) gives

$$\Theta'^2 = K^2 = \text{const}. \tag{46}$$

Thus K must take a constant value independent of a. This value will be given below as $\bar{K}$.

It can be suggested that $\bar{K}$ should be defined as the square root of the mean value of the function $K^2_{(a)}$ in the interval $[0, a_l]$ corresponding to the length of the horn. This gives

$$\bar{K} = \left[\frac{1}{a_l}\int_0^{a_l} K^2 da\right]^{1/2}. \tag{47}$$

It follows from (46) that knowing $\bar{K}$ the phase Θ can be calculated

$$\Theta = \bar{K}a. \tag{48}$$

Thus, solution (7) of the reduced wave equation (1) will in this approximation have the form

$$F = A_1\exp(i\bar{K}a) + A_2\exp(-i\bar{K}a), \tag{49}$$

where the first term of the sum in formula (49) corresponds to the wave travelling from the inlet to the outlet of the horn, while the second term corresponds to the reflected wave.

It can be noted that when $\bar{K}^2 < 0$ formula (49) takes the form

$$F = A_3 \exp(\bar{\chi}\alpha) + A_4 \exp(-\bar{\chi}\alpha), \tag{50}$$

where

$$\bar{K} = -i\bar{\chi}. \tag{51}$$

The present section can be concluded with formulae for the admittance of the horn in the zeroth approximation. Formulae (49) and (50) in the general form of (10) can be used for this purpose. The present consideration is limited to the most frequent case when the wave reflected from the outlet of the horn is neglected. This is the case of the so-called horn of infinite length [5, 8, 12, 15]. Accordingly the second term of the sum can be neglected in formulae (49) and (50) and the formula for admittance, (10), takes for $K^2 > 0$ the form

$$\beta = \frac{\bar{K}}{\mu} + \frac{i}{\mu}\frac{\varrho'}{\varrho}. \tag{52}$$

In turn, for $\bar{K}^2 < 0$

$$\beta = \frac{-i\bar{\chi}}{\mu} + \frac{i}{\mu}\frac{\varrho'}{\varrho}, \tag{53}$$

and for the boundary case $\bar{K}^2 = 0$

$$\beta = \frac{i}{\mu}\frac{\varrho'}{\varrho}. \tag{54}$$

The formulae obtained for the admittance have a similar form to the relations used generally in the literature for waveguides of a constant value of K [8, 9, 12]. It follows therefore that the approximation given in this section lies essentially in the substitution for a horn for which K is a function of position, by a hypothetical horn of a constant, i.e. averaged, value of K. This procedure can give satisfactory results only when the properties of the horn as a whole are of interest. This is the most frequent case in practice where as a rule only the frequency response of the inlet impedance of a horn is analysed. However, the application of the approximation of the zeroth order for study of phenomena occurring inside a waveguide is in the authors' opinion a useless attempt.

5. A numerical example

The object of calculations illustrating as an example the results of the foregoing considerations was a horn of catenoidal profile and annular cross-section whose area is defined by the formule

$$S_0 = S_0 \cos \mathrm{h}\alpha. \tag{55}$$

Considerations in [13, 14] showed that the wave equation for a horn of this geometry has no exact solution in a compact form. An analysis of the usefulness of the WKB approximation, made according to section 2 shows that the function $K_{(\alpha)}$ cannot be considered as slowly variable, while the coefficient γ (cf. formula (22)) reaches the value of several score percent. In this case the approximate methods proposed in the present paper were used. Fig. 2 shows the results calculated for the real part of the inlet admittance of the horn type under consideration, with the dimensions: the width of the inlet ring $-1.5 \cdot 10^{-3}$ m, the length $-15 \cdot 10^{-2}$ m, the diameter of the outlet $-2 \cdot 10^{-1}$ m.

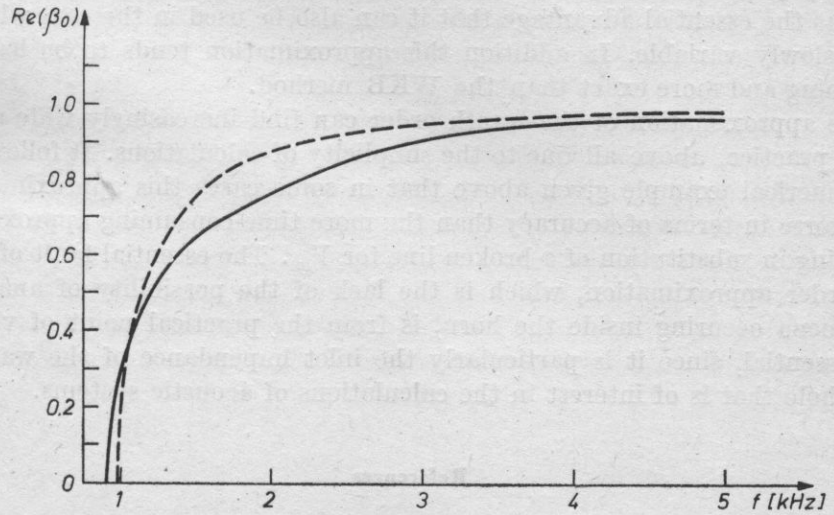

Fig. 2. The real part of the relative unit inlet admittance of a catenoidal horn of annular cross-section
– – – – the approximation of the zeroth order, —— the approximation of the function V_α by a broken line

The calculations were made with neglecting the effect of the wave reflected from the outlet. The continuous line in Fig. 2 shows the results obtained when the method of linear approximation of the function $V_{(\alpha)}$ was used, while the dashed line represents the calculations in the approximation of the zeroth order. It can be seen that in the case of the horn under consideration the approximation of the zeroth order gives satisfactory results, compared with the much more exact approximation by the linearization of the function $V_{(\alpha)}$ since the deviation does not exceed 15 percent.

6. Conclusions

The WKB approximation recommended in the acoustical literature for approximate solution of the equation of wave propagation in horns [1, 3, 9, 10], can be used above all for qualitative analysis of the transmission properties

of horns in the cut-off frequency region. Its use in numerical calculations is, however, limited, since it cannot be applied in the case of horns for which $K_{(a)}$ does not satisfy the requirement of slow variation. In addition, even in its applicability range, the WKB method may give very complicated formulae preventing their physical interpretation and good for computer calculations only.

When compared with the WKB method, the approximation proposed in the present paper, which consists in approximation of the function $V_{(a)}$ by a broken line, has the essential advantage that it can also be used in the case when $K_{(a)}$ is not slowly variable. In addition this approximation tends to be less time-consuming and more exact than the WKB method.

The approximation of the zeroth order can find increasingly wide application in practice, above all due to the simplicity of calculations. It follows from the numerical example given above that in some cases this approximation is little worse in terms of accuracy than the more time-consuming approximation consisting in substitution of a broken line for $V_{(a)}$. The essential fault of the zeroth order approximation, which is the lack of the possibility of analysis of phenomena occuring inside the horn, is from the practical point of view not very essential, since it is particularly the inlet impendance of the waveguide as a whole that is of interest in the calculations of acoustic systems.

References

[1] A. H. Benade, E. V. Jansson, *One plane and spherical waves in horns with nonuniform flare*, Acustica, **31**, 2, 79-98 (1974).

[2] I. N. Bronsztejn, K. A. Siemiendiajew, *A guide-book to mathematics for technologists and engineers*, The Macmillan Company, New York 1963.

[3] J. E. Freehafer, *The acoustical impedance of an infinite hyperbolic horn*, JASA, **11**, 467-476 (1940).

[4] E. Jahnke, F. Emde, F. Lösch, *Tables of higher functions*, McGraw- Hill Book Comp., New York 1960, pp. 55-60.

[5] I. Malecki, *Physical fundations of technical acoustics*, Pergamon Press, London 1969, pp. 426-432.

[6] O. K. Mawardi, *Generalized solutions of Webster's horn theory*, JASA, **21**, 4, 323-330 (1949).

[7] N. W. McLachlan, *Bessel functions for engineers* (in Polish), PWN, Warsaw 1964, pp. 37-38, 44-45.

[8] P. M. Morse, *Vibration and sound*, McGraw Hill Book Comp., New York 1948, pp. 265-283.

[9] V. Salmon, *Generalized plane wave horn theory*, JASA, **17**, 3 (1946).

[10] A. F. Stevenson, *Exact and approximate equations for wave propagation in acoustic horns*, JASA, **22**, 12, 1461-1462 (1951).

[11] A. G. Webster, *Acoustical impedance and the theory of horns and of the phonograf*, Proc. Natl. Acad. Sci. (U.S.), **5**, 275-282 (1919).

[12] R. Wyrzykowski, *A linear theory of the acoustic field of gaseous media* (in Polish), RTPN-WSP, Rzeszów 1972, pp. 287-317.

[13] T. Zamorski, R. Wyrzykowski, *Hyperbolic horns of annular cross-section* (in Polish), Proc. XXV Open Seminar on Acoustics, Poznań — Błażejewko 1978, 367-370.

[14] T. ZAMORSKI, *Finite length horn effect on the operating conditions of acoustic siren* (in Polish), Warsaw Technical University, Institute of Physics, Warsaw 1979, doctoral diss., pp. 79-81.

[15] Z. ŻYSZKOWSKI, *The fundamentals of electroacoustics* (in Polish), WNT, Warsaw 1966, pp. 145-150.

Received on June 12, 1980; revised version on January 30, 1981.

ARCHIVES OF ACOUSTICS
6, 3, 287-306 (1981)

AN ULTRASONIC *C.W.* DOPPLER METHOD OF MEASUREMENT OF THE BLOOD FLOW VELOCITY

T. POWAŁOWSKI

The Institute of Fundamental Technological Research
(00-049 Warszawa, ul. Świętokrzyska 21)

This paper presents an analysis of factors affecting the results of measurement of the blood flow velocity by the ultrasonic continuous wave (*C.W.*) Doppler method. For the parabolic flow velocity profile the effect on the spectrum of a Doppler signal of such factors as the ratio of the width of the ultrasonic beam to the inner diameter of the blood vessel and the coincidence of the transmitted ultrasonic beam with the one received inside the blood vessel, was analyzed. To that end, two variants of the position of the transmitting transducer and the transducer receiving the ultrasonic wave, with respect to the blood vessel were considered. In the first variant the point of intersection of axes of the transmitted ultrasonic beam and of the received from the flowing blood, was outside the blood vessel. In the second variant the axes of the ultrasonic beams intersected with each other in the middle of the blood vessel, on its axis. On the basis of analysis of the spectra of a Doppler signal the value of the factor of proportionality between the frequency of zero-crossings of the amplitude of the Doppler signal, measured by a Doppler flowmeter, and the mean Doppler frequency corresponding to the mean blood flow velocity in the blood vessel, was determined. This factor is the basis for quantitative estimation of the blood flow velocity from the Doppler frequency measured by the flowmeter.

1. Introduction

Of the currently used ultrasonic Doppler methods of measurement of blood flow the *C.W.* method was historically the first to find wide application in diagnostics of diseases of the human circulation system. It permits noninvasive measurement of the mean blood flow velocity in the cross-section of the blood vessel. Information about the blood flow velocity is contained in the Doppler frequency measured by the measuring apparatus, which is the difference between the frequency of the transmitted continuous wave and its frequency received from the flowing blood.

The previous investigations of the blood flow velocity by the ultrasonic *C.W.* method were mainly qualitative and consisted in registering variations in the blood flow velocity during the cardiac cycle. This resulted from the lack of sufficient information about the quantitative relation between the measured Doppler frequency and the real mean blood flow velocity.

This paper presents a detailed analysis of factors affecting the results of measurement of the blood flow velocity by the ultrasonic *C.W.* Doppler method and attempts to determine the quantitative relation between the measured Doppler frequency and the mean blood flow velocity in the cross-section of the blood vessel.

2. The principle of measurement of the blood flow velocity

The general principle of measurement of the blood flow velocity by the ultrasonic *C.W.* Doppler method is shown in Fig. 1. A piezoelectric transmitting transducer excited to vibration by a high-frequency electric signal trans-

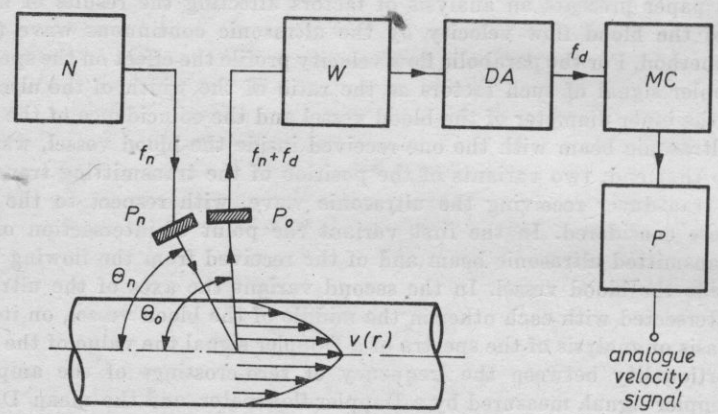

Fig. 1. A schematic diagram of the system for measuring the blood flow velocity by the *C.W.* method

N – the transmitter, P_n – the piezoelectric transmitting transducer, *P* – the piezoelectric receiving transducer, *W* – the high-frequency amplifier, *DA* – the amplitude detector, *MC* – the frequency meter, *P* – the frequency-to-voltage converter, f_n – the transmitted frequency, f_0 – the Doppler frequency, $v(r)$ – the velocity of blood cells in the cross-section of the vessel, θ_n, θ_o – the angles between the transmitted and received waves with respect to the axis of the vessel

mits a continuous ultrasonic wave towards the blood vessel. The ultrasonic wave scattered by flowing blood cells contains the spectrum of the Doppler frequencies f_d. The individual components of the Doppler spectrum are proportional to the velocity of blood cells flowing in the field of the transmitted ultrasonic beam, according to the relation

$$f_d = \pm f_n \frac{v(r)}{c} (\cos\theta_n + \cos\theta_0), \tag{1}$$

where c – the ultrasonic wave propagation velocity in blood, f_n – the frequency of the transmitted ultrasonic wave, $v(r)$ – the velocity of blood cells in the cross-section of the blood vessel at the distance r from its axis, θ_n – the angle between the direction of the transmitted ultrasonic beam and the blood vessel, θ_0 – the angle between the direction of the received ultrasonic beam and the blood vessel.

The Doppler frequency f_d is positive when blood cells approach the transmitting and receiving transducers in the ultrasonic head, and it is negative when they flow away from the transducers.

According to formula (1) the mean Doppler frequency f_s described by the following relation, corresponds to the mean blood flow velocity in the blood vessel of cylindrical cross-section

$$f_s = \frac{1}{\pi R^2}\left[\frac{f_n(\cos\theta_n + \cos\theta_0)}{c}\right]\int_0^R 2\pi r v(r)\,dr, \tag{2}$$

where R is the inner radius of the blood vessel.

In ultrasonic Doppler flowmeters the ultrasonic wave received from the flowing blood is transformed into an electric signal which after amplification is detected in terms of amplitude. In order to obtain information about the mean blood flow velocity the technique of measurement of the frequency of a Doppler signal by the method of zero-crossing is generally used. The mean frequency f_{zc} of the positive zero crossings of the amplitude of the Doppler signal depends on the power density spectrum $S(f)$ of the Doppler signal and is proportional to the mean velocity v_s of blood flow in the cross-section of the blood vessel, according to the relation

$$v_s = a\frac{cf_{zc}}{f_n(\cos\theta_n + \cos\theta_0)}, \tag{3a}$$

where

$$f_{zc} = \left[\frac{\int_0^\infty f^2 S(f)\,df}{\int_0^\infty S(f)\,df}\right]^{1/2}. \tag{3b}$$

The proportionality factor a in formula (3a) describes the relation between the Doppler frequency f_{zc} measured by the method of zero-crossing and the mean Doppler frequency calculated from formula (2).

The frequency of the Doppler signal measured by the method of zero-crossing is transformed in the receiver of the measuring apparatus into a voltage signal whose amplitude u_0 is proportional to the measured mean blood flow velocity v_s, according to the relation

$$v_s = \frac{ab}{\eta}\frac{cu_0}{f_n(\cos\theta_n + \cos\alpha_0)}, \tag{4}$$

where η — the constant of transformation of the measured Doppler frequency into voltage, b — a coefficient describing the relation between the measured frequency and the real frequency of zero-crossing of the amplitude of the Doppler signal.

The term $abc/\eta f_n$ in formula (4) describes the general form of the calibration coefficient of the Doppler flowmeter for a given angle at which the ultrasonic wave is transmitted and received with respect to the blood vessel. The parameters in the term, such as the ultrasonic wave velocity in blood c [10] the frequency of the transmitted ultrasonic wave f_n and the constant of transformation of the measured Doppler frequency into voltage η are known and given by the manufacturers of ultrasonic Doppler measuring apparatus. The value of the coefficient b in formula (4) is connected with the magnitude of the error occuring in measurement of the frequency of zero-crossing of the amplitude of a Doppler signal. The main causes of this error are: noise accompanying the Doppler signal and filtration of low-frequency components from the spectrum of the Doppler signal. This filtration is necessary so that components from pulsating walls of the blood vessel can be eliminated from the Doppler signal. The error in measurement of the Doppler frequency caused by the above factors is lower than 5 percent when the power ratio of the Doppler signal to noise is larger than 30 dB and when the maximum frequency of the Doppler signal is larger by the factor of ten than the lower frequency of the transmission band of the Doppler signal amplifier in the receiver of the apparatus [3, 4]. A detailed analysis of errors occurring in measurement of the Doppler frequency by the method of zero-crossing was presented in many papers [3-5], therefore, it will not be considered here. Instead the object of the present analysis is the value of the proportionality factor a between the mean Doppler frequency f_s (see formula (2)) and the frequency f_{zc} of the positive zero crossing of the amplitude of the Doppler signal (see formula (3b)).

In order to determine a quantitative value of the proportionality factor a, it is necessary to analyze the relation between the power density spectrum of the Doppler signal and the blood flow velocity profile in the blood vessel, with consideration given to such factors as the ratio of the width of the ultrasonic beam to the inner diameter of the blood vessel and the geometrical orientation of piezoelectric transducers of the ultrasonic probe with respect to the blood vessel.

3. The power density spectrum of the Doppler signal

Analysis of the whole of phenomena occurring in measurement of the blood flow velocity and affecting the spectrum of the Doppler signal is very complicated. The power density spectrum of the Doppler signal depends on many factors such as the spatial distribution of the density of blood cells scattering the

ultrasonic beam, the blood flow velocity profile in the blood vessel, the geometrical dimensions of the region common to the transmitted beam and the one received inside the blood vessel, and the geometrical orientation of transducers of the ultrasonic probe with respect to the blood vessel.

The spectral analysis presented in this paper concerns the measuring system with two rectangular piezoelectric transducers of dimensions $H \times B$ placed at the same side of the blood vessel. The transmitted and received ultrasonic beams pass symmetrically through the middle of the blood vessel at the angles θ_n and θ_0 with respect to its axis (Fig. 2a, b), respectively. The author will con-

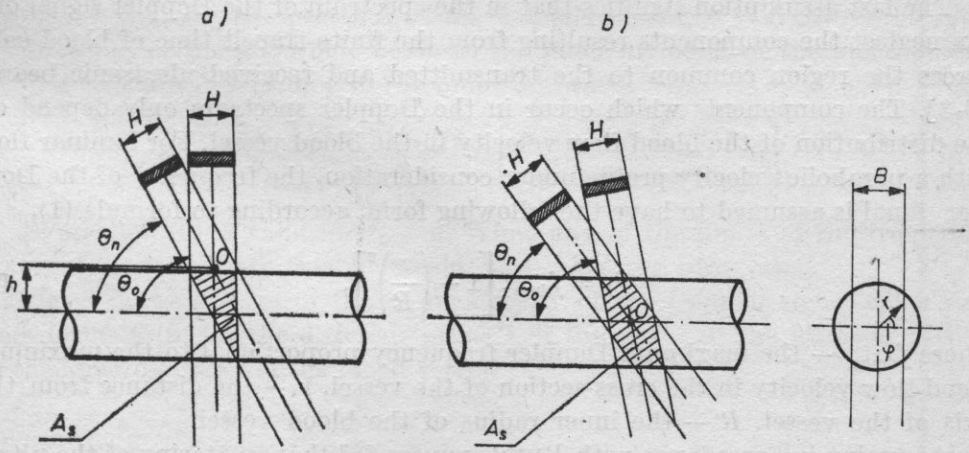

Fig. 2. The position of ultrasonic transducers with respect to the blood vessel
A_s – the region common to the transmitted ultrasonic beam and the one received inside the blood vessel, O – the point of intersection of axes of the ultrasonic beams

sider here two variants of coincidence of the transmitted ultrasonic beam with the one received inside the blood vessel. In the first variant (shown in Fig. 2a) the point of intersection of axes of the ultrasonic beams is outside the wall of the vessel at the distance h from the axis of the vessel, the distance being defined by

$$R+\frac{H\cos(\theta_n+\theta_0)/2}{2\cos(\theta_0-\theta_n)/2}\leqslant h\leqslant\frac{H\sin(\theta_0+\theta_n)/2}{2\sin(\theta_0-\theta_n)/2}-R. \tag{5}$$

In the second variant the point of intersection of axes of the ultrasonic beams is on the axis of the vessel (Fig. 2*b*). In this case the following assumptions were made

$$\frac{\sin(\theta_0-\theta_n)}{2\sqrt{\sin\theta_n\sin\theta_0}}\leqslant\frac{H}{B}\leqslant 1 \tag{6a}$$

and

$$0^\circ<\theta_n<\theta_0\leqslant 90^\circ. \tag{6b}$$

The spectrum of the Doppler signal will be analyzed for laminar, stationary flow in a cylindrical vessel with rigid walls. The following simplifying assumptions were made:

1. the distribution of the acoustic pressure in the field of the ultrasonic beam is uniform;
2. the spatial density distribution of flowing blood cells is uniform;
3. the mean dimensions (measured in the direction of the blood flow) of the region common to the ultrasonic transmitted beam and the one received inside the blood vessel are much larger than the ultrasonic wavelength in blood.

The last assumption signifies that in the spectrum of the Doppler signal one can neglect the components resulting from the finite transit time of blood cells across the region common to the transmitted and received ultrasonic beams [2-3]. The components which occur in the Doppler spectrum only depend on the distribution of the blood flow velocity in the blood vessel. For laminar flow with a parabolic velocity profile under consideration, the frequency of the Doppler signal is assumed to have the following form, according to formula (1),

$$f_d = f_{d\max}\left[1-\left(\frac{r}{R}\right)^2\right], \tag{7}$$

where $f_{d\max}$ – the maximum Doppler frequency proportional to the maximum blood flow velocity in the cross-section of the vessel, r – the distance from the axis of the vessel, R – the inner radius of the blood vessel.

Assuming in accordance with REID's papers [8] that scattering of the ultrasonic wave on flowing blood cells is of the first order, the power of the Doppler signal is proportional to the density of blood cells flowing across the field of the ultrasonic beam. Blood cells flowing at the distance r from the axis of the vessel at the velocity $v_1 < v < v_1 + dv$ are sources of a Doppler signal whose power dN can be expressed by the relation

$$dN = a\varrho r dr \int_{\varphi_1(r)}^{\varphi_2(r)} l(r,\varphi)\,d\varphi, \tag{8}$$

where a – the proportionality factor whose value depends among other things on the intensity of the transmitted ultrasonic wave, ϱ – the density of flowing blood cells, r, φ – the cylindrical coordinates describing the position of blood cells in the cross-section of the vessel, $l(r, \varphi)$ – the length of the region common to the transmitted and received ultrasonic beams in the direction of blood flow (cf. Fig. 2a, b).

The integration limits in formula (8) are a function of the coordinate r and depend on the ratio of the width B of the ultrasonic beam to the inner diameter $2R$ of the blood vessel (cf. Fig. 2a, b).

Differentiation of expression (7) with respect to r and consideration of the results of differentiation in expression (8) give an expression of the distribution of the power density spectrum of the Doppler signal. For the measuring system

shown in Fig. 2*a* where the point of intersection of the ultrasonic beams is outside the blood vessel, the power density spectrum of the Doppler signal calculated on the basis of expressions (7) nad (8) assumes the following form

$$S(f_w) = \begin{cases} \dfrac{2W}{\pi} \arcsin \dfrac{k}{\sqrt{1-f_w}} & \text{for} \quad 0 \leqslant f_w \leqslant 1-k^2, \\ W & \text{for} \quad 1-k^2 \leqslant f_w \leqslant 1, \end{cases} \tag{9}$$

where $S(f_w)$ – the power density spectrum of the Doppler signal, f_w – the relative frequency equal to the ratio of the current frequency f_d to the maximum frequency $f_{d\max}$ of the spectrum of the Doppler signal, $k = B/2R$ – the ratio of the width of the ultrasonic beam to the inner diameter of the blood vessel, W – a constant determined in the following way

$$W = \frac{\pi a \varrho H R^2}{f_{d\max}} \frac{\sin(\theta_0 - \theta_n)}{\sin\theta_n \sin\theta_0} \left[\frac{H \sin(\theta_0 + \theta_n)/2}{2 \sin(\theta_0 - \theta_n)/2} - h \right]. \tag{9a}$$

Expression (9) is valid for $f_w \geqslant 0$. When any of the limits of the frequency ranges does not satisfy this condition, this takes the zero value.

Fig. 3 shows spectra of the power density of the Doppler signal calculated from formula (9) for the different ratios k of the width of the ultrasonic beam to the inner diameter of the blood vessel.

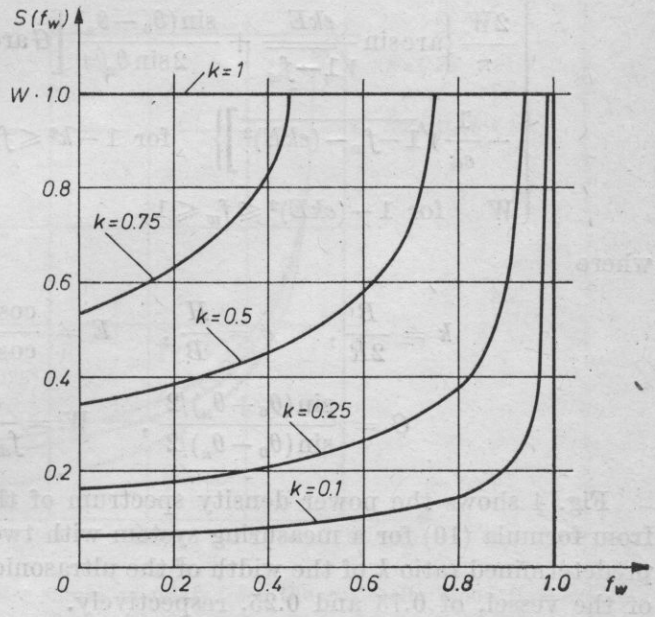

Fig. 3. The spectra of the Doppler signal for the parabolic blood flow velocity profile in the case when the point of intersection of axes of the ultrasonic beams is outside the blood vessel (cf. Fig. 2a)
k – the ratio of the width of the ultrasonic beam to the inner diameter of the blood vessel

For the measuring system shown in Fig. 2*b* where the point of intersection of axes of the ultrasonic beams is on the axis of the blood vessel, the spectrum

of the power density of the Doppler signal calculated from formulae (7) and (8) takes the form described by formula (10). This expression, as also expression (9), is valid for $f_w \geqslant 0$.

$$S(f_w) = \begin{cases} 0 \quad \text{for } 0 \leqslant f_w \leqslant 1-k^2(1+e^2G^2); \\ \dfrac{W\sin(\theta_0-\theta_n)}{\pi\sin\theta_n}\left\{G\left[\arcsin\dfrac{ekG}{\sqrt{1-f_w}} - \arccos\dfrac{k}{\sqrt{1-f_w}}\right]+\right. \\ \left.+\dfrac{1}{ek}\sqrt{1-f_w-(ekG)^2} - \dfrac{1}{e}\right\} \quad \text{for } 1-k^2(1+e^2G^2) \leqslant f_w \leqslant 1-(ekG)^2, \\ \dfrac{W\sin(\theta_0-\theta_n)}{\pi\sin\theta_n}\left[G\arcsin\dfrac{k}{\sqrt{1-f_w}} - \dfrac{1}{e}\right] \\ \qquad\qquad \text{for } 1-(ekG)^2 \leqslant f_w \leqslant 1-k^2(1+e^2E^2), \\ \dfrac{2W}{\pi}\left\{\left[\arcsin\dfrac{ekE}{\sqrt{1-f_w}} - \arccos\dfrac{k}{\sqrt{1-f_w}}\right]+\right. \\ \left.+\dfrac{\sin(\theta_0-\theta_n)}{2\sin\theta_n}\left[G\arccos\dfrac{ekE}{\sqrt{1-f_w}} - \dfrac{1}{ek}\sqrt{1-f_w-(ekE)^2}\right]\right\} \\ \qquad\qquad \text{for } 1-k^2(1+e^2E^2) \leqslant f_w \leqslant 1-k^2, \\ \dfrac{2W}{\pi}\left\{\arcsin\dfrac{ekE}{\sqrt{1-f_w}} + \dfrac{\sin(\theta_0-\theta_n)}{2\sin\theta_n}\left[G\arccos\dfrac{ekE}{\sqrt{1-f_w}} - \right.\right. \\ \left.\left.-\dfrac{1}{ek}\sqrt{1-f_w-(ekE)^2}\right]\right\} \quad \text{for } 1-k^2 \leqslant f_w \leqslant 1-(ekE)^2, \\ W \quad \text{for } 1-(ekE)^2 \leqslant f_w \leqslant 1, \end{cases}$$

where

$$k = \frac{B}{2R}, \qquad e = \frac{H}{B}, \qquad E = \frac{\cos(\theta_0+\theta_n)/2}{\cos(\theta_0-\theta_n)/2},$$

$$G = \frac{\sin(\theta_0+\theta_n)/2}{\sin(\theta_0-\theta_n)/2}, \qquad W = \frac{\alpha\pi\varrho HR^2}{f_{d\max}\sin\theta_0}.$$

Fig. 4 shows the power density spectrum of the Doppler signal calculated from formula (10) for a measuring system with two square transducers for the predetermined ratio k of the width of the ultrasonic beam to the inner diameter of the vessel, of 0.75 and 0.25, respectively.

Fig. 5 shows the spectrum of the Doppler signal calculated from formulae (9) and (10) and measured for the case when the point of intersection of axes of the ultrasonic beams is outside the tube (Fig. 5a, b) and when the point of in-

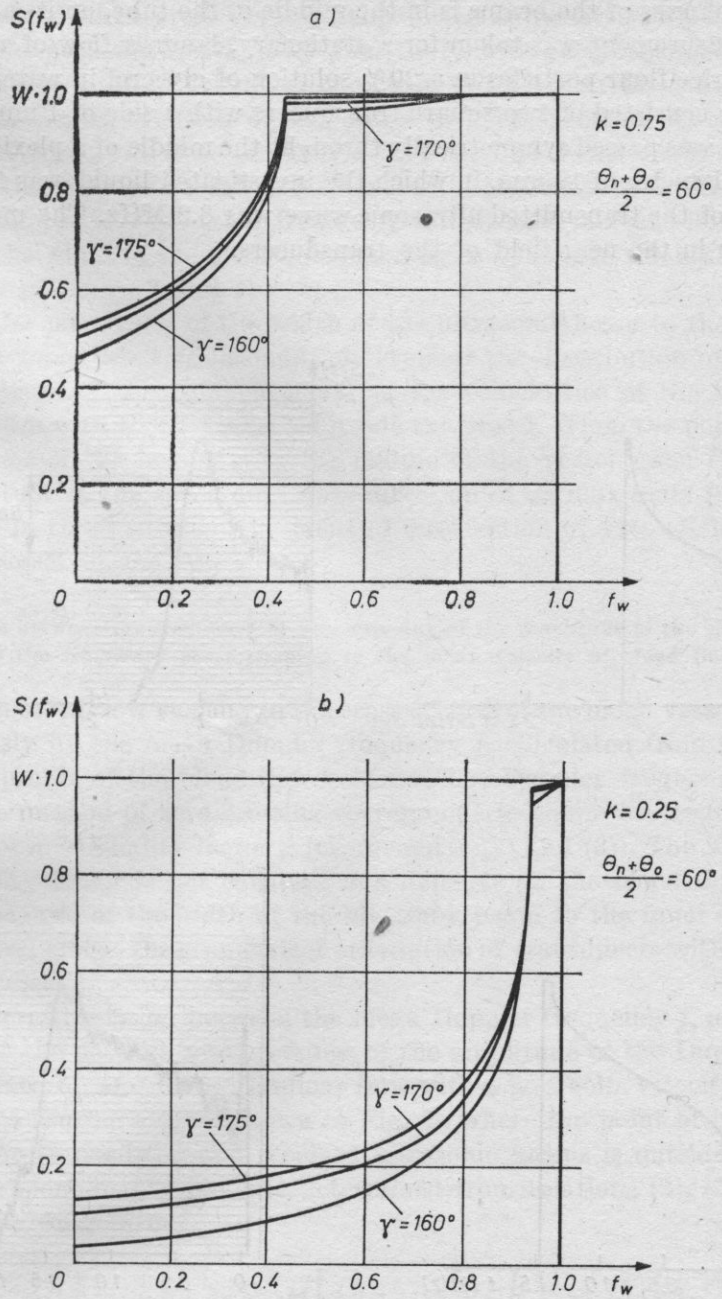

Fig. 4. The spectra of the Doppler signal calculated for the parabolic blood flow velocity profile in the case of a measuring system with two square transducers and when the point of intersection of axes of the ultrasonic beams is on the axis of the blood vessel (cf. Fig. 2b)
k – the ratio of the width of the ultrasonic beam to the inner diameter of the vessel, θ_n, θ_o – the angles between the transmitted and received ultrasonic beams and the axis of the vessel, γ – the angle between the transducers

tersection of axes of the beams is in the middle of the tube, on its axis (Fig. 5c, d). The measurement was taken for a stationary, laminar flow of a 0.01% suspension of rice flour particles in a 20% solution of glycerol in water. The ultrasonic probe consisted of two square transducers with a side of 4 mm. The ultrasonic beam was passed symmetrically throught the middle of a plexiglass tube of the inner diameter of 19 mm, in which the investigated liquid was flowing. The frequency of the transmitted ultrasonic wave was 8.2 MHz. The measurements were taken in the near field of the transducers.

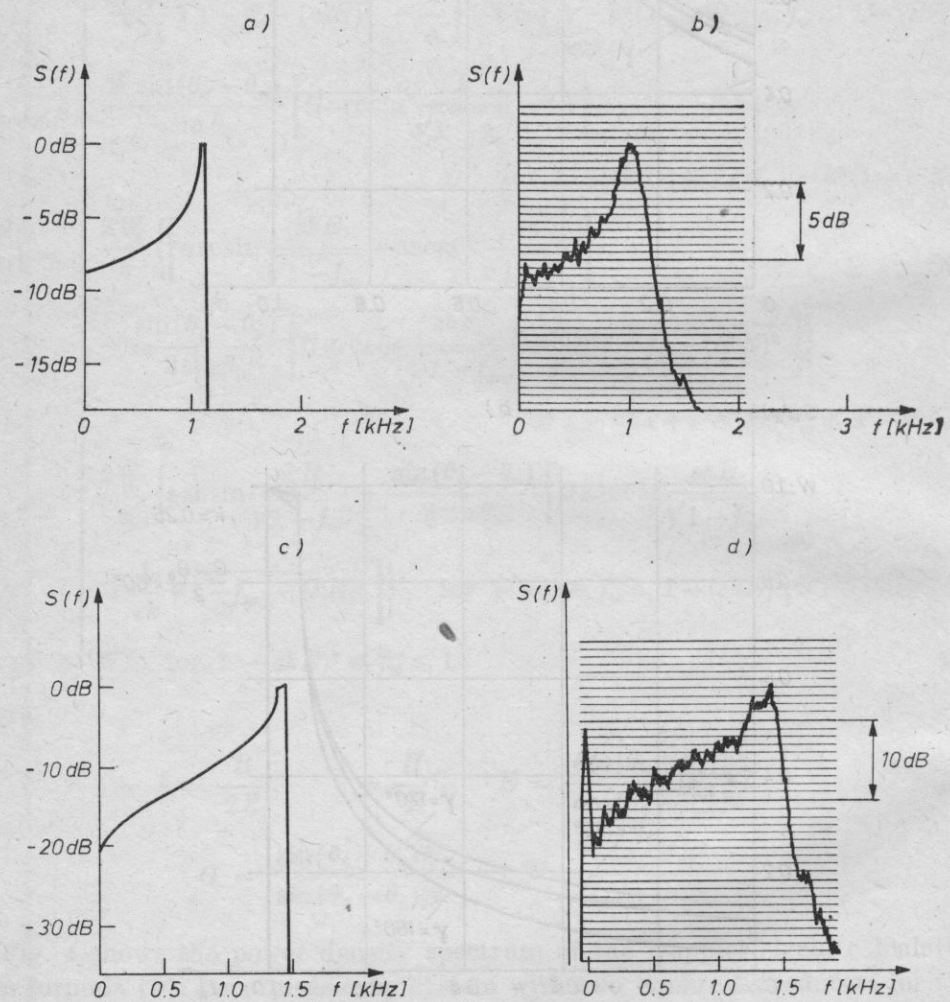

Fig. 5. The calculated (*a*, *c*) and measured (*b*, *d*) spectra of Doppler signals for laminar flow in the case when the point of intersection of axes of the transmitted and received ultrasonic beams was outside the wall of the tube (*a*, *b*) and when the point of intersection of axes of the ultrasonic beams was in the centre of the tube, on its axis (*c*, *d*). The ratio k of the width of the ultrasonic beam to the inner diameter of the tube was 0.21

On the basis of the theoretical analysis made and the results obtained from investigation of the spectra of the Doppler signal, the following conclusions were drawn:

(a) When the width of the ultrasonic beam is less than the inner diameter of the vessel, the distribution of the power density spectrum of the Doppler signal is affected by the ratio of the width of the ultrasonic beam to the inner diameter of the vessel. This effect can be seen in the increase in the amplitude of the spectrum over the higher frequency range. This increase is the greater the smaller the width of the ultrasonic beam is, compared to the inner diameter of the vessel (cf. Figs. 3 and 4).

(b) For the same ratio of the width of the ultrasonic beam to the inner diameter of the vessel what additionally determines the distribution of the power density spectrum of the Doppler signal is the coincidence of the transmitted ultrasonic beam with the one received inside the vessel. When the point of intersection of axes of the beams is in the middle of the vessel, then the increase in the amplitude of the spectrum in the direction of its maximum frequency is greater than in the case when the point of intersection of axes of the beams is outside the vessel (cf. Fig. 5).

4. The relation between the frequency of zero-crossing of the amplitude of the Doppler signal and the frequency corresponding to the mean velocity of blood flow

The mean blood flow velocity in the cross-section of the blood vessel is defined unambiguously by the mean Doppler frequency f_s calculated from relation (2) for the real profile of the blood flow velocity. The Doppler frequency f_{zc} measured by the method of zero crossing corresponds to the mean frequency f_s by way of the proportionality factor a (cf. formulae (2) and (3)). The value of the proportionality factor is not constant and depends on the blood flow velocity profile, on the ratio of the width of the ultrasonic beam to the inner diameter of the blood vessel and on the geometrical orientation of transducers with respect to the blood vessel.

The numerical relation between the mean Doppler frequency f_s and the frequency f_{zc} of the positive zero crossings of the amplitude of the Doppler signal will be analyzed for stationary, laminar flow with a parabolic velocity profile.

For the measuring system shown in Fig. 2a where the point of intersection of axes of the transmitted and received ultrasonic beams is outside the blood vessel the proportionality factor a determined from relations (2), (3b) and (9) takes the following form

$$a = \frac{f_s}{f_{zc}} = \begin{cases} \frac{\sqrt{3}}{2}\left[\frac{\arcsin k + k\sqrt{1-k^2}\left[3.2 + (1+2k^2)\left(\frac{4}{15}k^2 - 1\right)\right]}{\arcsin k + k\sqrt{1-k^2}}\right]^{-1/2} & \text{for } k < 1, \\ \frac{\sqrt{3}}{2} \quad \text{for } k \geqslant 1. \end{cases} \tag{11}$$

where k — the ratio of the width of the ultrasonic beam to the inner diameter of the blood vessel.

Fig. 6 shows the value of the proportionality factor calculated from formula (10) as a function of the ratio of the width of the ultrasonic beam to the inner diameter of the blood vessel. Variation in the value of the factor a results from variation in the distribution of the power density spectrum of the Doppler

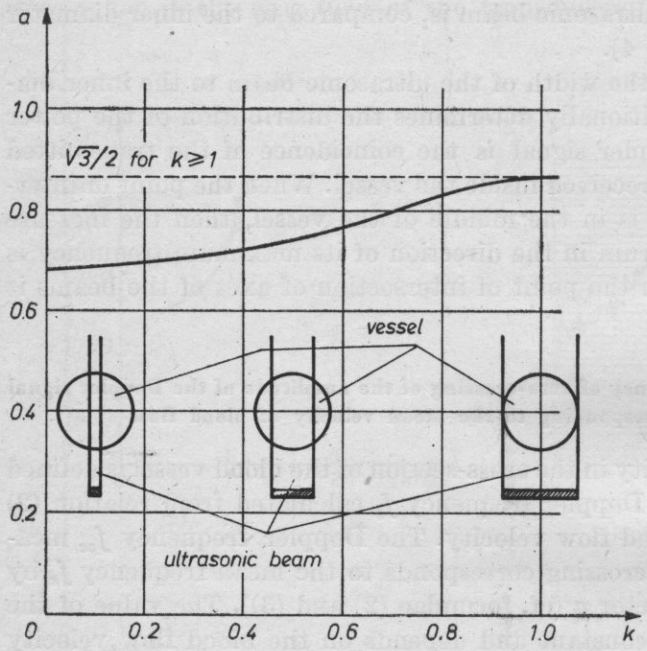

Fig. 6. The factor a of proportionality between the mean frequency and the frequency of zero crossing of the Doppler signal for the parabolic blood flow velocity profile and a measuring system in which the point of intersection of axes of the ultrasonic beams is outside the vessel (cf. Fig. 2a)
k — the ratio of the width of the ultrasonic beam to the inner diameter of the vessel

signal for the individual values of the ratio k. As was shown above (cf. Fig. 3), the spectrum of the Doppler signal does not depend on the width of the ultrasonic beam when this beam occupies the whole cross-section of the vessel. Hence the value of the proportionality factor a is constant for the ratio $k \geqslant 1$. However, when the ultrasonic beam is narrower than the diameter of the blood vessel, then the amplitude of the Doppler spectrum increases in the direction of its maximum frequency with decreasing ratio k of the width of the ultrasonic beam to the inner diameter of the vessel. This causes, in turn, an increase in the value of the Doppler frequency f_{zc} measured by the method of zero crossing for the constant mean frequency f_s. As a result the value of the factor of proportionality between the mean frequency f_s and the frequency f_{zc} measured by the method of zero crossing decreases with decreasing ratio k of the width of the ultrasonic beam to the inner diameter of the blood vessel.

The lack of the constant numerical relation between the mean frequency f_s and the measured frequency f_{zc} makes difficult interpretation of the results of measurement of blood flow in blood vessels with diameters larger than the

width of the ultrasonic beam, since in this case the lack of information about the real inner diameter of the blood vessel is an essential source of error in quantitative evaluation of the mean blood flow velocity on the basis of the Doppler frequency measured by the zero crossing method.

One can now consider a case-when the point of intersection of axes of the transmitted ultrasonic beam and the one received from the flowing blood is inside the blood vessel, on its axis (Fig. 2b). The proportionality factor a calculated for this case takes, according to relations (2), (3) and (10), the following form

$$a = 0.5 \times \left[\frac{C_n + A_{kn}(1-GL) + GL(E_{kn} + A_{km} - F_{km}) + L\left(E_{km} - E_{kn} - \frac{1}{e} C_{kmn}\right) + C_{kn} + A_{kmn} + R_{kn}}{B_{kn}(1-GL) + D_{kn} + B_{kmn} - \frac{2L}{\pi e}(m^2 - n^2) + GLB_{km}} \right]^{-1/2}$$

$$\text{for } 0 < k < \frac{1}{\sqrt{1+e^2G^2}}, \tag{12a}$$

$$a = 0.5 \times \left[\frac{C_n + A_{kn}(1-GL) + GL[E_{kn} + G_{kn} + 2(A_m - B_m)]}{B_{kn}1(-GL) + GL[k^2 + H_{kn} + 2(D_m - E_m)] - \frac{4L}{3\pi} k^2 + D_{kn} - \frac{2L}{\pi e}(1-k^2-n^2) + \frac{L}{k} G_m} + \right.$$

$$\left. + \frac{-LF_{kn} + C_{kn} - \frac{2L}{3\pi e}(1-k^2-n^2)^3 + \frac{L}{k} F_m - R_{kn}}{B_{kn}(1-GL) + GL[k^2 + H_{kn} + 2(D_m - E_m)] - \frac{4L}{3\pi} k^2 + D_{kn} - \frac{2L}{\pi e}(1-k^2-n^2) + \frac{L}{k} G_m} \right]^{-1/2}$$

$$\text{for } \frac{1}{\sqrt{1+e^2G^2}} \leqslant k < \frac{1}{eG}, \tag{12b}$$

$$a = 0.5 \times \left[\frac{C_n + A_{kn}(1-GL) + GL(F_{kn} + G_{kn}) - LE_{kn} + C_{kn} - \frac{2L}{3\pi e}(1-k^2-n^2)^3 - R_{kn}}{B_{kn}(1-GL) + GL(k^2 + H_{kn}) - \frac{4}{3\pi} Lk^2 + D_{kn} - \frac{2L}{\pi e}(1-k^2-n^2)} \right]^{-1/2}$$

$$\text{for } \frac{1}{eG} \leqslant k < \frac{1}{\sqrt{1+e^2E^2}}, \tag{12c}$$

$$a = 0.5 \left[\frac{C_n + 2A_n(1-GL) + 2B_nGL - \frac{L}{k} F_n + 2A_k - \frac{1}{3}(1-k^2)^3}{n + 2D_n(1-GL) + 2E_nGL - \frac{L}{k} G_n + 2D_k + k^2 - 1} \right]^{-1/2} \tag{12d}$$

$$\text{for } \frac{1}{\sqrt{1+e^2E^2}} \leqslant k < 1,$$

$$a = 0.5\left[\frac{C_n + 2A_n(1-GL) + 2B_nGL - F_nL\dfrac{1}{k}}{n^2 + 2D_n(1-GL) + 2E_nGL - G_nL\dfrac{1}{k}}\right]^{-1/2} \quad \text{for } 1 \leqslant k < \frac{1}{eE}, \tag{12e}$$

$$a = \frac{\sqrt{3}}{2} \quad \text{for } k \geqslant \frac{1}{eE}, \tag{12f}$$

where $e = H/B$ – the ratio of sides of the transducer (cf. Fig. 2), k – the ratio of the width of the ultrasonic beam to the inner diameter of the blood vessel;

$$E = \frac{\cos(\theta_0+\theta_n)/2}{\cos(\theta_0-\theta_n)/2}, \quad G = \frac{\sin(\theta_0+\theta_n)/2}{\sin(\theta_0-\theta_n)/2}, \quad L = \frac{\sin(\theta_0-\theta_n)}{2\sin\theta_n},$$

$$n = ekE, \quad m = ekG, \quad A_k = \frac{1}{\pi}\left\{\frac{k}{3}\sqrt{1-k^2}\left[3.2 + (1+2k^2)\left(\frac{4}{15}k^2 - 1\right)\right] + \right.$$

$$\left. + \frac{1}{3}\arcsin k - k^2\left(1 - k^2 + \frac{k^4}{3}\right)\frac{\pi}{2}\right\};$$

A_n and Q_m are described by expression A_k, when the parameter k is replaced with the parameters n or m, respectively;

$$D_k = \frac{1}{\pi}\left[k\sqrt{1-k^2} + \arcsin k - k^2\frac{\pi}{2}\right];$$

D_n and D_m are described by expression D_k when the parameter k is replaced with the parameters n or m, respectively;

$$C_k = \frac{1}{3}\left[1-(1-k^2)^3\right], \quad C_n = \frac{1}{3}\left[1-(1-n^2)^3\right], \quad B_n = \frac{1}{6}(1-n^2)^3,$$

$$B_m = \frac{1}{6}(1-m^2)^3, \quad E_n = \frac{1}{2}(1-n^2), \quad E_m = \frac{1}{2}(1-m^2),$$

$$G_n = \frac{4}{3\pi}\sqrt{(1-n^2)^3}, \quad G_m = \frac{4}{3\pi}\sqrt{(1-m^2)^3}, \quad F_m = \frac{32}{105\pi}\sqrt{(1-m^2)^5},$$

$$F_n = \frac{32}{105\pi}\sqrt{(1-n^2)^5},$$

$$A_{kn} = \frac{2}{\pi}\left\{\frac{nk}{3}\left[3 + (k^2+3n^2)\left(\frac{4}{15}n^2 - 1\right) + \frac{1}{5}(k^2+n^2)^2\right] + \right.$$

$$\left. + (k^2+n^2)\left[1-(k^2+n^2) + \frac{1}{3}(k^2+n^2)^2\right]\arcsin\frac{n}{\sqrt{k^2+n^2}} - \frac{\pi}{2}n^2\left(1 - n^2 + \frac{n^4}{3}\right)\right\};$$

$$B_{kn} = \frac{2}{\pi}\left[(k^2+n^2)\arcsin\frac{n}{\sqrt{k^2+n^2}} + nk - \frac{n^2}{2}\pi\right],$$

$$C_{kn} = \frac{2}{\pi}\left\{\frac{nk}{3}\left[3+(n^2+3k^2)\left(\frac{4}{15}k^2-1\right)+\frac{1}{5}(k^2+n^2)\right]+\right.$$

$$\left.+(k^2+n^2)\left[1-(k^2+n^2)+\frac{1}{3}(k^2+n^2)^2\right]\arcsin\frac{k}{\sqrt{k^2+n^2}} - \frac{\pi}{2}k^2\left(1-k^2+\frac{k^4}{3}\right)\right\},$$

$$D_{kn} = \frac{2}{\pi}\left[(k^2+n^2)\arcsin\frac{k}{\sqrt{k^2+n^2}} + nk - \frac{k^2}{2}\pi\right],$$

$$E_{kn} = \frac{2}{\pi}k^2\left[\frac{2}{15}(5-10n^2-6k^2)+\frac{2}{7}(k^2+n^2)^2+\frac{8}{105}n^2(5n^2+3k^2)\right],$$

$$F_{kn} = \frac{1}{3}\left[(1-n^2)^3-(1-n^2-k^2)^3\right],$$

$$G_{kn} = \frac{2}{\pi}\left\{\frac{k}{3}\sqrt{1-k^2}\left[3.2+(1+2k^2)\left(\frac{4}{15}k^2-1\right)\right]+\frac{1}{3}\arcsin k-(k^2+n^2)\times\right.$$

$$\left.\times\left[1-(k^2+n^2)+\frac{(k^2+n^2)^2}{3}\right]\arcsin\frac{k}{\sqrt{k^2+n^2}} - \frac{kn}{3}\left[3+(n^2+3k^2)\left(\frac{4}{15}k^2-1\right)+\right.\right.$$

$$\left.\left.+\frac{(k^2+n^2)^2}{5}\right]\right\},$$

$$H_{kn} = \frac{2}{\pi}\left[\arcsin k + k\sqrt{1-k^2} - nk - (k^2+n^2)\arcsin\frac{k}{\sqrt{k^2+n^2}}\right],$$

$$R_{kn} = \frac{1}{3}\left[(1-k^2)^3-(1-k^2-n^2)^3\right],$$

$$A_{kmn} = \frac{2}{\pi}\left\{(k^2+m^2)\left[1-(k^2+m^2)+\frac{1}{3}(k^2+m^2)^2\right]\arcsin\frac{k}{\sqrt{k^2+m^2}} -\right.$$

$$-\frac{km}{3}\left[3+(m^2+3k^2)\left(\frac{4}{15}k^2-1\right)+\frac{1}{5}(k^2+m^2)^2\right]-(k^2+n^2)\left[1-(k^2+n^2)+\right.$$

$$\left.\left.+\frac{(k^2+n^2)^2}{3}\right]\arcsin\frac{k}{\sqrt{k^2+n^2}} - \frac{kn}{3}\left[3+(n^2+3k^2)\left(\frac{4}{15}k^2-1\right)+\frac{1}{5}(k^2+n^2)^2\right]\right\},$$

$$B_{kmn} = \frac{2}{\pi}\left[(k^2+m^2)\arcsin\frac{k}{\sqrt{k^2+m^2}} + k(m-n) - (k^2+n^2)\arcsin\frac{k}{\sqrt{k^2+n^2}}\right];$$

$$C_{kmn} = \frac{2}{3\pi}\left[(1-k^2-n^2)^3-(1-k^2-m^2)^3\right],$$

$A_{km}, B_{km}, E_{km}, F_{km}$ are described by expressions $A_{kn}, B_{kn}, E_{kn}, F_{kn}$, respectively when the parameter n is replaced with the parameter m. The expressions given above (12a-f) take a very complicated form which results from successive transformations of relations (2), (3) and (10). The present investigation is the first attempt in the world literature to solve this problem analytically and, therefore, it seems purposeful to present the whole form of the solution.

The proportionality factor a described by expressions (12a-f) depends on the ratio k of the width of the ultrasonic beam to the inner diameter of the blood vessel, and in addition on the ratio H/B of the width of the ultrasonic beam along the blood vessel to its width across the vessel and on the angles θ_n and θ_0 at which the ultrasonic wave is transmitted and received with respect to the blood vessel. Fig. 7 shows values of the factor a calculated from relations (12a-f) for a measuring system with two square transducers placed at the angle $\gamma = 170°$ with respect to each other.

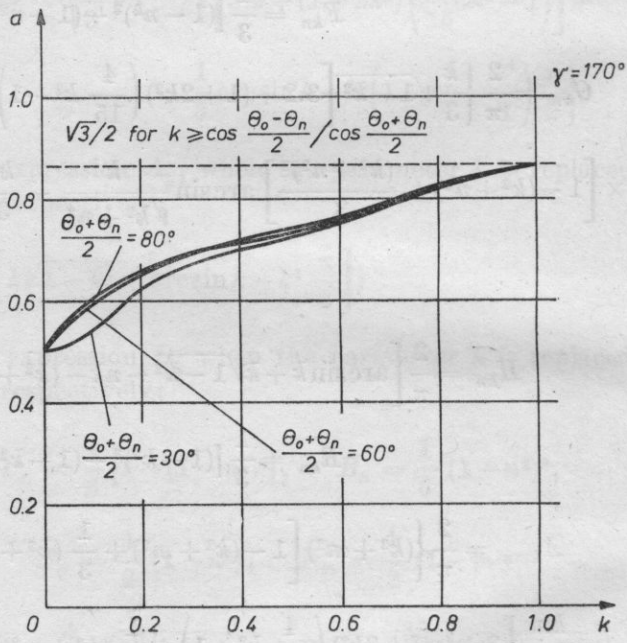

Fig. 7. The factor a of proportionality between the mean frequency and the frequency of zero crossing of the Doppler signal for the parabolic blood flow velocity profile and a measuring system with two square transducers, in which the point of intersection of axes of the ultrasonic beams is on the axis of the vessel (cf. Fig. 2b)

k – the ratio of the width of the ultrasonic beam to the inner diameter of the vessel, θ_n, θ_0 – the angles between the transmitted and received ultrasonic beams and the axis of the vessel, γ – the angle between the transducers

5. Limitations of the ultrasonic *C.W.* Doppler method in measurement of the absolute blood flow velocity

The ultrasonic *C.W.* Doppler method does not permit quantitative information about the blood flow velocity profile to be obtained. In the case when it is impossible to determine the profile analytically, then error can be committed in calculation of the mean blood velocity v_s on the basis of the Doppler frequency measured by the method of zero-crossing (formula (3a)). This results

from the fact that without quantitative information about the blood flow velocity profile it is impossible to determine the exact value of the factor of proportionality a between the measured Doppler frequency and the mean frequency f_s corresponding to the mean blood flow in the cross-section of the blood vessel (cf. formula (2)). Under the assumption that the mean blood flow velocity profile during the cardiac cycle is contained between the parabolic and flat profiles, the mean a_s of the factor a can be calculated from the relation [6, 7]

$$a_s = \frac{2a}{1+a}, \tag{13}$$

where a is a factor for a parabolic profile.

Assuming the factor a_s as the basis for calculating the mean blood flow velocity, the error which can result from the lack of information about the blood flow profile is contained in the following interval

$$0 \leqslant \left| \frac{v_0 - v_s}{v_s} \right| < (1 - a_s) \cdot 100\,\%, \tag{14}$$

where v_0 — the mean blood flow velocity calculated from the measured Doppler frequency, v_s — the real mean blood flow velocity. The numerical value of this error can be determined by calculation of the value of the factor a_s from relations (11) — (13). For the measuring system where the point of intersection of axes of the ultrasonic beams is outside the blood vessel (Fig. 2*a*), the error described by expression (14) is less than 7.2 % when the ultrasonic beam occupies the whole cross-section of the vessel.

An additional source of error in transcutaneous measurement of blood flow is the lack of information about the inner diameter of the blood vessel. This is mainly the case when the diameter of the blood vessel is greater than the width of the ultrasonic beam, since then the calibration coefficient of a Doppler flowmeter considerably changes its value, depending on the ratio k of the width of the ultrasonic beam to the inner diameter of the blood vessel (cf. Figs. 6 and 7).

The error in measurement of the mean blood flow velocity, determined from relations (11), (13) and (14) and resulting from the lack of information about the blood flow velocity profile and the diameter of the blood vessel, is less than 15 % for $k > 0.5$. From the point of view of diagnostics of the human circulation system this error is negligible, however, since blood flow velocities in normal and pathological cases are different by several times. The sources of error in measurement of the blood flow velocity also include the factors affecting the accuracy of measurement of the Doppler frequency by the method of zero-crossing (cf. section 2) and in addition the lack of information about the angle between the ultrasonic beam and the blood vessel. The problem of measurement of this angle was solved for peripheral vessels by application in the measurement of the

blood velocity of an ultrasonic probe consisting of two independent pairs of transmitting and receiving transducers placed at a known constant angle to each other [1, 6, 7].

6. Conclusions

In summary of the foregoing considerations of the ultrasonic *C.W.* Doppler method it should be stated that quantitative evaluation of the blood flow velocity by this method is very difficult and requires specification of conditions of the measurement, which is not always possible. It follows therefore that the technique of measurement of the Doppler frequency by the method of zero crossing, used in ultrasonic flowmeters, does not give direct information about the mean Doppler frequency proportional to the mean blood flow velocity in the cross-section of the vessel.

The sought information can be obtained from determination of the factor a of proportionality between the frequencies mentioned above. The value of the factor is not constant, however, and depends on such factors as the blood flow velocity in the blood velocity, the ratio of the width of the ultrasonic beam to the inner diameter of the vessel and the possition of the transducers transmitting and receiving the ultrasonic wave with respect to the blood vessel. The lack of information about the above parameters is a source of error in quantitative evaluation of the blood flow velocity on the basis of the Doppler frequency measured by the method of zero crossings. This error is smallest when the mean proportionality factor a_s described in this paper is taken as the basis of calculation of the mean blood flow velocity and when the ultrasonic beam occupies the whole cross-section of the blood vessel. In such a case for a measuring system in which the point of intersection of axes of the transmitted ultrasonic beam and the one received from flowing blood is outside the blood vessel, the error under consideration is less than 7.2% when the blood flow velocity varies and takes shapes contained between parabolic and flat profiles.

References

[1] K. Borodziński, L. Filipczyński, A. Nowicki, T. Powałowski, *Quantitative transcutaneous measurements of blood flow in carotid artery by means of pulse and continuous wave Doppler methods*, Ultrasound in Medicine and Biology, **2**, 189-193 (1976).

[2] W. R. Brody, J. D. Meindl, *Theoretical analysis of the C.W. Doppler ultrasonic flowmeter*, IEEE Trans. on Biomedical Engng., **21**, 2, 183-192 (1974).

[3] L. Filipczyński, P. Herczyński, A. Nowicki, T. Powałowski, *Blood flow-hemodynamics and ultrasonic Doppler measurement methods*. PWN (1980), pp. 87-114.

[4] S. W. Flax, J. G. Webster, S. J. Updike, *Noise and functional limitations of the Doppler blood flowmeter, Cardiovascular amplications of ultrasound*, Ed. R. S. Reneman, North Holland Publ. Comp. (1974), pp. 18-31.

[5] P. PERONNEAU, J. BOURNAT, A. BUGNON, A. BARBET, M. XHAARD, *Theoretical and practical aspects of pulsed Doppler flowmetry: real time application to the measure of instantaneous velocity profiles in vitro and in vivo, Cardiovascular applications of ultrasound*, Ed. R. S. RENEMAN, North Holland Publ. Comp. (1974), pp. 66-84.

[6] T. POWAŁOWSKI, *Quantitative blood velocity measurements by means of continuous wave Doppler method*, Proc. 9th Int. Congress on Acoustics, Madrid 1977, 928.

[7] T. POWAŁOWSKI, *Real time automatic transcutaneous determination of blood flow velocity by means of C.W. Doppler method eliminating angle dependence*, Proc. 2 Congress of FASE 1978, II, 157-160.

[8] J. M. REID, R. A. SIGELMANN, M. G. NASSER, D. W. BAKER, *The scattering of ultrasound by human blood*, Proc. 8th Int. Conf. Med. Biol. Engng. (1969), 10-7.

[9] S. RICE, *Mathematical analysis of random noise*, Bell System Tech. J., **23**, 282-330 (1944).

[10] R. J. URICK, *A sound velocity method for determining the compressibility of finely divided substances*, J. Ap. Physics, **18**, 983 (1947).

Received on July 14, 1980; revised version on February 12, 1981.

ARCHIVES OF ACOUSTICS
6, 3, 307-319 (1981)

ULTRASONIC VELOCITY MEASUREMENTS OF HYDRATION NUMBERS OF SUGARS IN ALCOHOL-WATER SOLUTIONS*

ADAM JUSZKIEWICZ

Institute of Chemistry, Jagiellonian University
(30-060 Kraków, ul. Karasia 3)

This paper describes a method for finding the hydration numbers of electrolytes and non-electrolytes based on ultrasound velocity measurements in a mixed ethanol-water solvent. The hydration numbers of sugars such as: glucose, mannose, arabinose, xylose, saccharose and lactose were determined. Interpretation of the results obtained on the basis of the theory of "specific hydration" for sugars was presented.

1. Introduction

Ultrasonic interferometry can be a useful instrument for investigation of the hydration of substances in an aqueous environment. The advantage of this particular method of hydration number determination is its great simplicity. The first method of determining the hydration number using ultrasonic velocity and density measurements was proposed by PASSYNSKY about forty years ago [1, 2]. PASSYNSKY assumed that the decrease of solution compressibility is connected with the strong compression of water in an ionic field and that this decrease of compressibility in solution is due to hydration. He found the following expression for determining the hydration numbers of molecules in an aqueous solution:

$$n_h = (1 - \beta_T/\beta_T^0)\frac{100 - x}{M_0}\frac{M_2}{x}, \tag{1}$$

where β_T and β_T^0 are the isothermal coefficients of compressibility of the solution and solvent respectively, x is the weight percentage of the solute, M_0 is the molecular weight of the solvent and M_2 is the molecular weight of the solute.

* The work described in this paper was partly financed by the U.S. Agricultural Dept. under Public Law 480 agreement.

All of the remaining methods using ultrasonic measurements for the determination of hydration numbers are based on this expression [3-8]. In deriving this expression PASSYNSKY assumed that an ion, together with its hydration shell, is incompressible. The other authors assumed ionic incompressibility, but the compressibility of the water in the hydration shell they assumed to be equal to the compressibility of free water. The incompressibility of an hydrated ion can only be valid for small ions such as: Mg^{2+} and Li^{+}. In the case of larger ions the electric field of these ions interacting with water molecules changes widely and the local compressibility of the water molecules in the hydration shells also changes ($0-4.5\cdot10^{-10}N^{-1}\ m^2$) [9]. For molecules of non-electrolytes and macromolecules the situation is still more complicated because besides the necessity of taking into consideration the compressibility of the water in the hydration shell, the compressibility of the solute itself has to be considered also. It has generally been believed that the small molecules of nonelectrolytes are incompressible and the compressibility of the hydration water is equal to the compressibility of normal ice [3, 4]. Thus, the hydration numbers of electrolytes and nonelectrolytes obtained by different authors on the basis of different assumptions cannot be relied upon because the possibility of experimental verification of these assumptions does not exist. For these reasons the method of measurement of hydration numbers which was first proposed by YASUNAGA at al. [10, 11] was used. This method gives valid results for electrolytes as well as for non-electrolytes and macromolecules. Using this method the hydration of the molecules can be determined by ultrasonic velocity measurements in alcohol-water solutions. It is known that the dependence of the ultrasonic velocity as a function of alcohol concentration in water-alcohol mixtures is parabolic, and the maximum is precisely defined for each temperature.

The addition of any given substance causes the maximum to shift in the direction of smaller alcohol concentration. The difference between the abscissae of the maxima of the curves obtained is caused by the molecules of the solute bonding part of the water.

With this assumption we have

$$\frac{A_0}{W_0} = \frac{A_1}{W_1 - W_x} = \text{const}, \tag{2}$$

where A_0 and W_0 are the amounts of alcohol and water corresponding to the maximum for alcohol-water mixtures without solute, and A_1 and W_1 are the amounts of alcohol and water at the maximum for alcohol-water solutions containing a certain amount of solute. W_x in this equation is the amount of water bound to the solute.

In a previous paper [12] the hydration numbers of polyethylene glycols of different molecular weights were determined using the method described above.

2. The structure of alcohol-water solutions

The addition of small amount of a non-electrolyte to water causes stabilization of the structure of the water [13, 14]. Stabilization of the structure of water implies effects connected with the passage of non-electrolyte molecules into the cages of this structure. According to DANFORD and LEVY [15] the structure of the water (particularly its short-range order) ought to be considered as a defective ice structure with partly filled cages. In the structure of ice every cage is surrounded by six water molecules. Thus every molecule neighbours with three cages and the number of cages in the structure of ice is equal to half the number of molecules. In water some of the molecules form a skeleton of cages and some fill up the cages. The presence of non-electrolyte molecules in the cages leads to a decrease in the translational mobility of the water molecules In effect it causes a decrease in the selfdiffusion coefficient of water, and change of the kinetic and equilibrium properties of a solution. For alcohol solutions an anomal dependence of some of the properties of the solution can be observed within the concentration range of 0.03 to 0.2 mole fraction of alcohol [16-18].

3. Investigation in alcohol-water solutions using infra-red spectroscopy and ultrasonic measurements

In Fig. 1 the results of measurements of ultrasonic velocity in alcohol-water solutions at 25°C (curve *1*) and the shifts of the valence-deformation band of water $\nu_\delta + \nu_{OH}$ with the maximum at 5180 cm^{-1} (curve *2*) are presented. Measurements of the ultrasonic velocity were performed using the "sing around" method described below and the spectroscopic measurements were made using infra-red spectrometer of high resolution Digilab produced by U.S.A.

As can be seen from Fig. 1 the ultrasonic velocity increses at first, reaches a maximum at a concentration $k_{mol} = 0.106$ and then decreases. On the curve of $\Delta\nu_{max}$ as a function of alcohol concentration an increase in the shift of the studied absorption band in the concentration range 0-0.1 k_{mol} is observed, and for the higher concentrations this shift is constant and independent of alcohol concentration up to $k_{mol} \sim 0.4$ [19]. Previous infrared spectroscopic investigations [19, 20] showed that the stabilization of the structure of water by non-electrolyte molecules is connected with an increase of the stability of the hydrogen bonds between the water molecules. This effect is reflected in the shift of absorption bands in the direction of lower frequencies. The observed order of water is due to the influence of non-polar groups of non-electrolyte molecules on water; around the non-electrolyte molecules associated molecules of water called non-polar group solvates appear. This type of solvation is defined as second order solvation [21].

Mathematical analysis of the shift of the absorption band at 5180 cm^{-1}, assuming a Gaussian character for the contour of this band, allowed the determination of the mean number of water molecules in the non-polar group solvate. For ethyl alcohol it equals 6 ± 1 [19] and 7 ± 1 [20] at 20°C and it decreases with increasing temperature.

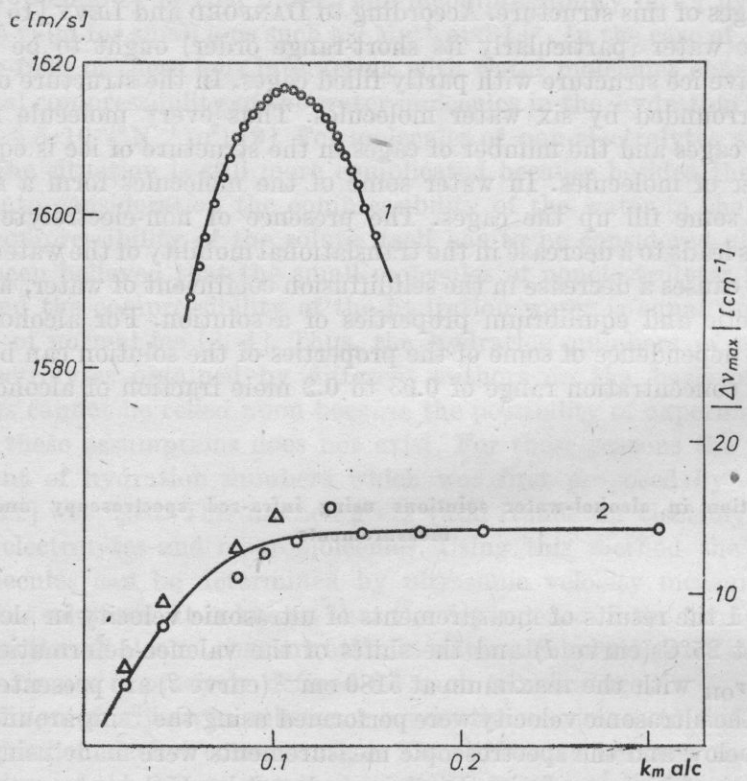

Fig. 1. Ultrasonic velocity (*1*) and the shift of the valence-deformation band of absorption of water with the maximum at 5180 cm^{-1} (*2*) versus k_{mol} of alcohol for an ethanol-water system

It is known that the maxima on the ultrasonic velocity curves (minima on the compressibilty curves) shift in the direction of lower concentrations with increasing temperature. This is caused by a decrease in the "open-work" structure of water with increasing temperature. The number of empty cages ("holes") which can be occupied by alcohol molecules decreases and the amount of "free" water molecules increases. Assuming that at 0°C all the water molecules occur in an ice-like skeleton it can be presumed, with a high probability, that the concentration at which the ultrasonic velocity maximum at 0°C occurs defines the number of molecules surrounding the non-polar molecule. Due to the impossibility of defining this concentration at 0°C with satisfactory accuracy (the error

of the velocity measurement ought not to exceed 2 cm/s) ultrasound velocities at higher temperatures were determined.

In Fig. 2 the results of our measurements in ethanol-water solutions in the temperature range 5-35°C are presented. As can be seen in Fig. 2 the ultrasound

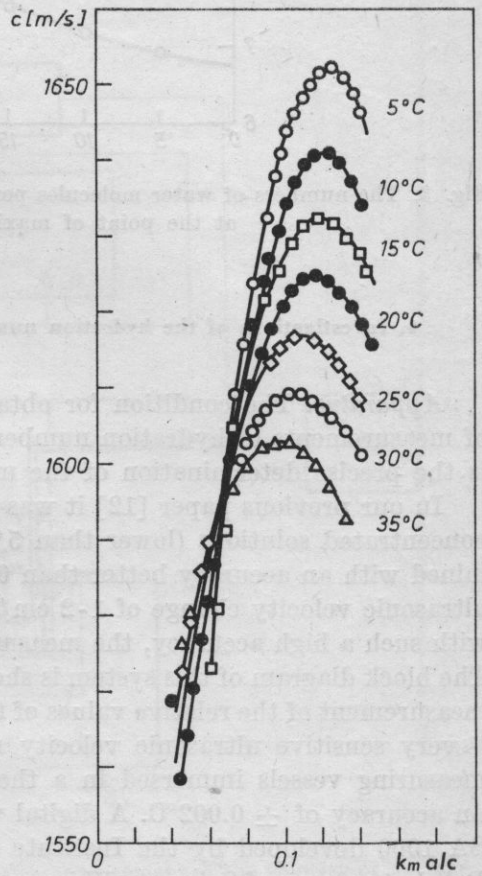

Fig. 2. Ultrasonic velocity versus k_{mol} of alcohol in the temperature range 5-35°C for the ethanol-water system

velocity maximum shifts in the direction of lower concentrations of alcohol. The number n (mole/mole) of water molecules per alcohol molecule were determined at the maximum points in the investigated temperature range and are graphically presented in Fig. 3.

Extrapolating to a temperature of 0°C a value of $n = 6.6$ was obtained. The results obtained are in good agreement with the results of infrared measurements. Theoretically at 0°C n should be equal to 6 for a perfect ice crystal lattice of ice (octahedral structure). However, due to the occurence of defects in the water structure (Frenkl and Schoottky defects), the number of empty cages is less and $n > 6$.

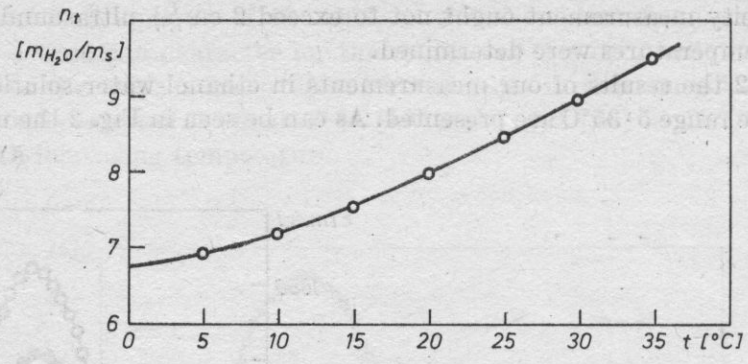

Fig. 3. The numbers of water molecules per alcohol molecule as a function of temperature at the point of maximum ultrasonic velocity

4. Investigations of the hydration numbers of sugars in alcohol-water solutions

Apparatus. The condition for obtaining reproducible and authentic results of measurements of hydration numbers from ultrasonic velocity measurements is the precise determination of the maximum point.

In our previous paper [12] it was shown that in the case of not too highly concentrated solutions (lower than 5%) the maximum point should be determined with an accuracy better than 0.2 ml of alcohol which corresponds to an ultrasonic velocity change of 1-2 cm/s. In order to perform the measurements with such a high accuracy, the measurement system described below was used. The block diagram of this system is shown in Fig. 4. Such a good accuracy in the measurement of the relative values of the ultrasonic velocity was obtained with a very sensitive ultrasonic velocity meter, with the construction of suitable measuring vessels immersed in a thermostat, with thermostatic control with an accuracy of $\pm$ 0.002°C. A digital velocity meter of the "sing around" type SA 1000 developed by the Institute of Fundamental Technological Research, Polish Academy of Sciences, Warsaw, was used for the ultrasonic velocity measurements. The change of the last figure on the wave meter display gives, depending on the measuring vessel used, a change in velocity of the order of 0.5-1 cm/s. A cylindrical measuring vessel of stainless steel which has a small coefficient of expansion (50 mm diameter) was immersed at a constant level in the thermostat. The termostat had a 25 dcm^3 capacity, double walls and was powered and controlled by a temperature regulator of the type 650 and power unit of the type 651 developed by UNIPAN, Warsaw. The regulator and the power unit are part of a microcalorimeter produced by that firm. The regulator and the power unit are automatically controlled by a resistance platinum sensor of type 2100 s-3 wire-100ohm of English production. The temperature in the measuring vessel was controlled by the same kind of resistance sensor with an

accuracy of $\pm$ 0.001°C. The thermostat was cooled by water from a second thermostat in which the temperature of the thermostating water was 2-3°C lower than the temperature of the water in the main thermostat. With the aim of assuring the stability of the "sing-around" velocity meter, the wavemeter and the regulator, the environmental temperature was held constant (21 $\pm$ 1°C).

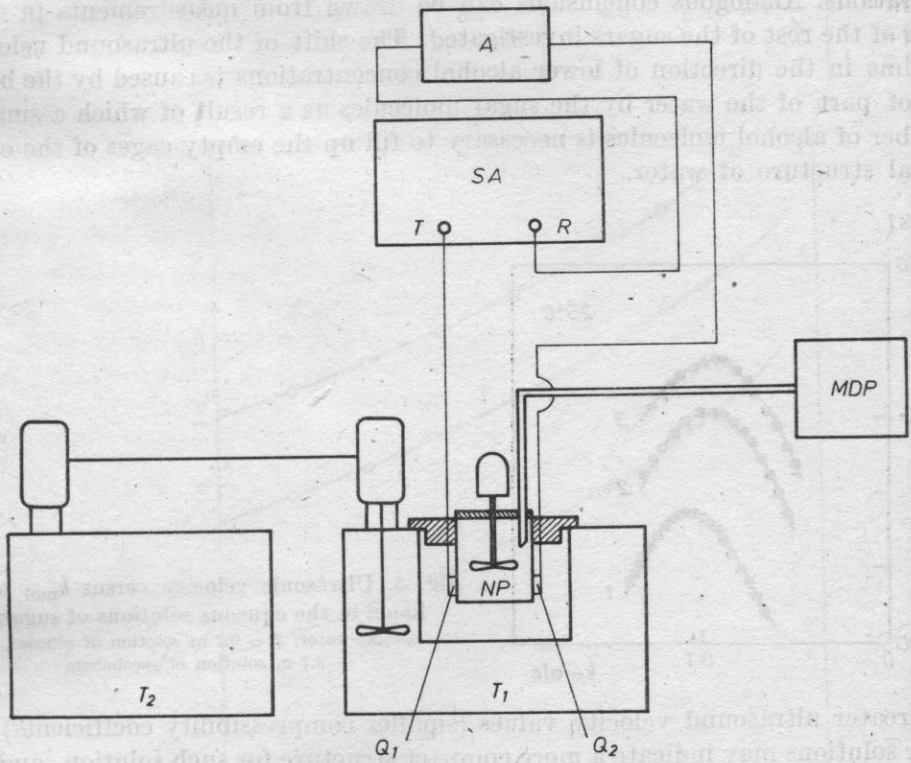

Fig. 4. Block diagram of the apparatus used for the measurement of the velocity of the ultrasonic waves

Procedure. Hydration number measurements of sugars such as: glucose, mannose, arabinose, xylose, saccharose and lactose were performed over a temperature range of 10-40°C. Furthermore, hydration number measurements of sugars as a function of concentration were performed at 25°C. The range of concentrations investigated was 3-25% wt. for glucose and saccharose, and 3-8% wt. for the remaining sugars.

The results of these measurements are presented in Tables I and II and also graphically in Figs. 5 and 6.

Results and discussion. In Fig. 5 the curves of ultrasonic velocity as a function of ethanol concentration, expressed as molar fractions for glucose (curve *2*) and saccharose (curve *3*) solutions having concentrations of 0.7 mole of sugar per 1000 g of water, are presented. As can be seen from the graphs, the ultrasonic velocities in ethanol-water solutions of glucose and saccharose are greater by 20-30 m/s than the velocities in alcohol-water solutions without sugar (curve *1*). Simultaneously the maximum velocity points occur at lower alcohol concentrations. Analogous conclusions can be drawn from measurements in solutions of the rest of the sugars investigated. The shift of the ultrasound velocity maxima in the direction of lower alcohol concentrations is caused by the binding of part of the water by the sugar molecules as a result of which a smaller number of alcohol molecules is necessary to fill up the empty cages of the octahedral structure of water.

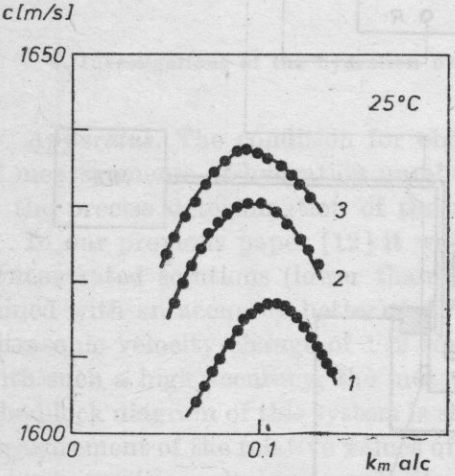

Fig. 5. Ultrasonic velocity versus k_{mol} of ethanol in the equeous solutions of sugars
1 – alcohol-water, *2* – 0.7 m solution of glucose, *3* – – 0.7 m solution of saccharose

Greater ultrasound velocity values (smaller compressibility coefficients) for sugar solutions may indicate a more compact structure for such solution and also the formation of strong hydrogen bonds between the hydroxyl groups of the sugar and the water molecules. The existence of such bonds has been confirmed repeatedly using magnetic resonance methods [22-24]. In Table 1 the results of hydration number measurements of the investigated substances at 25°C and their dependence on concentration expressed in weight per cent are presented.

From the above data it can be seen that in the concentration range of 3-25 % wt. of glucose and saccharose, and 3-8 % wt. of the other sugars, the hydration numbers (within experimental error) are not dependent on concentration. The results of hydration number measurements of glucose and saccharose and their dependence on temperature from 10-40°C are presented in Fig. 6. Similar curves were obtained for the remaining sugars. As can be seen from Fig. 6 the temperature dependencies of the hydration numbers of glucose (2) and saccharose (3) are of the same type as the temperature dependence (1) of the number

Table 1

Concentration (% of weight)	Glucose	Mannose	Arabinose	Xylose	Lactose	Saccharose
3	4.7	4.8	4.0	4.0	8.0	7.4
5	5.2	4.9	4.0	4.1	8.3	7.2
6	5.2	5.1	3.9	4.1	8.2	7.0
8	5.1	5.1	3.9	4.0	8.1	7.0
20	4.9					6.8
25	4.9					6.8

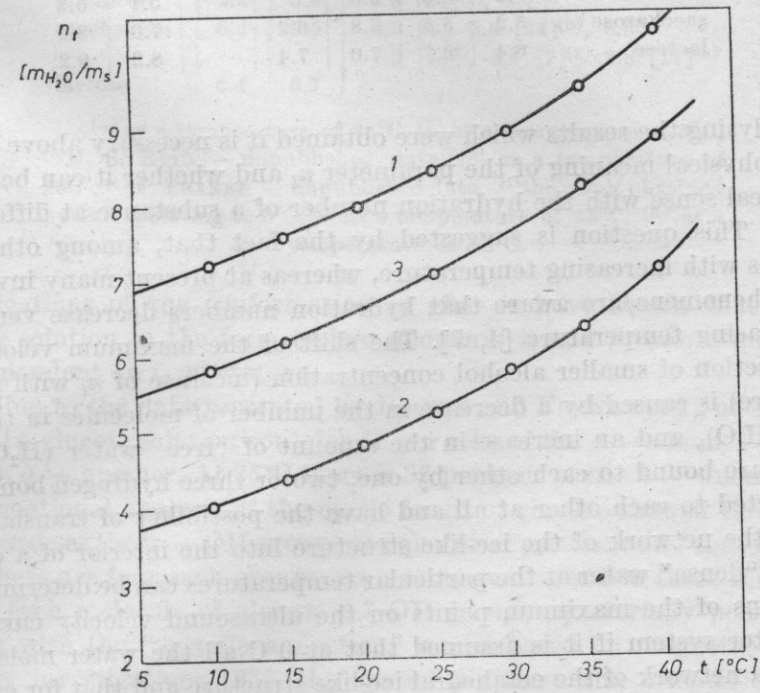

Fig. 6. The numbers of water molecules n_t per mole of solute as a function of temperature at the points of maximum ultrasonic velocity
1 – ethanol, *2* – glucose, *3* – saccharose

of moles of water for each mole of ethyl alcohol at the maximum velocity points (Fig. 3).

The curves in Fig. 3 and 6 can be described by the following equation

$$n_t = n_0 + At + Bt^2 \tag{3}$$

where n_0 is the hydration number at 0°C, and A and B are empirical coefficients equal to $3.83 \cdot 10^{-2}$ and $1.3 \cdot 10^{-3}$ respectively.

The numerical values of n_0 and $n_{5°C}$ calculated on the basis of the above equation, and the values of n_t obtained for the particular sugars at different temperatures are presented in Table 2.

Table 2

	n_0	$n_{5°C}$	$n_{t°C}$ 10	15	20	25	35
glucose	3.4	3.7	4.0	4.4	4.8	5.2	6.4
arabinose	2.2	2.5				4.0	5.2
xylose	2.3	2.6	3.0			4.1	
mannose	3.3	3.6	3.9			5.1	6.3
saccharose	5.2	5.5	5.8	6.2		7.0	8.2
lactose	6.4	6.7	7.0	7.4		8.2	9.2

In analysing the results which were obtained it is necessary above all to consider the physical meaning of the parameter n_t and whether it can be identified in a physical sense with the hydration number of a substance at different temperatures. This question is suggested by the fact that, among other things, n_t increases with increasing temperature, whereas at present many investigators of these phenomena are aware that hydration numbers decrease very quickly with increasing temperature [4, 7]. The shift of the maximum velocity point in the direction of smaller alcohol concentration (incerase of n_t with increasing temperature) is caused by a decrease in the number of molecules in the ice-like skeleton $(H_2O)_b$ and an increase in the amount of "free" water $(H_2O)_d^*$ whose molecules are bound to each other by one, two or three hydrogen bonds, or are not connected to each other at all and have the possibility of translating from a node of the network of the ice-like structure into the interior of a cage. The amount of "dense" water at the particular temperatures can be determined from the locations of the maximum points on the ultrasound velocity curves in an alcohol-water system if it is assumed that at 0°C all the water molecules are present in a network of the octahedral ice-like structure and that for each molecule of ethyl alcohol there are six molecules of water. If the amount of "dense" water occuring at the particular temperatures is subtracted from the values obtained for n_t, the same number n_0 is obtained, as was earlier defined as the hydration number at 0°C and which is found by extrapolation of the n_t dependence to 0°C.

Is it possible therefore to assign to the values of n_0 the physical meaning of hydration number?

---

* Consistent with the expressions used in previous papers [23, 26] water occuring in the ice-like structure is expressed as "bulky" – $(H_2O)_b$ and "free" water as "dense" – $(H_2O)_d$.

Based on contemporary knowledge of the structure of sugar solutions and the comparison of the results obtained with literature data (Table 3), the answer to this question should be affirmative.

Table 3

	n_0	$n_{5°C}$	Literature data
glucose	3.4	3.7	3.5 [4][a], 3.7 [24][b], 2.7[c], 4.0 [25], 5.0 [22], 4.5 [3][d], 3.5 [11][h]
arabinose	2.2	2.5	3.5 [4]
xylose	2.3	2.6	2.3 [4]
mannose	3.3	3.6	3.9 [24][b], 3.7[e]
saccharose	5.2	5.5	3.8 [4], 6.6 [24][b], 6.5[e] 5.3 [7][f], 4.1 [7][g] 3.8 [11][h]
lactose	6.4	6.7	

[a] at a temperature of 25°C, [b] at a temperature of 5°C, [c] D. S. REID – unpublished data, [d] at a temperature of 20C°, [e] F. FRANKS – unpublished data, [f] the result obtained by extrapolating to 0°C, [g] at a temperature of 15°C, [h] at a temperature of 25°C.

Investigations of the conformation of glucose have shown that it occurs in a water solution in the form of two anomers: α and β, whose quantitative ratio is dependent on temperature.

According to the data presented by BOCIEK and FRANKS [24], at a temperature of 5°C a glucose solution contains 68 per cent of the β – anomer and 32 per cent of the α – anomer. At 25°C there is 37 per cent of the α – anomer.

Conformational analysis of the cyclic forms of glucose showed that the α – anomer possesses theer – OH groups at equatorial positions and that in the β – anomer, there are four such groups. At a temperature of 5°C there remains therefore for each molecule of glucose 3.7-OH groups equatorially positioned. In agreement with the "specific hydration" model based on magnetic resonance and X-ray investigations [23], the spatial positions and orientations of the equatorial –OH groups eases the hydration interaction of these groups with water molecules. If it is assumed that only the equatorial –OH groups of the sugar are hydrated, from SUGGETT's data [24] indicates that each group is hydrated by one water molecule. At a temperature of 5°C the hydration number of glucose given by SUGGETT is 3.7 and is equal to the average number of equatorial –OH groups per molecule of glucose. As can be seen from Table 3, an identical value was obtained from ultrasonic measurements of glucose at 5°C. At 0°C, n_0 is smaller and is equal to 3.4 m H_2O/m of sugar. For the remaining sugars investigated the values of n_0 which were obtained were approximately equal to the number of equatorial –OH groups. In reference to the "specific hydration" model of sugars the n_0 parameter is, therefore, the hydration number of the given

sugar at a temperature of 0°C, which, it is proposed, should be called the absolute hydration number. The values of n_0 which were obtained for glucose and xylose correspond to the data obtained by SHIIO [4] at a temperature of 25°C using a slightly different method of determining the hydration numbers from the ultrasonic measurements. In order to produce an expression for the hydration number, Shiio assumed that the compressibility of sugar is equal to zero and the compressibility of the water in the hydration shell is equal to the compressibility of normal ice ($\beta = 1.8 \cdot 10^{10}$ m^{2}N^{-1}).

Both of these assumptions can be verified experimentally. However it seems that the second assumption, particularly, is more probable at a temperature of 0°C and that at higher temperatures the compressibility of the hydration water is certainly larger. As the temperature increases the compressibility will increase to the compressibility of pure water. Thus the hydration number values obtained by SHIIO are close to the values of n_0 obtained in this paper. If this discussion is accepted, then the rapid decrease of the hydration numbers of sugars with increasing temperature observed by many authors is probably only an apparent effect, and in reality the hydration numbers do not decrease with a temperature increase. If the participation of "free" water in the hydration of sugars is not taken into consideration, the above conclusion finds confirmation in the investigations which were conducted. The hydration number values which were obtained over a temperature range of 10-40°C are approximately equal to the absolute hydration number n_0.

References

[1] A. G. PASSYNSKY, *Shimaemost i solvatatsia rastvorov elektrolitov*, Zhur. Fiz. Khim. **11**, 606-612 (1938).

[2] A. G. PASSYNSKY, *Solvatatsia nieelektrolitov i shimaemost ikh rastvorov*, Zhur. Fiz. Khim., **20**, 989-994 (1946).

[3] H. SHIIO, T. OGAWA, H. YOSHIHASHI, *Measurements of the amount of bount water by ultrasonic interferometer*, J. Amer. Chem. Soc., **77**, 4, 4080-4982 (1955).

[4] H. SHIIO, *Ultrasonic interferometer measurements of the amount of bound water*, Saccharides, J. Amer. Chem. Soc., **80**, 1, 70-73 (1958).

[5] K. TAMURA, T. SASAKI, *Ionic hydration in an aqueous electrolyte solution and its parameter*, Bull. Chem. Soc. Japan, **36**, 975-980 (1963).

[6] D. S. ALLAM, W. H. LEE, *Ultrasonic studies of electrolyte solutions, Part II. Compressibilities of electrolytes*, J. Chem. Sod. (A), **1**, 5 (1966).

[7] S. GOTO, T. ISEMURA, *Studies of the hydration and the structure of water and their roles in protein structure. IV. The hydration of amino acids and oligopeptides*, Bull. Chem. Soc. Japan, **37**, 1697-1701 (1964).

[8] J. STUEHR, E. YEAGER, *Physical Acoustics*, New York 1965, vol. II, part *A*, chapter 6.

[9] J. E. DESNOYERS, R. E. VERRALL, B. E. CONWAY, *Electrostriction in aqueous solutions of electrolytes*, J. Chem. Phys., **43**, 243-250 (1965).

[10] T. YASUNAGA, Y. HIRATA, Y. KAWANO, M. MIURA, *Ultrasonic studies of the hydra-*

tion of various compounds in an ethanol-water mixed solved. Hydration of inorganic compounds, Bull. Chem. Soc. Japan, **37**, 867-871 (1964).

[11] T. Yasunaga, I. Usui, K. Iwata, M. Miura, *Ultrasonic studies of the hydration of various compounds in an ethanol-water mixed solvent. II. The hydration of organic compounds*, Bull. Chem. Soc. Japan, **37**, 1658-1660 (1964),

[12] A. Juszkiewicz, J. Potaczek, *Investigation of the hydration of polyethylene glycols using an acoustic method*, Archives of Acoustics, **2**, 3, 207-212 (1977).

[13] I. V. Kochniev, *O mekhanizmie stabilizatsii vody nieelektrolitami*, Zhur. Strukt. Khim., **13**, 362-364 (1973).

[14] O. Ya. Samoilov, *K osnovam kineticheskoj teorii gidrofobnoj gidratatsi v razbavlennykh vodnykh rastvorakh*, Zhur. Fiz. Khim., **52**, 1857-1862 (1978).

[15] M. D. Danford, A. H. Levy, *The structure of water at room temperature*. J. Amer. Chem. Soc., **84**, 3965-3966 (1962).

[16] K. Nakanishi, *Partial molal volumes of butyl alcohols and of related compounds in aqueous solution*, Bull. Chem. Soc. Japan, **33**, 793-797 (1960).

[17] G. Franks, D. J. G. Ives, *Alcohol-water mixtures*, Quart. Rev., **20**, 1-50 (1966).

[18] V. N. Karcew, V. A. Zabielin, O. Ya. Samoilow, *Izotermiczeskaja shimajemost razbawlennych wodnych rostworow riada nieelektrolitow*, Żur. Fiz. Chim., **53**, 1774-1778 (1979).

[19] I. N. Kochniew, A. I. Khaloimow, *Sostojanije wody w rostworach spirtow*, Żur. Strukt. Chim., **14**, 791-796 (1973).

[20] A. P. Zhukowsky, M. V. Dengina, *Spektroskopiczeskij mietod opriedielienija czisel gidratatci niepolarnych grup w wodnych rastworach nieelektrolitow*, Żur. Strukt. Chim., **17**, 446-449 (1976).

[21] H. G. Hertz, M. D. Zeidler, *Elementarvorgänge in der hydrathülle von ionen aus protonen – und deuteronenrelaxationszeiten*, Zeit. Elektrochem., **67**, 774-786 (1963).

[22] F. Franks, D. S. Reid, A. Suggett, *The physical chemistry of aqueous systems*, Plenum Press, New York 1973, pp. 1-20.

[23] F. Franks, *The solvent properties of water*, *Water – a comprehensive treatise*, Plenum Press, New York – London 1973, vol. 2, pp. 1-54.

[24] S. Bociek, F. Franks, *Proton exchange in aqueous solutions of glucose*, Faraday Trans., I, **2**, 262-270 (1979).

[25] A. B. Biswas, A. C. Kumash, G. Pass, G. Phillips, *The effect of carbohydrates on heat of fusion of water*, J. Solution Chem., **4**, 581-588 (1975).

[26] A. Suggett, *Polysaccharides*, *Water – a comprehensive treatise*, Plenum Press, New York–London 1975, vol. 4, pp. 519-567.

Received on June 12, 1980; revised version on December 16, 1980.

VII Symposium on Application of Noise and Vibration in Diagnostics of Machinery

The universally occurring acoustic phenomena which accompany the operation of machinery and technological equipment permit wide applications of acoustic signals in computer science and diagnostics. Application of this potential in practice requires development and sophistication of measurement methods, and particularly seeking qualitatively and quantitatively correct estimation of vibration and noise of given machinery.

These problems were discussed at the VII Symposium on Application of Noise and Vibration in Diagnostics of Machinery. As previous Symposia it was organized by Institute of Motor Transport of Silesian Technical University on January 11-16, 1981 at Wisła-Malinka.

The papers delivered at the Symposium continued the problems discussed at previous conferences. Prof. Dr. Ludwik MÜLLER was the Scientific Chairman of the Symposium. The Symposium was concluded with a panel session chaired by Prof. Dr. Stefan CZARNECKI of Institute of Fundamental Technological Research, Polish Academy of Sciences, Warsaw.

Janusz Gadulski

BOOK REVIEWS

Daryl N. MAY (ed.), *Handbook of noise assessment*, Van Nostrand Company, New York 1978 (391 pages).

An increase of noise in the environment of man makes it necessary to present more closely the effects of noise on man, both from the psychological and physiological points of view. For this reason Van Nostrand Reinhold Environmental Engineering Series published a collective work on the effect of noise on man, featuring chapters by prominent experts and edited by Daryl N. MAY.

The book has two parts. The first concerns the psychological aspects of the effect of noise on man, while the second deals with the health aspects.

The first part is divided into ten chapters:

1. Basic subjective responses to noise – D. N. MAY.

This chapter presents the basis criteria of noise loudness assessment and noise annoyance under the steady-state and transient conditions. It also discusses the effect of noise on the intelligibility of speech.

2. Noise of surface transportation to nontravelers – M. J. CROCKER.

This part presents the main sources of surface transportation, with a division into aircraft and helicopteres at airport, automotive and rail transportation, recreational vehicles such as scooters, motorcycles, motorbicycles, snowmobiles and speedboats. It also presents

the problem of the annoyance of the transportation means ennumerated above, and the criteria for their assessment and measurement methods. It also outlines the basic standards in this field.

3. Noise of air transportation to nontravelers – M. J. Crocker.

The peculiarity of aircraft noise has made it necessary to introduce different criteria of noise annoyance assessment, compared to these for surface transportation discussed in the preceding chapter. It also encloses a list of the basic legislative acts in the USA on the aircraft noise control.

4. Recreational vehicle noise to nonusers – E. Rose.

This chapter presents the problems of the effect on the environment of man of recreational and sports vehicles such as motorcycles, motorbicycles, go-karts, motorboats, snowmobiles and dune buggies.

5. Noise of transportation to travelers – G. Crépeau.

This chapter discusses the effect of noise from transportation means on the crew and passengers. The enclosed tables of noise within different automotive types and the proposed admissible levels can be the basis for improved comfort of passengers and for better working conditions of drivers. The conclusion of this chapter deals briefly with vibration problems.

6. Interior noise environment – L. W. Hegvold, D. N. May.

This section discusses briefly the problem of noise annoyance in apartments and public interiors, gives the admissible levels, and deals with the problems of speech intelligibility in offices.

7. Noise in hospitals – J. G. Walker.

This chapter concerns the problem of the effect of noise on patients and hospital personnel, and discusses briefly the criteria.

8. Exterior industrial and commercial noise – R. Taylor.

This part deals briefly with the problem of division of urban agglomeration into zones, depending on the level of industrial and commercial noise.

9. Construction site noise – R. J. Alfredson, D. N. May.

Beginning with a discussion of the successive building stages from site preparation through foundation laying to interior finish, the authors present the problems of noise in these stages and then go on to discuss the noise from construction machinery and auxiliary equipment.

10. Noise in and around the home – D. N. May.

This chapter deals with the sources of external and internal residential noise, including appliances.

The second part is divided into four chapters:

1. Occupational deafness and hearing conservation – A. M. Martin, J. G. Walker.

A short discussion of the fundamentals of the performance of a hearing aid is followed by presentation of methods of audiometric and dosimetric measurements, and the problem of noise control by setting the admissible noise doses.

2. The nonauditory effects of noise on health – D. Stephens, G. Rood.

This section presents the little investigated effect of noise on the respiratory, central nervous and circulatory systems of man, and discusses the effect of infra- and ultrasound on the particular systems.

3. Noise and sleep: a literature review and a proposed criterion for assessing effect – J. S. Lukas.

This chapter discusses the little known, but very important, effect of noise on human sleep. It gives averaged numerical data on the responses of specific human groups to noise in sleep, with consideration of their sex and age. It also proposes preliminary assessing criteria.

4. Effects of noise on human work efficincy – G. R. J. HOCKEY.

This chapter discusses the problem of the effect of continous and interrupted noise on work efficiency, the problem of localization of a noise source with respect to an observer, and finally the consideration of the future in this respect.

The book concludes with a short appendix containing a list of chosen standards, periodicals and international centres, and a short glossary of most important terms related to the problems discussed. This book is an original, valuable source of information in the field of the effect of noise on man, which in addition to encyclopedic information discusses a number of new aspects with a future bearing.

Stefan Czarnecki

Building acoustics, L'acustica nell'edifizia, ESA Edizioni Scientifiche Associate Roma 1979

Proceedings of a two-day symposium on building acoustics, which was held in Torino on 5-6 June, 1979 (259 pages, in Italian).

The symposium was organized by the Gallileo Ferraris Institute of Electrotechnology and was sponsored by Italian Acoustical Society.

The proceedings consist of sixteen papers by Italian authors and one in French by a French author, and in terms of subject can be divided into two parts.

The first part, which contains the materials from the first day of the symposium, is concerned with the problems of standardization and, in addition to short papers, includes a long monographic review of E. BROSIO on the standardization of measurement methods in building.

The second part, which contains the materials from the second day of the symposium, concentrates on technical aspects. This part includes a large monographic paper of G. FRANZITTA on the insulating properties of barriers. Technical aspects of the insulating properties of different kinds of barrier are examined by R. PISANI and M. CURIONI. The second part also includes a paper of R. ROSSE on different aspects of noise control in residential buildings in France.

The proceedings as a whole testify to high rank of building acoustics in Italy and to the need for further development in fundamental research, technology and standardization.

Stefan Czarnecki

Mario COSA, *Urban and industrial noise, Il rumore urbano e industriale,* Instituto Italiano de Medicina Sociale, Roma 1980 (937 pages, in Italian).

This book contains a large material on the environmental acoustics and concerns the problems of the noise hazard and annoyance to man, and also the technical aspects of industrial and urban noise.

In addition, the book contains an ample list of standards in different countries, a unique presentation of chosen data in the field of the standardization of vibroacoustics and environmental acoustics.

Another interesting material is a large review of the basic definitions of the field discussed.

The book has ten chapters.

Chapter 1 discusses the basic notions in sound and noise and presents the criteria for their subjective assessment.

Chapter 2 concerns the manner of noise perception by the hearing organ and the effects of noise on man. It also discusses the primary kinds of noise-induced hearing loss.

Chapter 3 deals with urban acoustics, namely with methods for measurement and evaluation of transportation noise and includes a broad discussion of corrections for external factors, methods for calculating urban barriers, methods for averaging urban noises in time and standards for admissible noise levels in different countries, particularly those in different districts of Italy.

Chapter 4 deals with noise inside apartment houses both from the viewpoint of the effect of external and internal noise (neighbours, facilities) and discusses methods for measurement and standard for numerical values of insulating power of partitions.

Chapter 5 presents the problems of noise at work stands, including transient noise, and discusses standards in this field in particular countries. It also gives the basic methods for the reduction of noise propagation in industrial interiors and in ventilation channels (mufflers).

Chapter 6 deals with the problems of areadynamic noise and is devoted mainly to aircraft noise and the criteria for their assessment. It also presents the possibilities of aerodynamic noise control.

Chapter 7 is devoted to the problems of ariborne and structure-borne sound in buildings, and gives the values of the absorption by different types of carpeting, and the information of floating floors and suspended ceilings.

Chapter 8 contains 266 basic definitions of technical and medical notions and of generally used abbreviations of most important notions and units. This is a large material of about 100 pages, in which, in addition to definitions, some entries include basic formulae, figures, or tables.

Chapter 9 gives a long list (about 100 pages long) of most important standards in environmental and building acoustics from about 30 countries, including the standards of ISO and IEC. The titles of the standards are given in one of the following languages: Italian, English, French or German.

The standards are divided into fourteen groups:

1. The basic notions, terminology of acoustics and electroacoustics.
2. The criteria for the assessment of noise hazard and annoyance.
3. Noise measurement methods.
4. Measurements of machinery noise.
5. Acoustic measurements in interiors, acoustic and antivibration materials.
6. Measurements of noise from motorcars, railway and ships.
7. Audiometers and hearing aids.
8. Measurements of aricraft noise.
9. The basic vibration standards.
10. The basic criteria for the assessment of vibration hazard and annoyance.
11. Vibration measurements.
12. Measurements of machinery vibration.
13. Vibration measurements in environmential acoustics.
14. Physical properties of materials.

Chapter 10 is a short appendix which gives the most important data and the current proposals in standardization.

This book as a whole is a large source of information on environmental acoustics and a valuable aid to engineers, physicians and others related to the problems.

Additional advantages of this book are a large number of tables (over 80) and figures (also over 80), and a very long list of references, of nearly 900 items.

Stefan Czarnecki